Effect of Heat on the Properties of Automotive Airbag Materials

Submitted in fulfilment for the degree of

MPhil Materials

School of Materials

Faculty of Engineering and Physical Sciences

The University of Manchester

Mohammad Bin Rokan

2013

DECLARATION

With the exception of any statement to the contrary, all the material presented in this report is the result of my own efforts. In addition, no parts of this report are copied from other sources. I understand that any evidence of plagiarism and/or the use of unacknowledged third party materials will be dealt with as a serious matter.

ACKNOWLEDGEMENTS

First and foremost I thank almighty God for everything He has given me so far. I also thank my parents for their continuous support. I would like to thank Dr. Prasad Potluri for allowing me to work with him in this project. I must thank Autoliv for providing this research opportunity. I would also like to thank Dr. Haseeb Arshad, Dr. Richard Kennon, Dr. Arthur Wilkinson, Professor John Hearle, Professor Peter Lovell and Professor Robert Young for their valuable contributions to this project. Lastly, but not least, I want to thank all my friends who have always been there for me.

Contents

Abstract

Automotive airbags are subjected to extreme temperatures (up to 900°C) during deployment which is achieved by using pyrotechnic inflators. Although the airbag fully inflates within a few milliseconds, the heat often causes physical damage to the airbags fabric and seams in this short period of time. In this study, the effects of heat on airbag yarns (highly drawn Nylon 6,6) and airbag fabrics were investigated with the goal of understanding whether or not high heat causes the internal structure of the material to change. The degree of crystallinity of the material was found to increase as the delta H values of the material increased with heat and heating rate in a Differential Scanning Calorimeter (DSC) for both unheated and heated fibres (extracted from airbag yarns) as well as unfired and fired airbag fabrics. The storage modulus of the material was also found to drop gradually as the material was heated from sub-zero temperature to melting point in a Dynamic Mechanical Analyzer (DMA) with sharp drops in the glass-transition and melting regions. The initial stiffness and the breaking strength of the material were found to decrease in a tensile tester as the temperature and heating rate at which the material was heated increased. This unusual behaviour, i.e. a reduction in stiffness and strength with a rise in the degree of crystallinity was found to be due to a reduction in the molecular orientation of the fibres as high levels of shrinkage were observed for both yarns and fabrics when the material was heated. The shrinkage increased with increasing temperature and heating rate which caused the diameter of the fibre to increase. Upon correlation with shrinkage, the initial stiffness and breaking strength of the material were found to be inversely proportional to shrinkage while the breaking strain was proportional to shrinkage.

Chapter 1: Introduction to Automotive Airbags

This chapter gives a brief introduction to automotive airbags – how they are constructed, how they work and the different types of airbags. This chapter also explains why Nylon is the material of choice for airbags and why understanding the heat effects on Nylon is important.

1.1 Introduction to Airbags:

Airbags are among the most important automotive safety products, as the concept of inflating a textile cushion can be used in both frontal impacts and side impact collisions to protect different body parts. Airbags are classified as Passive Safety Devices (devices for injury mitigation) as opposed to Active Safety Devices (devices for crash prevention).

Fig 1: Airbag deployment during crash testing. (Source: Autoliv)

Airbags are now very widely adopted and are considered to be very important in reducing fatalities in crashes. Autoliv, a major manufacturer of airbag products estimates that, in frontal impacts, driver airbags reduce fatalities by 25% for belted drivers and serious head injuries by over 60%.

Nylon is widely used in airbag manufacture. Nylon yarns are woven together to produce the airbag fabric. The woven fabrics are then cut and sewn to the required size and shape, depending on the vehicle. The size of the airbags, weave patterns and sewing geometry varies depending on the application, such as driver side airbags, passenger side airbags, side curtains, etc.

Traditionally most airbag fabrics were coated with an elastomeric material, such as neoprene or silicone. The use of coated materials in this application has been largely due to their ability to act as a heat shield and the relative ease in predicting their performance in a deployment. However, there are some inherent problems with coated airbags, which include their excessive thickness, inability to be folded into small spaces, and tendency to degrade over time. (Mukhopadhay and Partridge, 1999)

The various types of airbags and their uses will be discussed in more detail in the section titled “Types of Automotive Airbags”.

1.2 Working Principle of Automotive Airbag Systems

Automotive airbag systems are made up of three general components.

1. A sensor system.
2. A deployment mechanism.
3. The airbag or the cushion.

In the event of a crash, the sensor system sends a signal to the deployment mechanism only if a set of conditions are met including acceleration pulse and pulse duration. These sensors can also detect the direction of impact, so the front airbags will not deploy during a side impact for example.

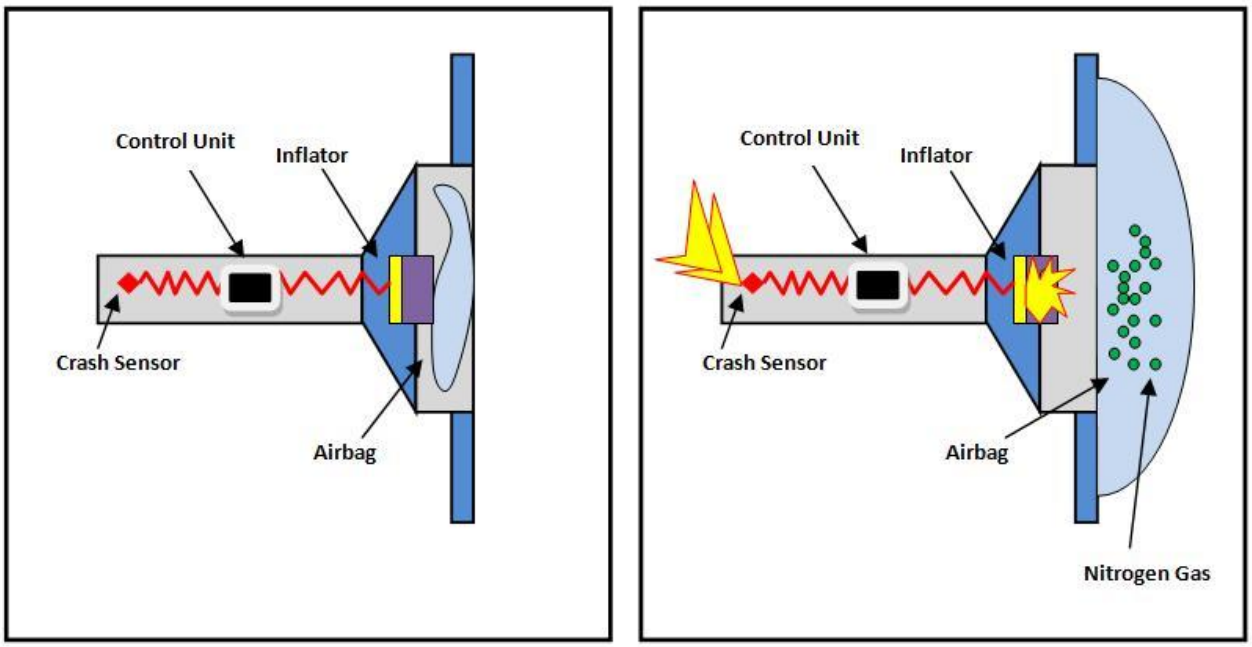

Fig 2: Crash sensing and deployment (Source: The Clemson University Vehicular Electronics Laboratory)

When the sensor system sends a voltage pulse to the deployment mechanism, the heat of the voltage pulse ignites the pyrotechnic material or the inflator. The inflator generates an inert gas that fill up the airbag very rapidly as shown in Figure 2.

Pyrotechnic inflation technology has changed over the past few years from reliance on sodium azide to the use of organic propellants in order to minimise environmental impact of the propellant and to increase efficiency. For frontal airbag systems the need for better protection of out-of-position occupants has led to the development of multi-stage devices

that have the potential to provide large or small volumes of gas as deemed necessary by the sensor system.

The main function of the cushion or the airbag is to contain the hot high pressure gas, allowing a safe and efficient deceleration of the occupant during the rapid deceleration of the vehicle in a crash. This is achieved through elastic fibre deformation and controlled hot gas flow through the fabric. The gas flow is controlled by the structural elements of the airbag, such as the seam and vents.

1.3 Types of Automotive Airbags

There are 2 main types of airbag systems:

1. Frontal Airbags
2. Side-impact Airbags

1.3.1 Frontal Airbags

Frontal airbags are an integral part of the full protection system for occupants in the front seating positions. Located in the steering wheel (for driver seat) or instrument panel (for passenger seat), these airbags inflate during frontal collisions in order to provide protection for the driver and passenger.

During a collision, crash sensors send signals to a micro-processor in an Electronic Control Unit (ECU), which determines the crash severity. If the crash severity exceeds a predetermined limit, an electrical impulse is sent to the inflator in the airbag module. An igniter in the inflator starts a chemical reaction that produces gas which fully inflates the airbag within 50 thousands of a second, twice the speed of a blink of an eye. The airbag

automatically deflates within a few milliseconds as the gas escapes through vents.

Frontal airbags can be further subdivided into 3 categories:

1. Driver Airbags
2. Passenger Airbags
3. Lower-body Protection

Driver airbag modules consist of the textile airbag, inflator and an initiator. This module is housed inside the steering wheel.

Pyrotechnic inflators are the most common. They contain a gas generant and during a crash, this generant is ignited and produces a harmless nitrogen gas.

The textile airbag or the cushion is made from nylon fabric which is folded inside the module in such a way as to ensure fast and safe deployment during a crash. It has vent holes on the back of the fabric which lets out gas to assure a soft landing of the occupant on the bag.

The **passenger airbag** module is very similar to the driver airbag module, with the exception of a larger cushion and a larger inflator to inflate the larger bag to the desired level.

Both the driver and passenger air bag materials are often manufactured with a heat shield coating to protect the fabric from scorching, especially near the inflator assembly, during deployment.

For car occupants who are protected by airbags and their seatbelts, leg injuries are the most frequent problem in frontal crashes. Autoliv estimates that leg injuries account for 40% of the moderate to severe injuries to these occupants, of which 60% are below the knee.

Lower-body protection airbags are still not well established compared to driver and passenger airbags. However, there is an increasing demand for lower-body protection airbags (knee airbags and anti-sliding airbags) to prevent fatal leg injuries and ensure that people not only survive a crash but also are able to walk and lead a normal life after a crash.

1.3.2 Side-Impact Airbags

Side-impact collisions account for a quarter of all injuries to car occupants, but they account for more than one third of the serious and fatal injuries according to Autoliv. One major reason is that the side of the vehicle is a thin crumple zone and the space between the occupant and the side of the vehicle is small.

Side-impact airbags can be subdivided into 5 categories:

1. Inflatable Curtain
2. Thorax Bag
3. Head Thorax Bag
4. Pelvis-Thorax Bag
5. Door Mounted Inflatable Curtain

Inflatable curtains are stored in the headliner above the doors and are used to absorb the energy of a direct side impact, often known as the "first impact" and to provide energy absorption in roll-overs, often known as "second impact". The US federal law has made it mandatory for all new vehicles of 2013 model sold in the US to contain this kind of airbag.

Thorax bags are stored in back rests of the front seats or in the front doors. These airbags are meant to protect the occupant from serious chest injuries from side-impact collision by pushing the occupant away from the impact zone, thus dampening the blow. These bags usually have

a small volume to keep the force on the occupant as gentle as possible while providing sufficient protection.

Head Thorax bags are used in vehicles where inflatable curtains cannot be used, for example in convertible cars. The module is usually located in the seat frame and works to protect the occupant very much similar to that of inflatable curtains.

Pelvis-Thorax bags are used to increase side impact restraint performance by increasing the coverage area with the help of an added cell which is inflated to a higher pressure in order to distribute load over the thorax (abdomen area) and pelvis (area between the abdomen and the lower limbs) parts of the occupant's body more efficiently. This concept takes advantage of the pelvis' ability to take higher loads, while it limits pressure on the sensitive thorax area.

Door Mounted Inflatable Curtains (DMICs) provide a large side coverage area in vehicles which have no roof, such as convertibles. It has a chamber design which offers even protection and real inflatable curtain (IC) performances, including improved ejection (situation where the seat belts of the driver or passengers are released) protection in roll-over accidents.

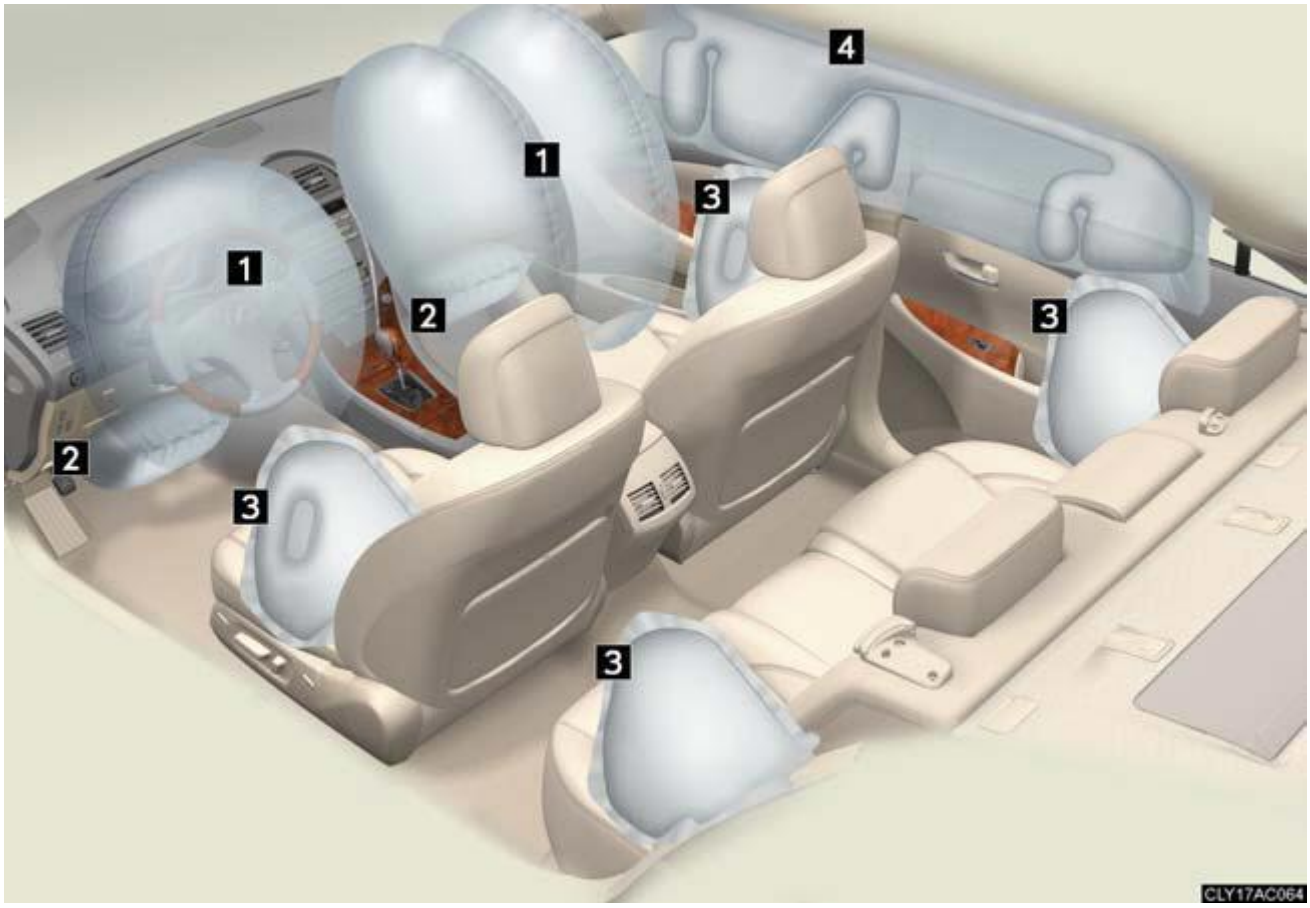

Fig 3: Different types of airbags in the Lexus ES 350. (1. Driver airbag/Front Passenger airbag, 2. Knee airbags. 3. Side-impact airbags, 4. Inflatable Curtains) [Source: Lexus]

1.4 Nylon in Airbags

Nylon is the material of choice for airbags because Nylon offers various advantages in airbag application compared to other fibres. In general, the Nylon fibre exhibits high specific strength, abrasion resistance, and toughness or energy-absorption properties. The aging characteristics of Nylon are also very good (Keshavaraj et al., 1996), which is important because airbags typically need to have a replacement period of at least 15 years (Sun and Barnes, 2010)

Nylon fabric has a greater bi-axial elongation compared to other fabrics due to its lower stiffness. This is a major advantage because it provides a more uniform bi-axial stress distribution. (Keshavaraj et al., 1996)

Compared to poly(ethylene terephthalate) [PET] for example, Nylon 6,6 has a number of advantages. They have similar melting points, but there is a large difference in *specific heat capacity.* This means that the amount of energy required to melt PET is about 30% less than that required to melt Nylon 6,6. Hence in any inflation event that uses a pyrotechnic inflator, cushions made from PET are far more susceptible to burn or melt in the body of the cushion or at the seam. Nylon 6,6 has a lower density than PET. This means that for fabrics made with yarns of identical diameter and in the same construction, PET fabric is 20% heavier than the fabric made from Nylon 6,6. The lower mass of Nylon allows the production of lightweight cushions which helps to lower the kinetic energy of impact on the occupant in out-of-position situations thus enhancing safety, while allowing the overall weight of the vehicle to be reduced. If lightweight cushions using the high density PET were to be made, the fabric coverage would have to be sacrificed. But this is impractical, because the lower fabric coverage would mean higher gas permeation, which would reduce the thermal protection for the occupants. In addition to that, seam performance would be reduced because seam strength is strongly dependent on the cover factor (Sun and Barnes, 2010).

Another advantage of Nylon is its hygroscopic nature which assists with quenching of the hot gases generated by the airbag's pyrotechnic inflator. Absorption of moisture by Nylon also helps in lowering the glass transition temperature of the polymer. The lower T_g can increase fabric permeability at lower temperatures and provide a pneumatic damping action of the airbags, especially in vent-less airbag modules. (Keshavaraj et al., 1996)

1.5 Understanding the Effects of Heat on Airbags

Pyrotechnic inflation techniques have changed over the years and these changes have increased the demands on the airbag cushion as they have led to higher inflation temperatures and in some cases greater risk of hot particulate ejection with the potential to lead to melting of the cushion fabric. Therefore it is important to understand and predict the changes in fibre and fabric level that occurs due to the effect of the gas at a very high temperature and pressure.

1.51 Aims and Objectives

There were 4 main aims to this research:

1. Understanding effects of heat (post deployment) on the crystallinity of airbag material – at fibre and fabric level.
2. Understanding effects of heat (post deployment) on mechanical properties of airbag fibres.
3. Understanding how the modulus of the material changes with temperature - the objective was to establish a path which the modulus takes when exposed to temperature and generate data for future modelling work.
4. Understanding the shrinkage behaviour of the material with heat - because molecular orientation often plays a key part in determining the mechanical properties of fibres.

Chapter 2: Literature Review

Polymers are very interesting materials and they are in use today in many diverse places all around us. In fact, humans are made up of polymers because the human DNA is a type of polymer. Few decades ago, the term "plastics" was more common, but now the term "polymer" has become mainstream and the term "plastics" is rightly used to describe a certain category of polymers with a particular mechanical behaviour.

This chapter reviews existing literature and aims to highlight some of the key developments made in the last few decades to better understand the heat effects on polymeric fibres. The chapter begins by looking into polymers in general. It then moves on to look at Nylon 6,6, which is extensively used to manufacture airbags. Nylon is a certain type of polymer which can be classed as a "thermoplastic" and more specifically as a "polyamide". Finally, this chapter will highlight the thermal properties (the effect of heat and rate) on Nylon 6,6.

2.1 Introduction to Polymers

A polymer is essentially a material which is composed of large molecules. They are also often known as "macromolecules". These molecules are made of one or more types of atoms which are covalently bonded to each other. Two elements in particular form the backbone of polymers and these are carbon and silicon. Polymers are formed by linking a large number of repeated chemical units in sequence.

The International Union of Pure and Applied Chemistry (IUPAC) defines a polymer as "a substance composed of molecules characterised by the multiple repetition of one or more species of atoms or groups of atoms linked to each other in amounts sufficient to provide a set of properties

that do not vary markedly with the addition or removal of one or a few of the constitutional units". The chain structure of polyethylene is shown in Figure 4.

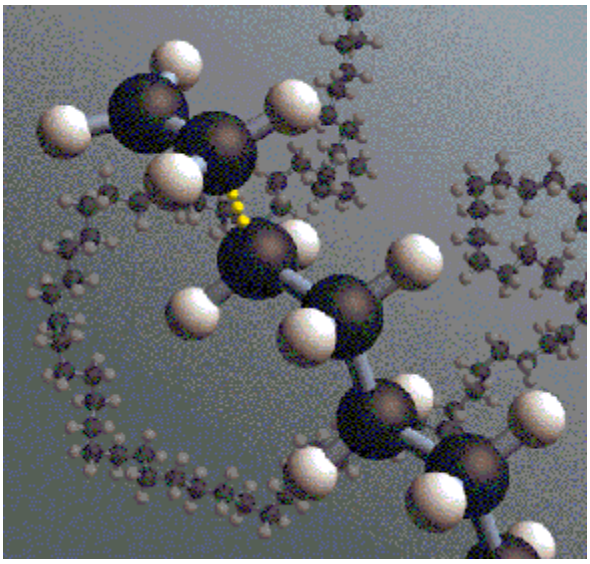

Fig 4: Polymer chain structure of polyethylene, one of the most common types of polymer. (Source: European Commission)

2.11 Structure of Polymers:

Some polymers contain two different regions and their structures are often known as "two-phase structures". Different views have been offered over the years as to how two different phases can co-exist within the same polymer.

One way to depict polymers is the "fringed micelle concept", as shown in Figure 5. This concept arose from the suggestion that perhaps the polymer chains are precisely aligned over distances corresponding to the dimensions of the crystallites, and that there are disordered segments of these same chains which do not crystallise, and contribute to the amorphous phase.

Because each polymer molecule is very long, it was therefore assumed that it would contribute to several crystalline and amorphous regions. This view led to the structure known as the fringed micelle model.

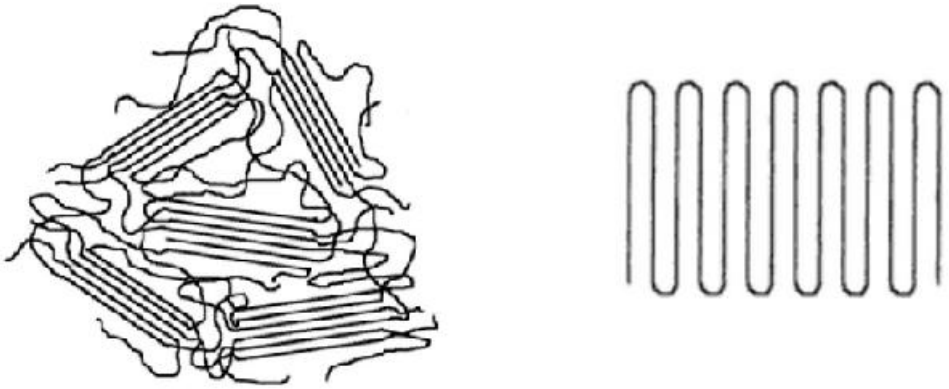

Fig 5: Fringed Micelle Model [left] and Chain-folded Crystal Model [right] (Source: Bower, 2002)

In a chain-folded lamellar crystal model (Figure 5), semi-crystalline polymers are thought to be made up of folded-chain lamellae which are held together by tie-molecules. These tie-molecules go from one crystalline layer to another (Pai et al., 1989). In Nylon 6,6 the thickness of these lamellae is 50-100 Angstroms, corresponding up to six repeat units (Narten et al., 1991).

2.12 Glass-transition of Polymers:

When the melt of a polymer is cooled, it becomes more viscous and flows less readily. If the polymer is not able to crystallise and the temperature is reduced low enough, it becomes rubbery and then as the temperature is reduced further, it becomes a relatively hard and elastic polymer glass. The temperature at which the polymer undergoes the transformation from a rubber to a glass is known as the "glass transition temperature, T_g". (Young and Lovell, 2011)

The glass-transition of polymers is commonly explained in terms of rapid molecular motion of polymer chains above T_g and the substantially reduced chain mobility below T_g. Above the T_g, a polymeric material can flow and be stretched or shaped into useful forms (Jenekhe and Roberts, 1993).

The value of T_g is thought to be determined by such factors such as chain stiffness, molecular symmetry, the presence of a side group (and its size and flexibility), molecular weight, chain branching, cross-linking, and intermolecular forces such as hydrogen bonding, dispersion forces, dipole-dipole forces and induction forces (Jenekhe and Roberts, 1993).

Jenekhe and Roberts, 1993 have shown that it is possible to influence the T_g of a polymer by weakening the intermolecular forces. The authors achieved this by a process called Lewis acid-base complexation on Nylon 6,6. The Nylon was reacted with a metal halide (Lewis acid) which caused the intermolecular hydrogen bonds to break and the T_g reduced to -4°C as compared to 55°C for pure Nylon 6,6.

2.13 Degree of Crystallinity:

The crystallisation of polymers is of enormous technological importance. Many thermoplastic polymers will crystallise to some extent when the molten polymer is cooled below the melting point of the crystalline phase. This is a procedure that is done repeatedly during polymer processing and the presence of the crystals has an important effect upon polymer properties. There are many factors that can affect the rate and extent to which crystallisation occurs for a particular polymer. They can be processing variables such as the rate of cooling, the presence of orientation in the melt and the melt temperature. Other factors include the tacticity and molar mass of the polymer, the amount of chain

branching and the presence of any additives such as nucleating agents (Young and Lovell, 2011).

The fraction of crystalline material in the polymer is called the "degree of crystallinity". The degree of crystallinity is the single most important characteristic of a polymer because it reflects the morphology of the polymer and determines mechanical properties, such as yield stress, elastic modulus and impact resistance. These mechanical properties increase progressively with crystallinity (Kong and Hay, 2002).

For example, amorphous poly(ethyleneterephthalate) [PET] is of little commercial value since it has poor mechanical properties, low dimensional stability and high gas permeation rate; on the other hand, crystalline PET has higher strength, good dimensional stability and chemical resistance. It is widely used in the production of fibres and in carbonated beverage containers because of its strength and low gas permeability, especially to carbon-dioxide and oxygen.

Degree of crystallinity is not expected to directly affect the glass-transition temperature of a polymer. However it can affect the glass-transition indirectly because the amorphous chain segments are constrained by the crystalline regions by means of linkages between the crystalline and amorphous regions. (Murthy, 1997)

A two-phase (amorphous-plus-crystalline) model described previously has been used widely to interpret crystallinity results. However, imperfections, and disorders within the crystals may also contribute to the amorphous component. Hence, the level of crystallinity measured is best interpreted as a level of order (White and Cakmak, 1986).

2.14 Industrial Production of Polymer Fibres:

Polymer fibres such as Nylon are widely produced industrially using a technique known as "melt spinning" (Figure 6). The melt spinning of fibres is an industrial processing operation of great commercial importance and the most important aspect of this operation is that of development of structure, in particular crystallinity and orientation (White and Cakmak, 1986).

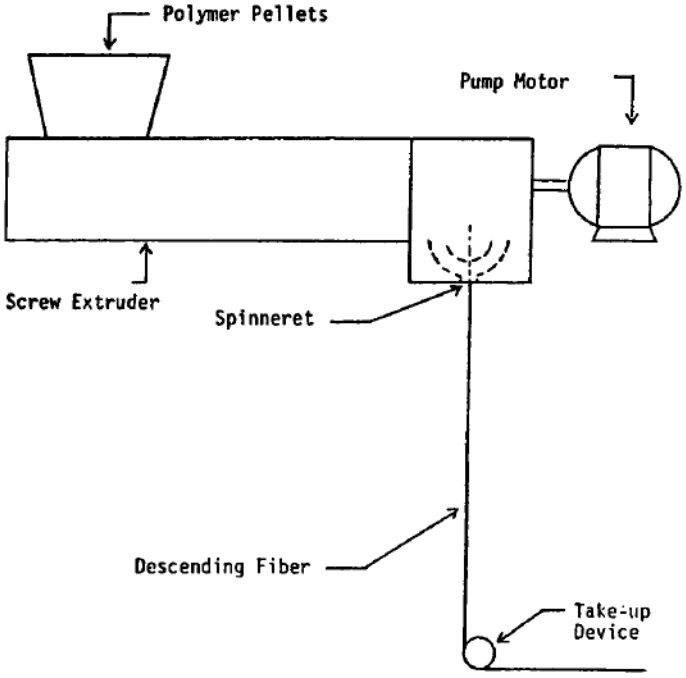

Fig 6: Melt Spinning of Polymer Fibres (White and Cakmak, 1986)

An important part of the melt-spinning process is "drawing". This is the process which develops the structure and orientation of the fibre. The glass-transition temperature of Nylon 6 fibre has been reported to increase with increasing draw ratio (Murthy, 1997). The author explained that this increase could be due to increased amorphous orientation.

In fact, the author suggested that for drawn fibres, the amorphous orientation has a greater influence on the glass-transition temperature than the degree of crystallinity does. Although drawing may produce a

more oriented fibre, the morphology might not change. Bell and Hughes, 1978 have found that the morphology of drawn Nylon 6,6 fibres is very similar to its morphology before drawing. This has also been reported by Crystal and Hansen, 1968.

Drawing can be done in the solid state or in the molten state at elevated spinning speeds. The elevated speeds give rise to an enhanced orientation within the melt. This orientation is expected to be transferred at least partially to the solid state, hence influencing fibre properties (Frank and Wendorff, 1988). The authors investigated the dependence of the mechanical properties of Nylon 6,6 with this processing parameter. The authors found that fibres drawn in the solid state show a lower deformation at break and a steeper increase of stress with increasing strain compared to the fibre which were drawn in the molten state. The authors interpreted this in terms of tie-molecules. The drawing of the sample after the melt spinning process gives rise to a high concentration of nearly extended tie-molecules which break during elongation.

Some polymers contain both crystalline (ordered) and amorphous (disordered) regions. The crystalline regions contribute to strength and rigidity while the amorphous regions contribute to elasticity. The fraction of crystalline material in the polymer is called the "degree of crystallinity".

The crystalline component of a given semi-crystalline polymer can also be divided into 2 parts – the part which re-crystallises when melted at a given heating rate and the part which does not re-crystallise upon melting at a given heating rate (Bell, 1972). The ratio of re-crystallisable to non-crystallisable material can be varied at will. Completely crystallisable and completely non-crystallisable material can be produced during melt spinning. Bell, 1972 found that as the rate of drawing is decreased, or the temperature at which drawing in done is increased, the amount of re-crystallisable material decreases.

2.2 Nylon:

Nylon is a synthetic polymer (man-made polymer) made up of repeating units which are linked by amide bonds. To make the repeating unit or the monomer, molecules with an acid (-COOH) group on each end are reacted with molecules containing amine ($-NH_2$) groups on each end. The monomers are then reacted together to form long polymer chains.

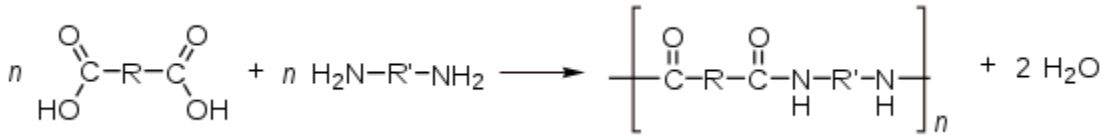

The resulting Nylon is named on the basis of the number of carbon atoms donated by the monomers, the diamine first and the diacid second. So for example, Nylon 6,6 refers to the diamine and the diacid donating 6 carbon atoms each to the polymer chain. So for Nylon 6,6, R will be 4-C and R’ will be 6-C in the equation above.

The earliest study of the crystal structure of Nylon 6,6 was that of Fuller, 1940 and Fuller et al., 1940. These authors established that the crystalline form consisted of extended polyamide chains. A more extensive study was conducted by Bunn and Garner, 1947 who determined the structure of a primary form of crystallites and suggested the existence of secondary forms.

2.21 Effect of Moisture on the Properties of Nylon:

Nylons are well known to readily absorb moisture. Water is first absorbed on the surface. When the surface layer is saturated with moisture, absorbed water starts diffusing inside the body. The moisture diffuses mostly in the amorphous regions. Once the diffused water reaches an accessible –CONH- group, it is chemically absorbed. Excess water which is

not chemically bound increases the volume of the samples and cause swelling (Pai et al., 1989).

The water absorption process depends on the thickness of the samples. Because diffusion of water is a slow process, sample thickness influences the early part of the water absorption process but not the equilibrium value (Pai et al., 1989). Also, the amount of water absorbed decreases with increasing density and is proportional to the amorphous fraction (Starkweather JR. et al., 1956).

Nylon 6,6 is hydrophilic due to the amide groups. Moisture is readily absorbed from normal laboratory atmospheres (Starkweather JR. et al., 1956). Pai et al., 1989 have shown that the melting peak of Nylon 6,6 polymers tend to broaden as moisture content increases. The authors have also shown that the tensile strength and modulus of Nylon 6,6 decreases as moisture content increases.

This can be explained by thinking of water as a plasticiser. It lowers the glass-transition temperature of Nylon 6,6, slightly decreases the degree of crystallinity and dilutes the amorphous phase (Pai et al., 1989).

Water absorption has effects opposite to that of drawing. It is stronger than the effect of orientation and weakens the inter-chain bonding which leads to the plasticising effect (Leung et al., 1984).

2.22 Use of Nylon 6,6 in Airbags:

Nylon 6,6 is widely used in the manufacture of automotive airbags and the previous chapter shed some light as to why Nylon 6,6 is chosen for this application. The reasoning and evidence for this are very well understood in the industry. However, one aspect which existing literature

has very limited information on is the effect on Nylon 6,6 when the airbag is deployed. During deployment the Nylon fabric experiences a very high temperature at a high pressure for a very short time. The time-scale of an airbag deployment is shown in Figure 7.

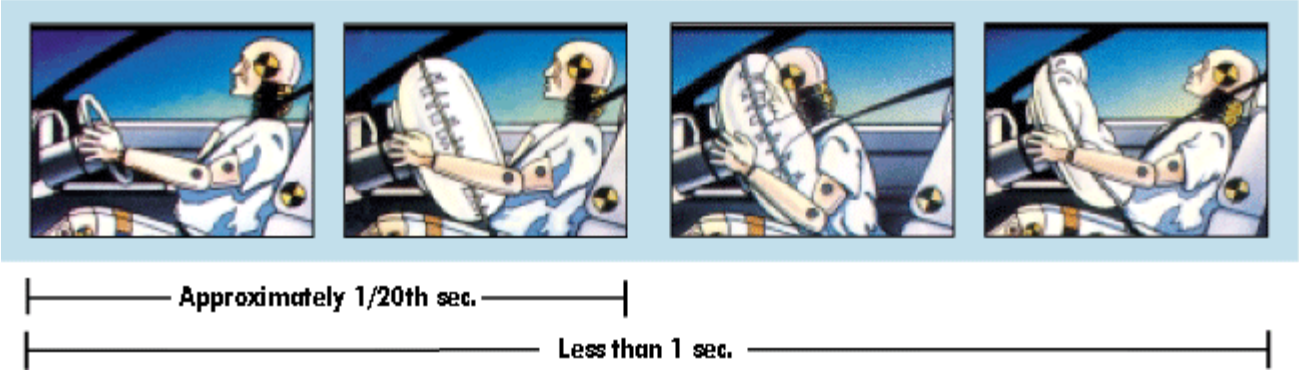

Fig 7: Complete airbag deployment cycle. (Source: Airbag 101)

There is not much information on what happens at the fabric and fibre level when the airbag is subjected to extreme temperatures and heating rates. Some of the information found from the literature regarding the effects of heat on polymeric fibres (not necessarily Nylon 6,6) and fabric (not necessarily airbags) are provided in the next few sections.

2.3 Effects of Heat on Polymeric Fibres:

Metals are accustomed to a level of certainty where temperature-dependent behaviour is concerned. Polymers do not provide such certainty (Sepe, 2011). Aluminium, for example, has essentially the same mechanical properties between room temperature and 250-300°C, and even when approaching the melting point, retention can be as high as 80% of room-temperature performance. This level of consistency is even better for materials like copper, brass, and steel, where the melting points are higher. This certainty is due to the fact that the building blocks for metallic substances are small and readily organise into a well-defined and predictable crystal structure.

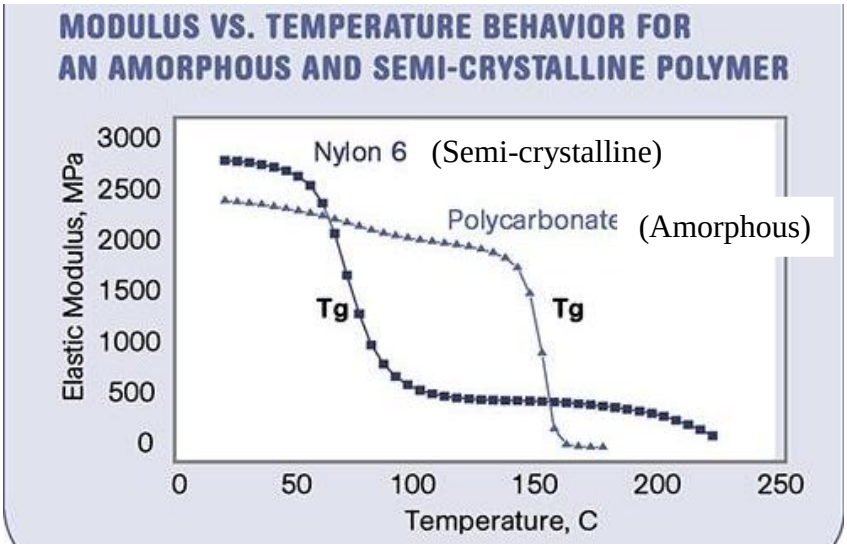

Fig 8: Modulus vs. Temperature behaviour for an Amorphous and Semi-crystalline Polymer (Sepe, 2011)

That is not the case for polymers. The individual molecules that make up polymeric materials are very large and have an extended chain-like shape that results in an entangled structure. This entanglement is beneficial in some respects. The relatively high levels of elongation that most polymers exhibit without breaking are due in large part to chain entanglement. However, this entanglement also restricts the freedom required at a molecular level to organise into crystals. Hence, no polymer under normal processing conditions is fully crystalline, and some polymers do not crystallise to any significant degree. Figure 8 shows the difference in mechanical behaviour due to a difference in crystallinity. This lack of a predictable and repeatable structure gives rise to a situation where changes in temperature always influence the mechanical properties of these materials (Sepe, 2011).

The effect of heat is usually measured in terms of the change in "enthalpy". Enthalpy is a fundamental thermodynamic of materials; it is temperature dependent and any change in enthalpy accompanying a phase change is also temperature dependent. (Kong and Hay, 2002)

2.31 Types of Thermal Change

It is important to understand the types of thermal change that can occur when a polymer is heated. Three different distinctions can be made in this regard (Morton and Hearle, 1993):

- **Firstly**, there is the difference between chemical and structural changes. Structural change is due to the relaxation of molecular chains and the chemical changes involve the breaking of chains or possibly the formation of cross-links.

- **Secondly**, there is the thermodynamic distinction between first-order and second-order transitions. A first-order transition involves a change of structure and is shown experimentally by changes in volume, V, in heat capacity, H (by latent heat), and by other major changes of form or properties. The most common first order transition is melting, which is the change from the regular order of a crystal to the disorder of a liquid. A second-order transition involves no change of molecular arrangement, i.e. snapshots of molecular arrangement above and below the transition would be virtually the same. But there is change in response of the structure, shown by changes in the second-order quantities. An important second-order transition in polymers is the change from the glassy-amorphous to the rubbery-amorphous state.

- **Thirdly**, there is a distinction between sharp and broad transitions. In polymer materials, this often is a reflection of local variations in structure, for example, in crystal size or perfection or in local packing, so that the observed effect is really a collection of sharp transitions spread over a range of temperatures.

2.32 Heat Effects on Fibre Structure:

Jain and Vijayan, 2002 took scanning electron micrographs of Nylon 6,6 fibres which depicted the characteristics of the fibres. Prior to heat treatment, faint lines parallel to the fibre length were observed on the surface. Tiny specks of extraneous material were found.

Aging the fibres at 175°C for 1750 hours caused a large number of holes and groove-like openings on the surface of the fibres. The deposit of extraneous material also increased compared to the unheated fibres. These features seemed to intensify at 225 and 245°C. Formation of holes and material deposits on the surface of heat treated fibres suggests that during thermal ageing some solid material has evolved from within the fibre via the holes and surface openings and have deposited on the surface. The material could be associated with chemical degradation of the polymer induced during thermal ageing. In addition to the solid deposits seen in the micrographs, gaseous components formed during heat treatment were also likely to have got evolved. The gaseous components could account for the weight loss. Thermally induced holes, pits, and longitudinal discontinuities were expected to be the cause of deterioration in the initial tensile properties of the fibre (Jain and Vijayan, 2002).

Murthy, 1997 analysed the changes in fibrillar structure of drawn Nylon 6 fibres with heat. Lamellar spacing and the length of the lamellar stack were found to increase with heat. The author suggested that annealing does not change the number of lamellae within a lamellar stack; either, new stacks are formed or the existing stacks grow laterally during annealing.

2.33 Weight Loss due to Heat:

An increase in temperature causes enhanced weight loss (Jain and Vijayan, 2002). This is shown in Figure 9. In addition, for a constant value of T [temperature], increase in the $t_{cum}(T)$ [duration] value also causes a progressive reduction in weight i.e. during any high temperature application, if the fibres are used at a fixed temperature for long durations, it will undergo a progressive weight loss.

The weight loss suggested that thermal exposures have led to a material loss which could be a consequence of thermally induced chemical degradation. Weight loss of this type was expected to lead to changes in the initial tensile characteristics of the fibre (Jain and Vijayan, 2002).

Holland and Hay, 2000 found that the weight loss of Nylon 6,6 with time only followed first order kinetics over a short initial period. After this period, a pronounced curvature was observed. The authors attributed this to the formation of involatile char.

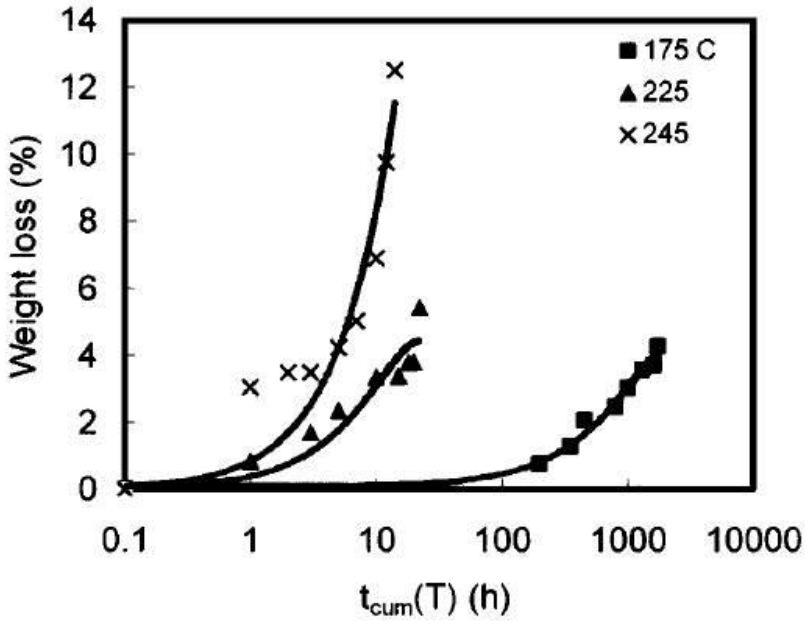

Fig 9: Weight loss (%) of Nylon 6,6 for various T and $t_{cum}(T)$ values (in air). (Jain and Vijayan, 2002)

It is worth noting that these data on weight loss (Figure 9) apply to thermal exposures carried out in air. Exposures in controlled atmospheres like nitrogen gas may be expected to alleviate the deterioration (Jain and Vijayan, 2002).

2.4 Thermo-mechanical Properties of Polymers:

The effects of heat also depend on the mechanical loading applied and the way a polymer reacts to the combination of heat and mechanical loading is known as the thermo-mechanical behaviour of the polymer. The general thermo-mechanical behaviour can be described broadly in terms of the two-phase structure which was mentioned before.

At very low temperatures the amorphous phase is in the glassy state, and therefore rigid. In addition, there may be significant inter-chain attractions (such as H-bonding or benzene ring interactions). The amorphous chain conformations are fixed because there is insufficient energy to permit rotation about the backbone covalent bonds. In this temperature range the stress-strain curve would be in effect a straight line, and the fibre brittle. As the temperature is increased, there is limited molecular mobility and some freedom of rotation about the single covalent bonds in the chains. However, H-bonding and/or other inter-chain forces remain active. These secondary bonds provide a mechanism for stress build-up as the structure is stretched. The fibre is therefore likely to exhibit moderate extensibility combined with a relatively high initial modulus. It will probably also yield, since the secondary bonds cannot extend far without rupturing. As they break, they tend to re-form in new positions, which stabilises the extension (and so impairs recovery) but also helps to maintain the stress as further strain is applied. Thus, the tenacity is expected to be quite high in this region of temperature. As the temperature is further increased, the H-bonds or other secondary forces

tend to dissociate. At high stresses crystal yielding may also take place (Morton and Hearle, 1993)

Dry isotropic Nylon 6,6 exhibits three relaxations at low frequency in the range of -180 to 160°C. The α relaxation is the most prominent and is associated with large-scale segmental motions in the amorphous phase which involve rupture of hydrogen bonds. The β relaxation is ascribed to the motions of non-hydrogen-bonded amide groups, while the γ process involves the local-mode motions of both $-CH_2-$ and amide groups (Leung et al., 1984).

2.5 Effect of Crystal Size and Size Distribution:

Crystalline solids consist of regular three-dimensional arrays of atoms. In polymers, the atoms are joined together by covalent bonds along the macromolecular chains. These chains pack together side-by-side and lie along one particular direction in the crystals. It is possible to specify the structure of any crystalline solid by defining a regular pattern of atoms that is repeated in the structure. This repeating unit is known as the "unit cell" and the crystals are made up of stacks of the cells. The spatial arrangement of the atoms is controlled by covalent bonding within a particular molecular segment, with the polymer segments held together in the crystals by secondary Van der Waals forces or hydrogen bonding. Since the polymer chains lie along one particular direction in the cell and there is only relatively weak secondary bonding between the molecules, the crystals have very anisotropic physical properties (Young and Lovell, 2011)

As Figure 10 shows, the observed melting point of a crystal is not an absolute temperature, but actually depends on its size and state of perfection. Both the overall crystallinity and the sizes (and distribution of

sizes) of crystallites depend on many factors such as chain flexibility and thermal history. Yongqiang et al., 2001 derived a relationship between the melting point and the size of crystals using the Kelvin equation. The size effect comes about because of the surface energy contribution to melting.

This is equivalent to the 'surface tension' at the interface between, say, a liquid and a vapour, or between one liquid and another. In the case of a polymer (fibre), the interface would typically be that between a crystallite and the amorphous phase. Although it is perhaps only a small component, it can nonetheless be significant if the crystal itself is very small, so that it has a large 'specific surface'. From the thermodynamics of melting, it can be shown that the observed melting point of a crystal ought to vary with its size (Yongqiang et al., 2001).

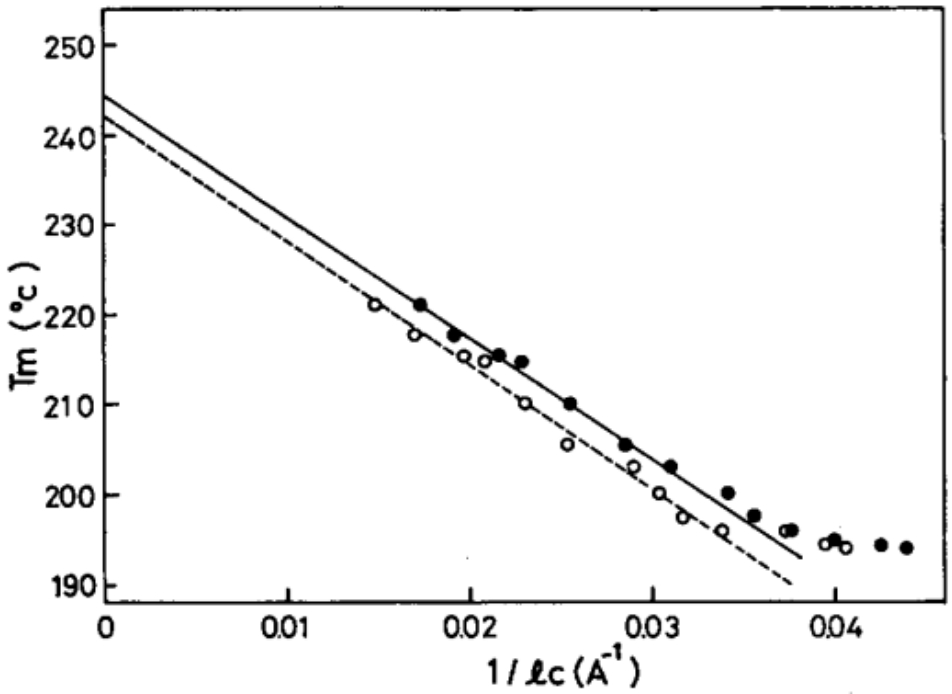

Fig 10: Relation of melting temperature (T_m) to the crystallite size in the direction of fibre axis for drawn Nylon 6 annealed at various temperatures between 150 and 215°C; ℓc calculated by using crystallinity values from (◦) the density and (•) the heat of fusion. (Arakawa et al., 1969)

In the case of metals, the observed melting point is always close to the theoretical value and a sharp melting peak would generally be obtained in, say, a differential scanning calorimetery analysis. This is certainly not the situation for polymers and fibres. There is likely to be a range of crystallite sizes present. The crystallite size distribution is in fact quite broad in most cases. Figure 11 shows the distribution for linear polyethylene.

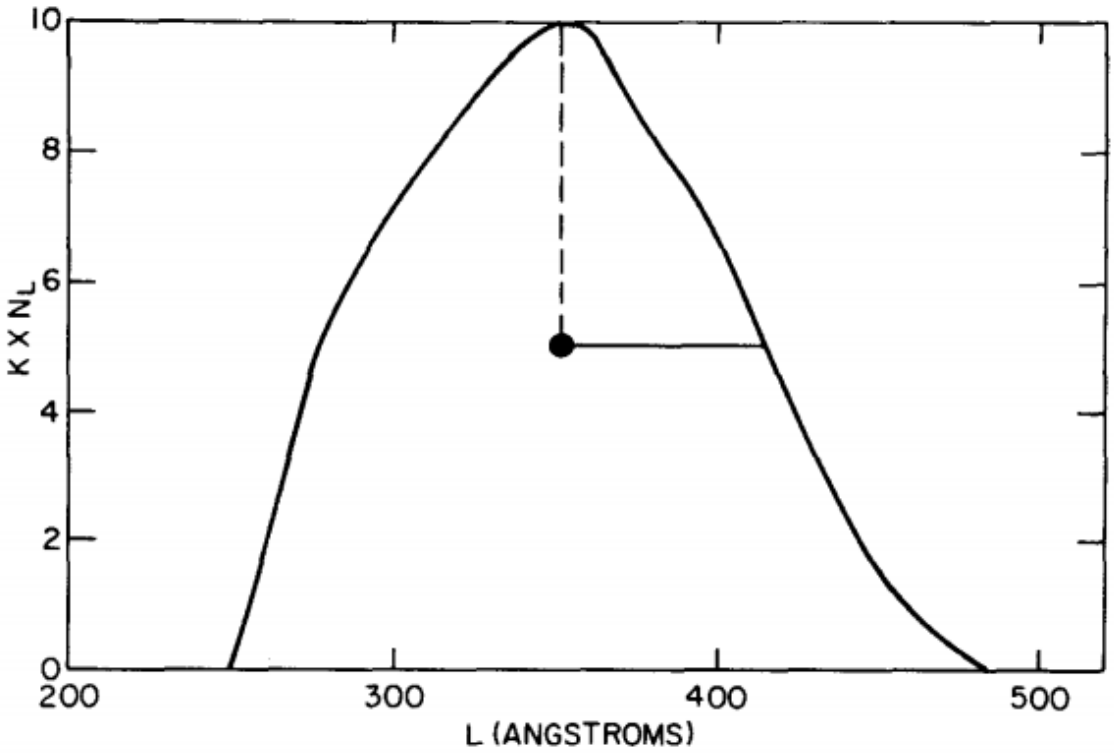

Fig 11: Plot of normalized number of ordered sequence lengths against length L in Angstroms. For fraction (M_W = 70,000, M_N = 65,000) crystallized at 126°C for 165 min. N_L is number of sequences of length L; K is normalization constant (Stack et al., 1982)

2.6 Melting of Polymers

The melting temperature range observed for a polymer depends on the thermal stability of the lamellae present in the sample, and to their

thickness distribution. Thickening of the lamellae with time isothermally or on heating makes the observed melting endotherms heating rate dependent and melting occurs over a wide range of temperature. It is common to observe multiple melting endotherms, crystallisation exotherms and shifts of the endotherm to higher temperatures with heating rate (Kong and Hay, 2002).

Highly viscous melts mean that polymer crystallisation is limited by kinetic rather than thermodynamic parameters. Due to dynamic chain entanglements not all of the molecular segments crystallise, defects are present in the crystals and the dimensions of the critical nuclei limit the lamellar crystal thickness. Accordingly these lamellae undergo reorganisation and progressive thickening on heating. The rate of heating and annealing alter the observed enthalpy of fusion and the temperature range over which melting is observed (Kong and Hay, 2002).

Elad and Schultz, 1984 reported that with isothermal heat treatment, the melting point of drawn Nylon 6,6 fibres increase, but only up to a certain level, at which point it starts to decrease. The authors explained this in terms of changes in crystal perfection and thickness, and changes in the melt state. As crystallites thicken and become more perfect, their net free energy decreases relative to the melt and hence the melting point increases. As the temperature is increased further, the tie-chains relax and the crystallites rotate. This causes the melt to become more random as the initial high melt orientation is no longer present. This increased melt entropy leads to a decrease in melting point as the melting point is inversely proportional to the entropy difference between crystal and melt (Elad and Schultz, 1984).

Unlike low molecular weight materials, polymer crystals melt over a wide range of temperature and the temperature dependence of the enthalpy of fusion cannot be neglected. The observed melting endotherms reflect the

thermal stability of the lamellae present as melting is approached and not in the initial sample prior to heating. The melting enthalpies are not comparable directly unless they are measured over the same temperature range (Kong and Hay, 2002).

While tests in the DSC are useful, they do not provide any information on the actual strength of the material. For this reference needs to be made to stress-strain curves and examine the relationship between stress and strain as a function of changes in temperature.

2.7 Tensile Properties of Polymers

Figure 12 shows the stress-strain curves of glass fibre reinforced Nylon 6,6 at different temperatures. Despite the fact that almost half of the compound is made up of the non-polymeric glass fibre, the shape of the stress-strain curve changes significantly. In general, strength and stiffness decrease with increasing temperature while elongation at break, a good relative indicator of ductility, increases (Sepe, 2011).

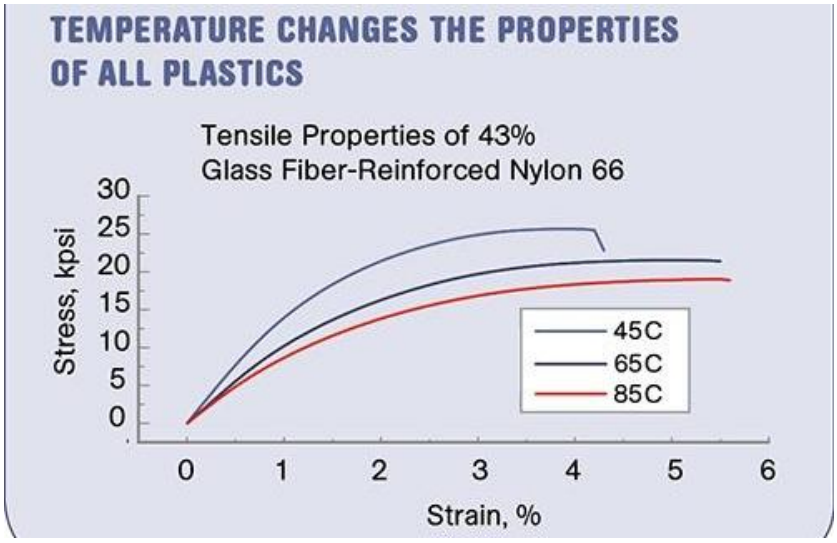

Fig 12: Stress-strain curves of 43% Glass Fibre reinforced Nylon 6,6 at different temperatures. (Sepe, 2011)

The tensile behaviour is however affected by many factors, including the degree of crystallinity and the amount of re-crystallisable material present in the sample. Bell, 1972 found that polymers with a greater ratio of non-re-crystallisable material to crystallisable material have greater ultimate tensile strength and lower elongation.

Tensile tests on heat treated Nylon 6,6 fibres have been carried out by Jain and Vijayan, 2002 and have demonstrated the effects of heat treatment on the tensile characteristics of the fibre. One thing to note here is that the heat treatment was done in air and in an isothermal environment.

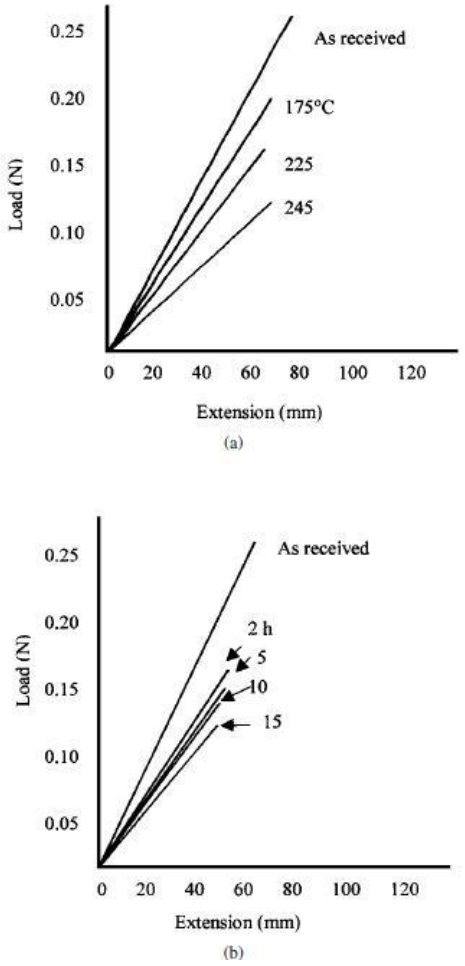

Fig 13: Typical load-extension curves recorded from individual Nylon 6,6 fibres prior to and after heat treatment. (a) As a function of T and (b) As a function of t_{cum} (T) at 225°C. (Jain and Vijayan, 2002)

Figure 13 (a) and (b) present the typical load-extension curves for Nylon 6,6 fibres. The former shows the effect of T [temperature] and in the latter, the role of $t_{cum}(T)$ [duration] for a constant T has been depicted. The progressive changes in the slope and the breaking load indicate that increase in temperature as well as $t_{cum}(T)$ lead to deterioration in the tensile modulus and strength respectively (Jain and Vijayan, 2002). This is due to the fact that the degree of orientation decreases with treatment time and the rate at which disorientation occurs increases with increasing temperature (Elad and Schultz, 1984).

Figure 14 (a), (b) and (c) shows the reductions in the tensile modulus, tensile strength and percentage elongation at break due to thermal-oxidation. Here, M_t^T, S_t^T, and ϵ_t^T represent the values of tensile modulus, strength and percentage elongation at break respectively for fibres exposed to temperature T for a duration of $t_{cum}(T)$. It may be noticed that after 800 h at 175°C, the tensile modulus and strength decrease by 40% and 70% respectively. At any stage of ageing at 175°C, the reduction in the tensile strength is noticeably more than the corresponding reduction in modulus. The preferential degradation of tensile strength suggests that the structural features connected with the tensile strength of the fibre deteriorate faster than those associated with the initial tensile modulus (Jain and Vijayan, 2002).

In contrast with the behaviour at 175°C, fibres aged at 225 and 245°C do not show such a preferential enhanced degradation in tensile strength. At these higher temperatures, both tensile modulus and strength appear to degrade by nearly equal amounts. The associated structural changes thus appear to occur simultaneously and perhaps in equal measures. As in the case of tensile strength and modulus, the percentage elongation at break (Figure 14c) also decreases with cumulative thermal exposure at any chosen temperature (Jain and Vijayan, 2002).

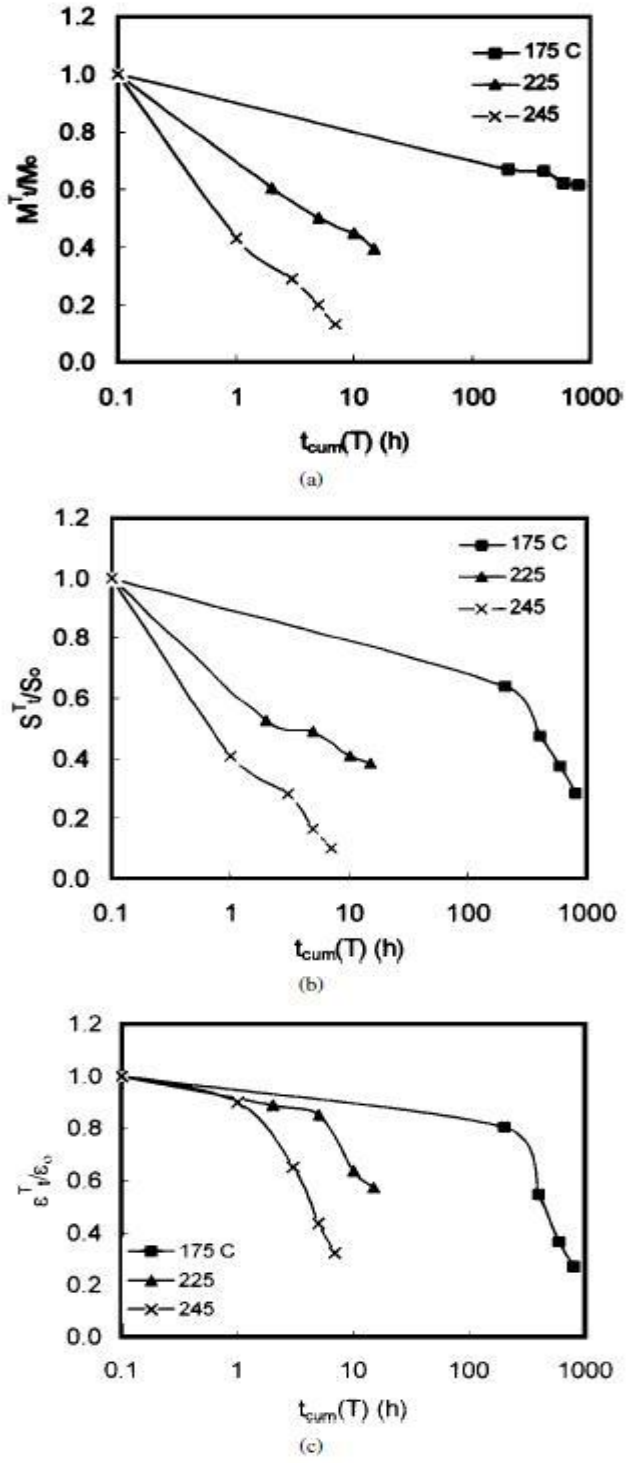

Fig 14 (a) Variation of M_t^T/M_o with t_{cum} (T) and T (b) Variation of S_t^T/S_o with t_{cum} (T) and T (c) Variation of ϵ_t^T/ϵ_o with t_{cum} (T) and T. (Jain and Vijayan, 2002)

2.8 X-ray Analysis of Semi-Crystalline Polymers:

Nylon-6,6 shows a crystal-to-crystal transition on heating, which is known as the Brill transition. The room-temperature triclinic structure transforms into a pseudo-hexagonal structure at elevated temperatures, and the transition is reversible. The nature of the Brill transition (T_B) is considered to be the effect of conformational motion due to temperature and is associated with a packing change within the crystal (Ramesh et al., 1994). The diffraction pattern of Nylon 6,6 obtained by the authors is shown in Figure 15.

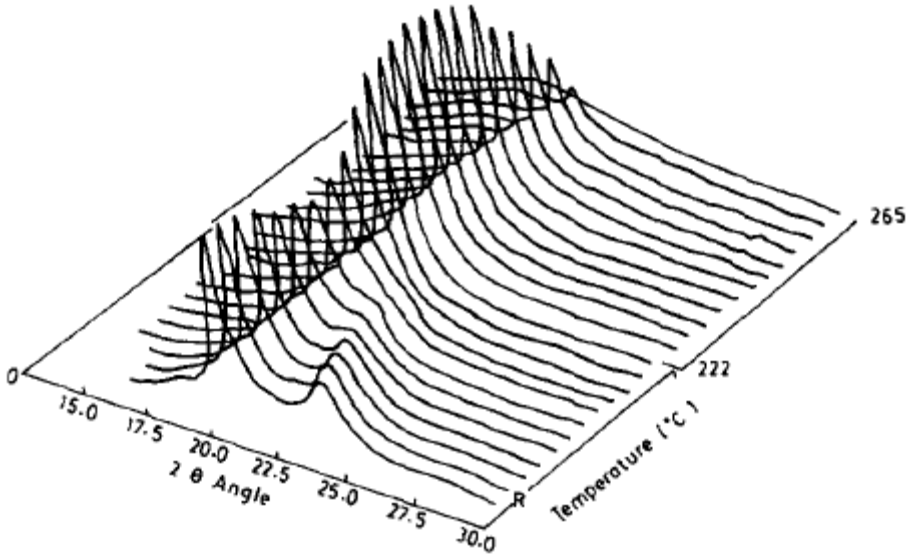

Fig 15: 3D view of the X-ray diffraction patterns of Nylon 6,6 on heating from room temperature to melting. (Ramesh et al., 1994)

From their work, Ramesh et al., 1994 concluded that crystallization from the melt takes place directly into the Brill structure, which then transforms at T_B into the triclinic structure on cooling to room temperature.

Jain and Vijayan, 2002 also carried out X-ray diffraction tests as shown in Figure 16. It was found that at each of the chosen temperatures, at some

stage of the prolonged thermal exposures, the intensities of reflections reach values where they are no longer observable above the background i.e., at this stage of thermal exposure, the sample has no crystalline fraction left to diffract.

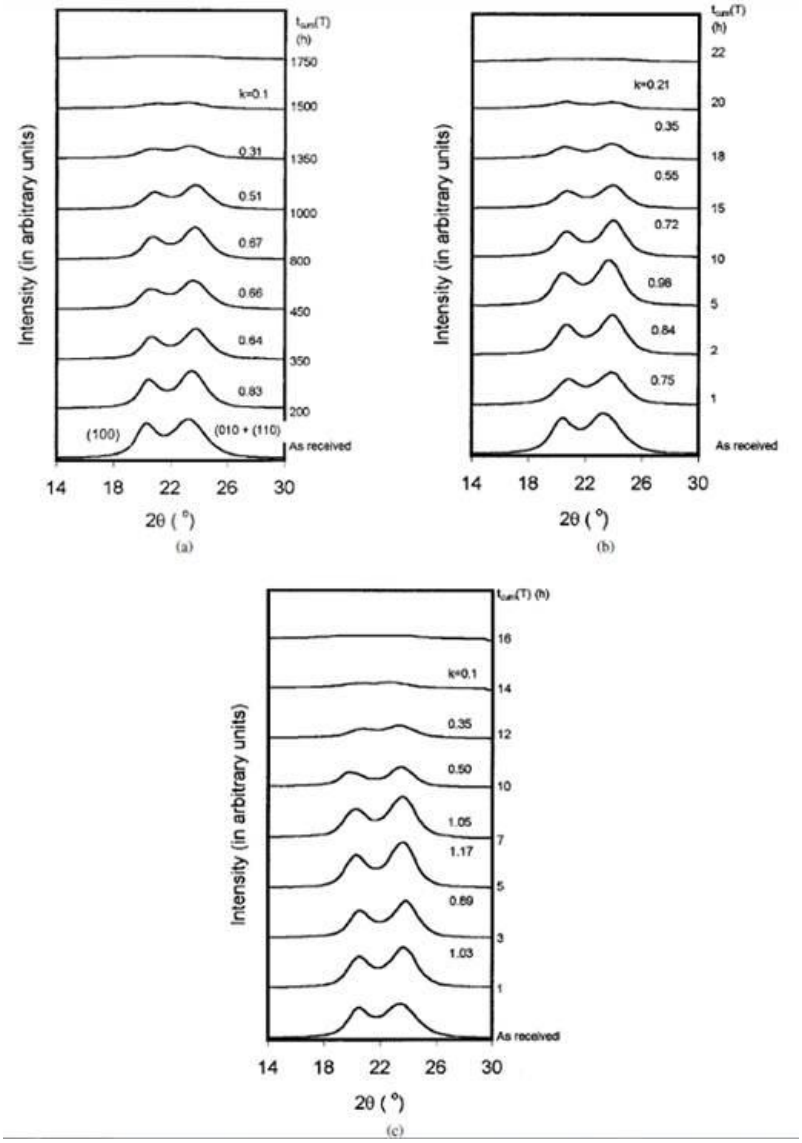

Fig 16 (a) X-ray diffraction profiles recorded prior to and at various stages of exposure to 175°C. (b) X-ray diffraction profiles recorded prior to and at various stages of exposure to 225°C. (c) X-ray diffraction profiles recorded prior to and at various stages of exposure to 245°C. (Jain and Vijayan, 2002)

This stage is referred to as the zero crystallinity state. The time needed for the 100% loss in crystallinity is referred to as t_{100}. It must be emphasized that the zero crystallinity state is reached as a result of cumulative exposure to a constant temperature. Jain and Vijayan, 2000 found that at 175, 225 and 275°C, 1750, 22 and 16h respectively of exposures are needed to reach the zero crystallinity state.

The authors' observations on the time dependent variations in relative intensities suggest that the first few thermal exposures of Nylon 6,6 cause changes in the atomic/molecular arrangement which in turn lead to changes in the relative intensities of the equatorial reflections. Subsequent exposures, however, cause progressive degradation and an eventual total loss in the crystallinity of the fibre.

Jain and Vijayan, 2002 presented the logarithmic variation of t_{100} with T. This is shown in Figure 17. Values of k depicting the progressive reduction and an eventual total loss in crystallinity have been marked in each set of the diffraction patterns in Figure 16. From these values, the time needed for 50% reduction in the initial crystallinity, t_{50}, has been derived and included in Figure 17.

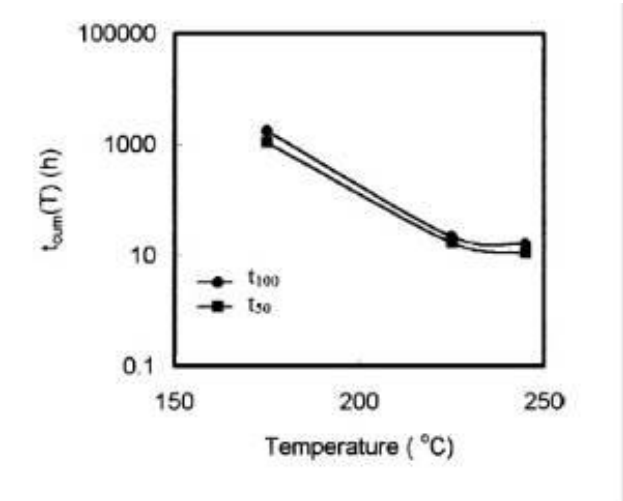

Figure 17: t_{100} and t_{50} vs. T. Here, t_{100} and t_{50} refer to the respective cumulative exposure time needed for 100 and 50% reduction in crystallinity. (Jain and Vijayan, 2002)

The parameters, t_{50} and t_{100} are useful because it allows to predict the duration of exposure which will cause any deterioration in the initial crystallinity, for a chosen T value (Jain and Vijayan, 2002).

2.9 Shrinkage and Change in Diameter:

In general, fibre shrinkage due to heat can be attributed to 2 processes: disorientation of the crystallites, and the transformation of the oriented amorphous chains into folded chain crystals (Murthy, 1997).

Emri et al., 2006 described a procedure of obtaining real time shrinkage results, using a special chamber, thermocouples and a thermal camera. The procedure allowed to accurately monitor the temperature and the heating rate.

The authors used their equipment to analyse the shrinkage of two different fibres, PA6 and PA66, undergoing the same thermal treatment. There were two clear observations. First, the total shrinkage of the two fibres is significantly different; however this effect may also be observed using a standard method of testing. Second, the rate of shrinking is dissimilar, which indicates that the effect of temperature on inherent structural changes in fibres must be different.

Since shrinkage is related to the inherent structure of the fibre, study of the shrinkage dynamics may provide insights into fibre structure and may be used in the process of material development and spinning process optimization.

Hou et al., 2008 carried out shrinkage tests on polyacrylonitrile (PAN) fibres. The PAN fibres undergo characteristic shrinkage during heating due to cyclization and cross-linking reactions. The shrinkage consists of two

categories: physical shrinkage (due to the relaxation of molecular chains) and chemical shrinkage (due to breaking of chains or possibly the formation of cross-links), or initial shrinkage and secondary shrinkage.

The authors observed that the physical shrinkage is not largely affected by the heating rate. In comparison, the amount of chemical shrinkage and the total amount of shrinkage fall off sharply and then increase rapidly, showing the least shrinkage at 5°C/min. The results are shown in Figure 18.

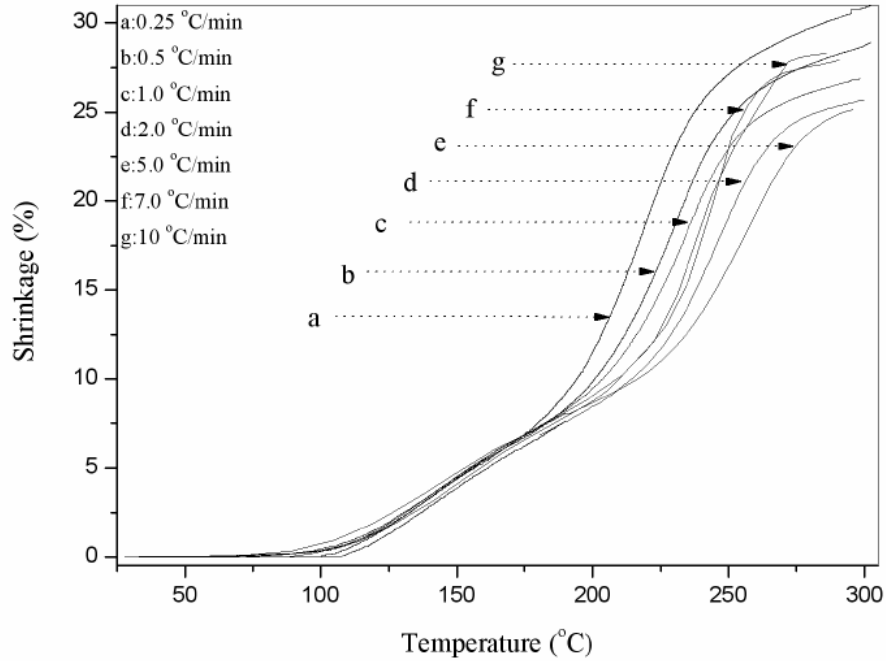

Fig 18: Shrinkage (%) of PAN fibres at different heating rates (Hou et al., 2008)

At heating rates lower than 5°C/min, the intra-molecular cyclization was the main reaction and the extent would decrease with the increase in heating rates. Above 5°C/min, an intermolecular cross-linking reaction also became obvious and the extent would increase with the increase in heating rate (Hou et al., 2008).

Zhang et al., 2012 carried out heat treatment experiments on PSU (polysulfone) electrospun nanofibrous membrane. The authors have

shown that under relaxation heating (no tension), the fibre diameter increases with an increase in heat treatment temperature. However, under tension heating, the fibre diameter decreases with an increase in heat treatment temperature. This is shown in Figure 19.

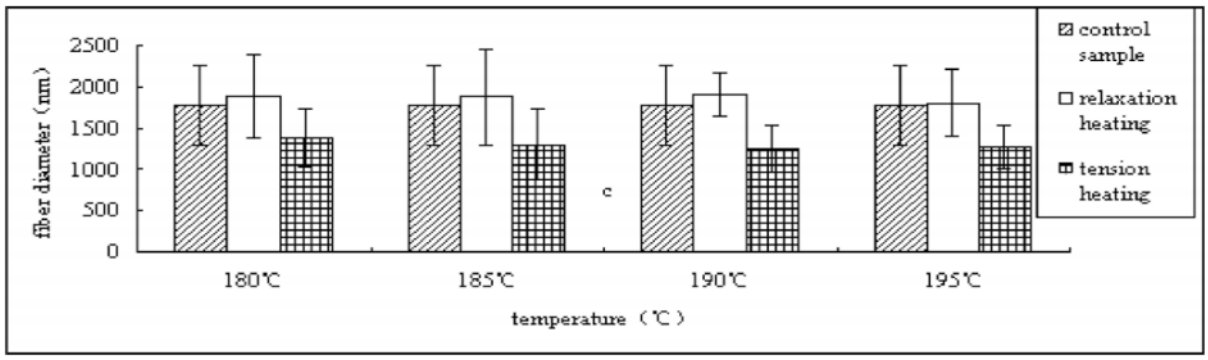

Fig 19: Diameter distributions of PSU electrospun fibres (Zhang et al., 2012)

When in the relaxation state, the molecular chains tended to stay in a stable state with minimum energy; thus the PSU fibre shrank, but due to the restrain of the cross-link entanglement between fibres, the shrunk fibre bends to form a curve at the same time. When the membrane was held by the clamps, the molecular chains would stretch and rearrangement along the direction of the external force would take place under the effect both of heat and tension, and gave rise to both the enhancement in the structural density of the internal fibres and the decrease in the fibre diameter (Zhang et al., 2012).

During relaxation heating, the movement of the molecules caused the internal stress of the fibre to relax, therefore the fibre tended to shrink and curve lengthways, and swell in the radial direction, which appeared as shrinkage in membrane size and an increase in membrane thickness at the macroscopic level. For the tension heating, the molecules would rearrange along the direction of the external force and reach a new stable state for the fibre structure, and this will also restrain the curvature (Zhang et al., 2012).

Chapter 3: Experimental Work

This section explains the experimental studies conducted in order to understand the effects of heat on airbag fibres and fabrics. Experimental studies include thermal tests, X-ray diffraction, shrinkage and diameter tests, and tensile tests.

3.1 Thermal Study

Thermal tests were conducted at both fibre and fabric level using two techniques:

1. Differential Scanning Calorimetry (DSC)
2. Dynamic Mechanical Analysis (DMA)

These two techniques will now be explained in more detail along with the experimental procedures used.

3.11 Differential Scanning Calorimetry (DSC)

Differential Scanning Calorimetry, or DSC, is a thermal analysis technique that looks at how a material's *heat capacity (Cp)* is changed by temperature. A sample of known mass is heated or cooled and the changes in its heat capacity are tracked as changes in the heat flow. This allows the detection of transitions like melting, glass transitions, phase changes, and curing.

As heat capacity increases with temperature, the DSC reading of a sample should show a slight upward slope toward higher temperature as well as a step change in the baseline across the melt as the heat capacity of a

molten material is higher than that of a solid. This allows easy determination of the melting temperature of a fibre.

Change in heat capacity is also important in determining the glass transition of the polymeric fibre. In amorphous and semi-crystalline polymer of any type – synthetic polymers like polypropylene and polystyrene, natural polymers like rubber, or biological polymers like proteins – the glass transition is the best indicator of material properties. As the glass transition changes due to either different degrees of polymerization or modification by additives, the physical properties of the material change. Similarly, material properties also change dramatically above the T_g. For example, materials lose their stiffness and flow as is the case in molten glass and their permeability to gases increases dramatically.

3.111 Types of DSC

There are 2 classes of DSC which differ in terms of their design and operation as shown in Figure 19.

1. Power-compensation DSC
2. Heat-flux DSC

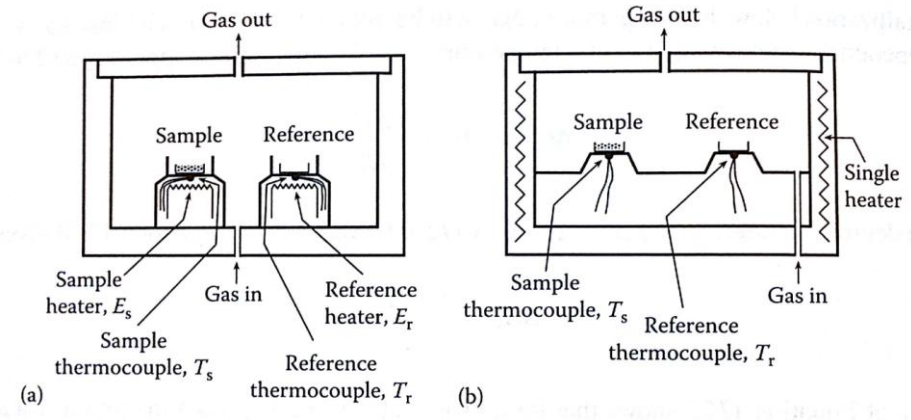

Fig 19: (a) Power-Compensation DSC (b) Heat-Flux DSC (Source: Young and Lovell, 2011)

In power-compensation DSC, the sample and inert reference material are independently heated (or cooled) at a controlled rate in adjacent, separate cells whilst simultaneously recording their temperature. The difference in heat input to keep the sample and the reference at exactly the same temperature is monitored. In heat-flux DSC, the sample and inert reference material are heated (or cooled) at a controlled rate side by side in a single cell. The temperature difference between them is recorded simultaneously. The test methodology for both types is very similar. Typical data obtained from both types of DSC is shown in Figure 20.

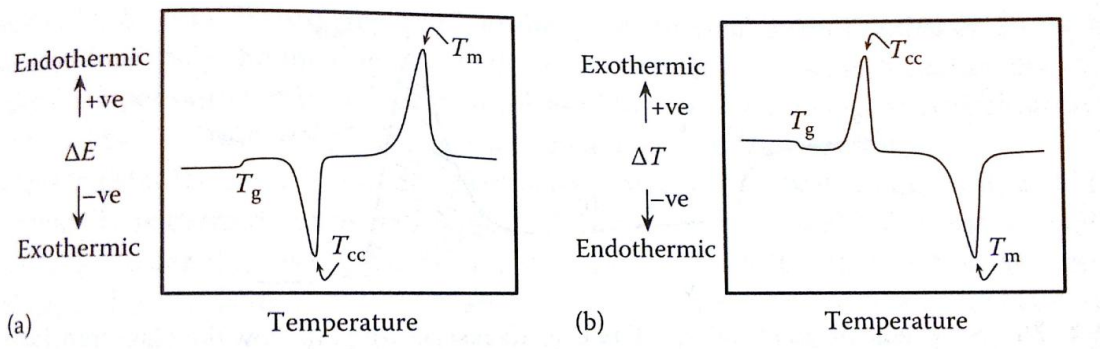

Fig 20: (a) Typical curve obtained from Power-Compensation DSC (b) Typical curve obtained from Heat-Flux DSC (Source: Young and Lovell, 2011)

3.112 Test Methodology

DSC tests were conducted at fibre level using PA66 yarns used to manufacture airbags. The unheated yarn was separated into fibres and a bundle of fibre was used to carry out the test.

An empty DSC pan was then weighed. The fibre bundle was placed inside the pan and weighed again. The difference between the two gave the mass of the fibres being used. Once the fibre mass was measured, a lid was placed on the pan and the pan was sealed.

The DSC was then switched on. Nitrogen was used as the purge gas at a flow rate of 20 ml/min. But before the sample pan was placed in the DSC, a sealed empty pan was run in the DSC. The empty pan data would later act as baseline data to be deducted from the sample data to give a more accurate result.

Once the pans were placed inside the furnace and the furnace cover was closed, the DSC software was started. The software allowed all the information about the sample to be added and to set up the program. The program was set to go from 30°C to 300°C at 10°C/min. This heating step showed a melting peak, from which information on the crystallinity of the fibre at the melting temperature could be found out.

The same procedure was repeated for 2 other heating rates, 100 and 300°C/min. This was done to check if the heating rate had an effect on the DSC results.

The DSC had to be calibrated each time a different heating rate was used. Indium and Zinc standards were used for the calibration. Once calibrations were done for the three heating rates, it was just a matter of choosing the right calibration file for the relevant heating rate. Apart from calibration, all other procedures were exactly the same.

These tests were conducted on unheated yarn samples. But to understand the effect of heat, the same tests needed to be carried out on heated samples. As the main objective was to understand what happens in airbag deployment, the temperature used to heat the yarn had to be very high and the exposure time had to be very low, as the temperature seen in airbag deployment reaches about 900°C and the blast only lasts for about 20ms.

It was clear that these extreme parameters were not possible to duplicate manually on a single yarn. A heat gun which could reach a maximum temperature of 600°C, was used to heat the yarn. As the temperature and pressure of the hot air gun was lower than that in actual airbag deployment, a higher exposure time was used. An exposure time of 45s was used. This high exposure time also ensured even heating of the yarn.

Different experimental set ups were tried, but in the end manual heating of a bundle of yarns tied to a tile showed the most consistent results. As shown in Figure 21, the bundle of yarns was heated with the hot air gun by hand. To record the temperature on the surface of the yarn, a fine thermocouple was placed in the middle of the bundle of yarn. The thermocouple was connected to a computer and the software recorded the temperature in real time. To ensure that the yarns experienced the maximum possible temperature from the start of the heating procedure, the heat gun was run for 30 seconds at maximum temperature pointing away from the yarns. Once the maximum temperature was reached, the heat gun was positioned 5cm above the bundle of yarns. Although the heat gun had a maximum temperature of 600°C, the maximum temperature on the surface of the yarns recorded by the thermocouple was 500°C.

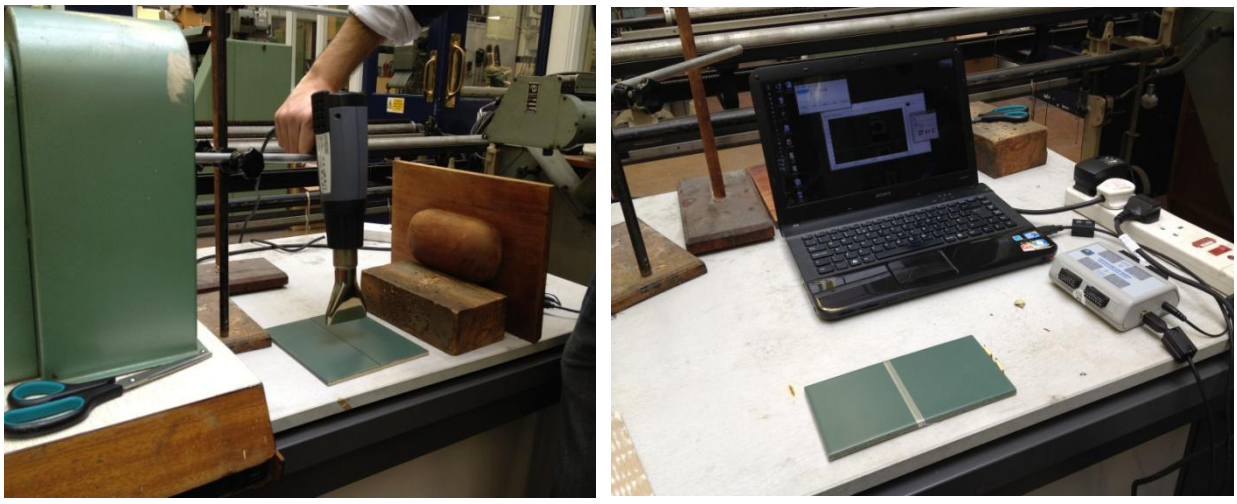

Fig 21: The experimental set up for heating yarn samples.

After the yarn bundle was heated, fibres from the yarn were extracted and tested in the DSC using the same procedure as the unheated yarn samples.

The DSC results from the heated and unheated yarn samples were compiled and the differences in Delta H calculated.

A notable difference was seen in the delta H values for different heating rates. This difference led to the thinking that if different heating rates have an effect on the Delta H value, the way the sample cools should also have an effect on the Delta H value. Hence, tests were carried out at different cooling rates, but keeping the heating rate constant.

This was done by initially heating the sample from 30°C to 300°C at 10°C/min, and then cooling the sample very slowly (5°C/min) back to 30°C. This was followed by another heating step to 300°C, keeping the heating rate constant at 10°c/min, followed by a faster cooling step (10°C /min). This was repeated for a few more steps to get the data for different cooling rates (5, 10, 20, 50, 100, 200, 300, 400, 500 and 600°C/min). It is worth mentioning that different cooling rates do not need different calibrations. A single calibration (associated with the heating rate) was used.

For DSC tests at fabric level, two airbags were provided by Autoliv. Of these two airbags, one was unfired and the other was fired (deployed) as shown in Figure 22.

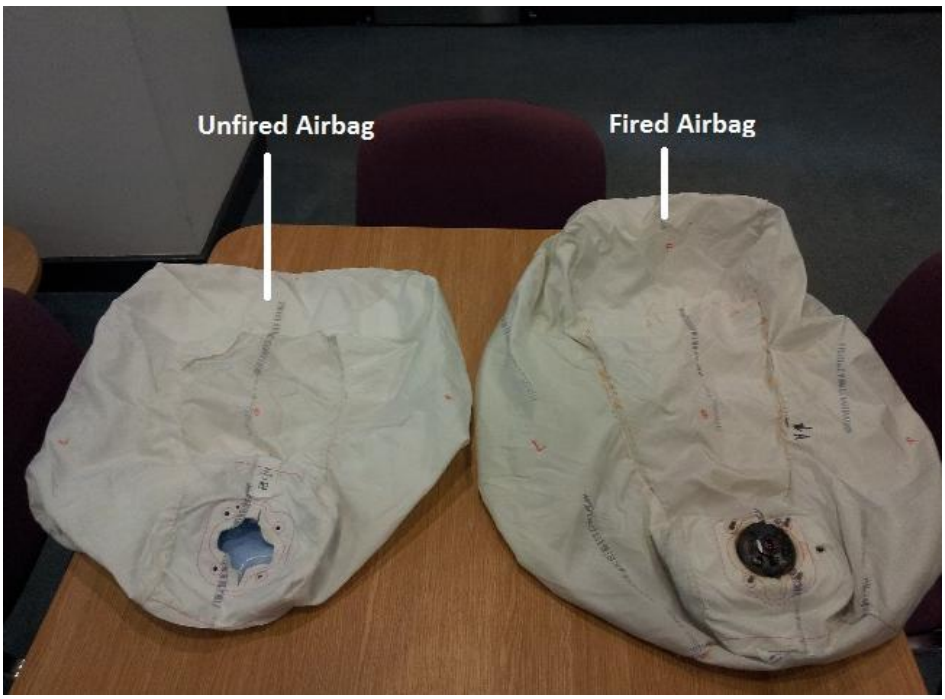

Fig 22: Unfired and fired airbags.

The main aim of tests at fabric level was to understand the effects of heat on particular areas of the bag. Hence, the bags were cut into sections. Figure 23 shows the right panel of both the unfired and fired airbags. Tests conducted on fabric from this panel would help understand the effect on heat specifically on the right panel of the airbag.

Fig 23: Right side panel of fired and unfired airbags

However, this study went into more detail and divided the panel into sections to understand the effects on a particular area inside a particular panel. For the right panel for example, 2 sections were made as shown in Figure 24.

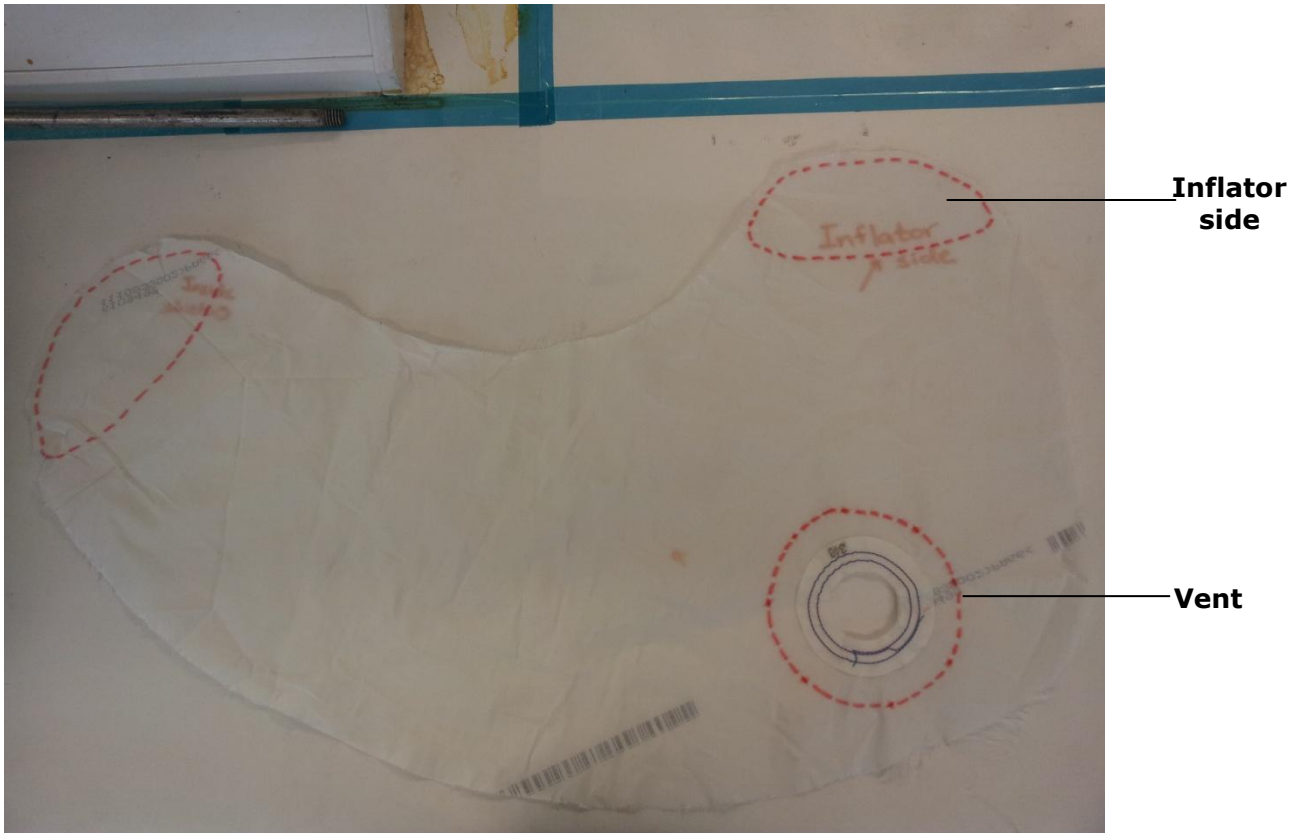

Fig 24: 2 zones, inflator side (top) and vent (bottom) marked on the fired panel.

Fabric samples were prepared in a similar way to fibre samples and tested in the DSC using the same temperature range of 30°C to 300°C at 300°C/min. The differences in Delta H for unfired and fired airbag fabric from a particular region inside the right panel were calculated.

3.12 Dynamic Mechanical Analysis:

Dynamic Mechanical Analysis, otherwise known as DMA, is a technique where a small deformation is applied to a sample in a cyclic manner. This allows the materials response to stress, temperature, frequency and other values to be studied. The term is also used to refer to the analyser that performs the test. DMA is also called DMTA for Dynamic Mechanical Thermal Analysis.

3.121 Working Principle of DMA

DMA works by applying a sinusoidal deformation to a sample of known geometry. The sample can be subjected by a controlled stress or a controlled strain. For a known stress, the sample will then deform a certain amount. In DMA this is done sinusoidally. How much it deforms is related to its stiffness. A force motor is used to generate the sinusoidal wave and this is transmitted to the sample via a drive shaft.

3.122 Measurements Taken Using DMA

DMA measures stiffness and damping, these are reported as modulus and tan delta. The modulus can be expressed as an in-phase component, the storage modulus, and an out of phase component, the loss modulus. The storage modulus, either E’ or G’, is the measure of the sample’s elastic behaviour. The ratio of the loss to the storage is the tan delta and is often called damping. It is a measure of the energy dissipation of a material. Modulus values change with temperature and transitions in materials can be seen as changes in the E’ or tan delta curves. This includes not only the glass transition and the crystalline melting, but also other secondary transitions that occur in the glassy or rubbery plateau.

3.123 Test Methodology:

The same Nylon yarn sample which was provided by Autoliv and used for the DSC tests was used again for the DMA tests. One end of the unheated yarn was clamped inside the upper jaw of the DMA. The other end of the yarn was pulled through the lower jaw and a slight tension was applied manually to ensure the yarn is not slack. The lower jaw was then closed. This set up is shown in Figure 25.

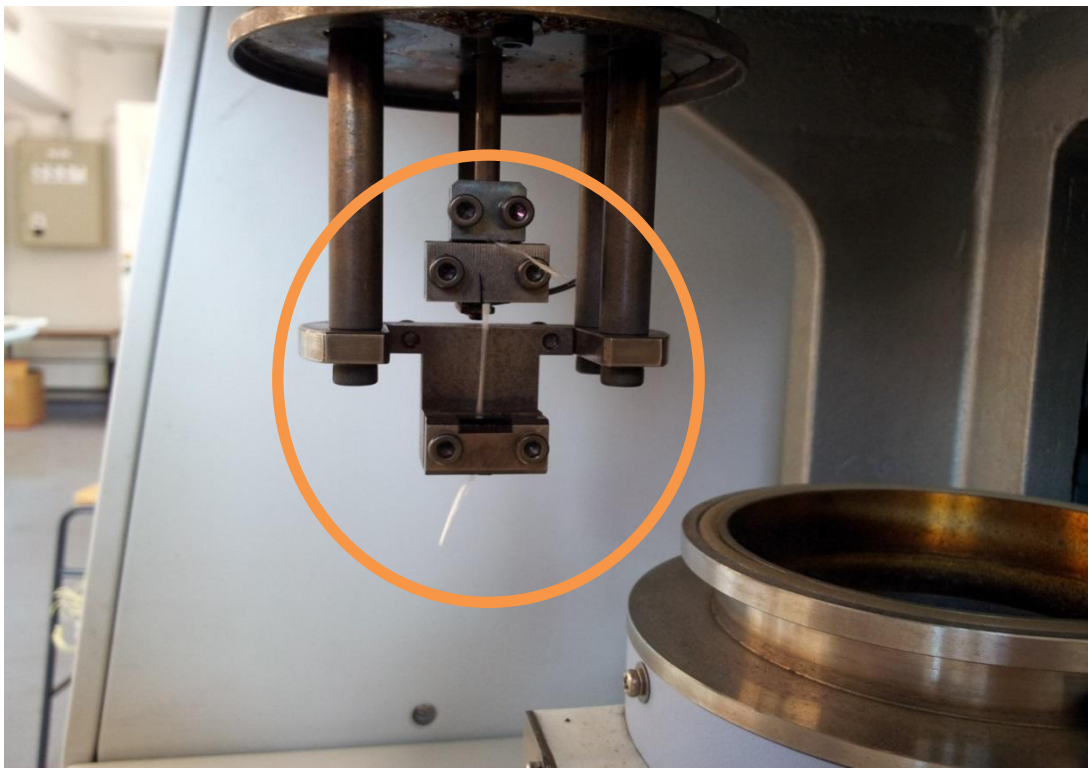

Fig 25: Nylon yarn sample clamped between the upper and lower jaws inside the DMA.

In the beginning it was not clear as to whether the test should be carried out using a single fibre or a whole yarn. Hence, both were tried out to see which gives the most consistent results. The yarn sample was mounted as shown in Figure 25. A single fibre is so thin that it is not possible to mount it on the DMA directly. Therefore, to mount a single fibre, a whole yarn was first mounted as in Figure 25. However, the top and the bottom

jaws were clamped a bit loose. A sharp pin was then used to separate fibres from the yarn until there was just a single fibre on one side of the pin and the rest of the fibres on the other side. Scissors were used to cut the portion with the rest of the fibres. Because the yarn was not clamped tightly, the fibres that were cut could be pulled out from above the top jaw and from beneath the bottom jaw, leaving just the single fibre. The fibre was then clamped tightly. From the results obtained it was clear that using a single fibre was not right as the fibre tends to slip between the jaws.

Once the sample was clamped, the furnace cover was closed and the software which controls the DMA was started. The software allowed the user to input a number of variables including frequency, starting temperature, end temperature and heating rate. The frequency was set at 1Hz. The starting temperature was set at 30°C and the end temperature was set at 300°C. The heating rate was set at 10°C/min.

From the results it was not quite clear if the drop in modulus in the glass transition region started below or above 30°C. Hence, a few tests were carried out using a starting temperature of -50°C. This sub-zero temperature ensured that the starting point of the drop in modulus was clearly identified. To get the temperature down to -50°C, liquid nitrogen was used.

In an actual airbag deployment, the heating rate is very high. In order to understand what happens in an actual deployment scenario, a few DMA tests were run at very high heating rates (up to 300°C/min). However, from the results it was very clear that it was not possible to get reliable results using this high rate because the number of readings that the software takes cannot cope with the high heating rate used. Hence, it does not give a smooth curve, which makes it impossible to determine the loss in modulus due to glass transition and melting.

It was evident that DMA tests were best carried out at low heating rates as they give the most accurate and reliable results. Therefore, DMA tests were carried out from -50°C to 300°C at 2°C/min.

3.2 Tensile Tests

Tensile tests were carried out on Nylon 6,6 fibres to find out the change in tensile properties due to heat exposure. First, unheated fibre samples were tested. A paper frame as shown in Figure 26 was used to secure a single fibre. This was then mounted on the tensile tester, and the two sides of the frame were cut as shown in Figure 26. A gauge length of 25mm was used.

Once this was done, heated fibre samples were tested. For this, a bundle of Nylon fibres was placed inside an airbag and the airbag was fired so that the heat exposure on the fibres would resemble the heat exposure on a deployed airbag. The fibres were mounted on the frame and tested on the tensile tester in the same way as with the unheated fibres.

Although heating in this way resembles actual deployment conditions, the heating itself is uncontrolled and there is no way of knowing the rate of heating or even the temperature which the fibre goes up to. For this, another batch of fibres was heated, this time using the DSC. Using the DSC to heat up the fibres ensures controlled conditions.

Two different heating rates were used 10°C/min and 300°C/min. The reason for using two different heating rates was to see if the heating rate influenced the tensile characteristics or was it only the final temperature which influenced it. Two different end temperatures (210°C and 230°C) were used. The end temperature was kept below the melting point to avoid complete decomposition of the fibre.

Once the fibres were heated, the DSC pan was cut and the fibres taken out. The fibres were then mounted on paper frames and tested on the tensile tester in the same way as before.

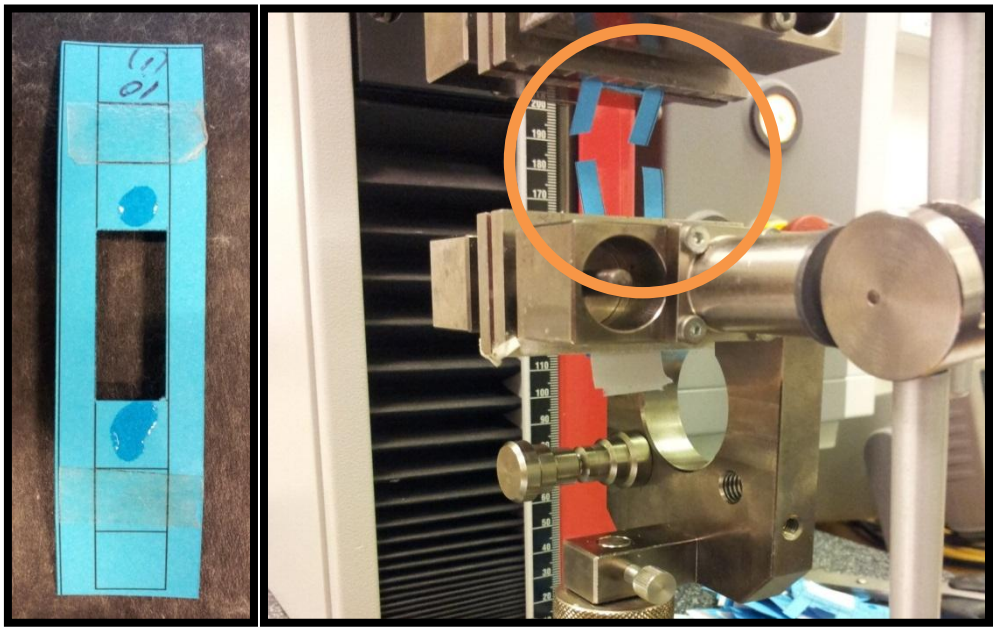

Fig 26: (a) Single fibre glued to a paper frame. (b) Paper frame with single fibre mounted on a tensile tester and sides cut off.

These tests were followed by cycling tests on the tensile tester. Virgin fibres were taken to a strain of 15% and heated fibres were taken to a strain of 20% (because the fibres had increased elongation properties after being exposed to heat) and allowed to recover. The strain at zero force was then measured.

3.3 Wide-angle X-ray scattering (WAXS)

Wide-angle X-ray diffraction is another way of determining the degree of crystallinity. Figure 27 shows a typical WAXS curve for a semi-crystalline polymer. The Y-axis is "intensity", i.e. the number of photons detected and the X-axis is the angle at which the X-ray hits the sample.

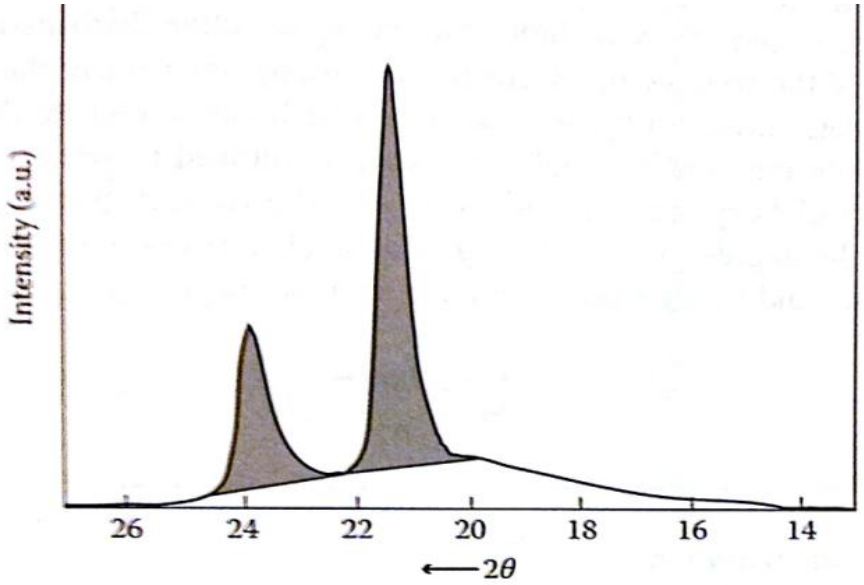

Fig 27: Typical WAXS curve for a semi-crystalline polymer (Source: Young and Lovell, 2011)

The peaks are due to scattering from the crystalline regions and the broad underlying base, also known as the "halo" is due to scattering from non-crystalline or amorphous areas.

The degree of crystallinity can be calculated from the relative areas under the crystalline peaks (shown shaded) and the amorphous halo.

$$X_c = A_c / (A_c + A_a)$$

where,

X_c = degree of crystallinity

A_c = area under the crystalline peaks

A_a = area under the amorphous halo

For WAXS on airbag material, yarn samples were wrapped on a frame and place inside the instrument as shown in Figure 28. The arm on the left fires X-ray at the sample at different angles and the right arm collect the scattered X-ray.

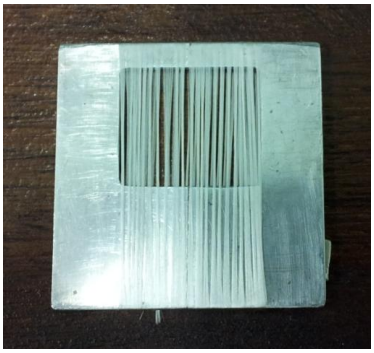

Fig 28 (a): Sample prepared for X-ray diffraction.

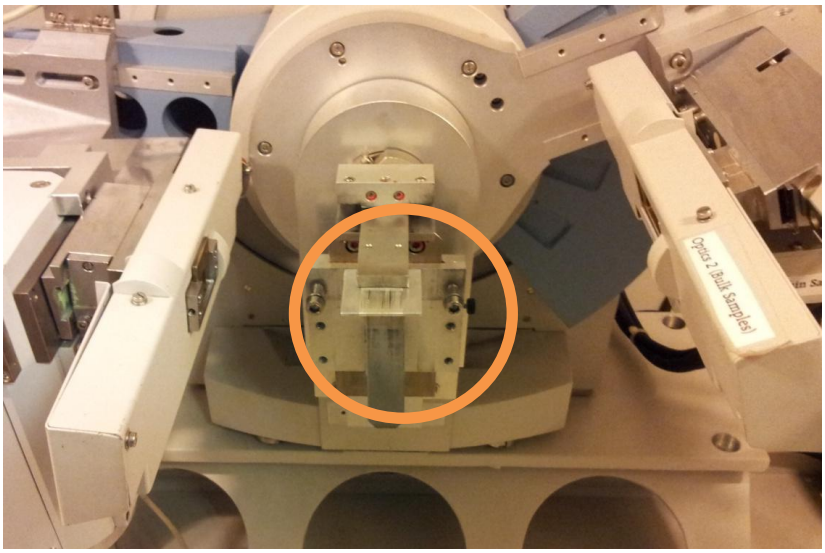

Fig 28 (b): Sample being fired with X-ray.

The same test was repeated with fabric taken from the vent and inflator side of fired and unfired airbags.

3.4 Shrinkage

The fibre structure consists, in principle, of three distinct components: viscoelastic plastically deformed long chains, the crystalline phase and the remaining amorphous phase. The shrinking of fibres is a consequence of the frozen-in elastic deformation of long chains, which is released upon heating the fibre.

Fibre shrinkage is normally used as one of the criteria to characterise fibre performance. The amount of fibre shrinkage depends on both the material, from which it was made, and the processing technology.

In most cases, measurement of shrinkage consists of measuring the initial length of the fibre, exposing the fibre to boiling water or hot air for certain period of time, without taking into account the rate of temperature change, and afterwards measuring the final length. From the change in length the magnitude of shrinkage is then obtained.

Experimental Procedure (Heating in an oven):

1. For fibres, loose yarns 7cm in length were heated in an oven at 220°C for 15 minutes. After heating, the length was measured again using a ruler and the difference calculated.
2. For fabrics, square pieces of fabrics (7cm x 7cm) [Figure 29] were heated in an oven at 220°C for 15 minutes. After heating, the lengths in the warp and weft directions were measured again using a ruler and the difference calculated.

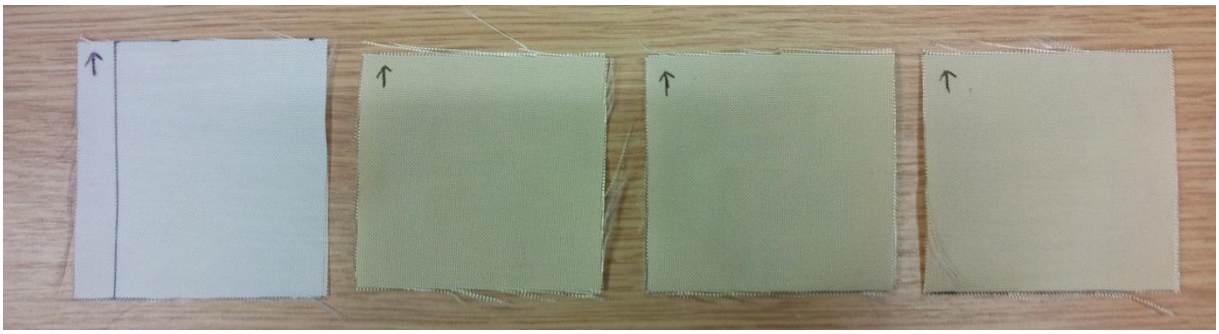

Fig 29 (a): Unheated and 3 heated samples with an arrow indicating warp direction

Fig 29 (b): Unheated and heated samples placed on top of each other with the arrow indicating warp direction.

While tests such as these are sufficient for monitoring shrinkage, they do not take into account the rate of heating. To understand how shrinkage varies at different temperatures and different heating rates, another set of tests were done using the DSC to heat the samples. The DSC allowed a controlled heating environment with the scope of using different heating rates.

Experimental Procedure (Heating in DSC):

1. A small length of a fibre bundle was placed inside the DSC pan. The length of this fibre bundle was measured using an optical microscope at 10x magnification.
2. The pan was sealed and heated in the DSC from 30°C to 210°C at 10°C/min.
3. The pan was taken out and the edges cut to expose the heated fibre sample.
4. The length of the heated sample was then measured using the optical microscope at 10x magnification (Figure 30).

5. The same process was repeated 3 times using 3 different DSC pans and the average values were taken.
6. This test was repeated at different test conditions, i.e. 210°C at 300°C/min, 230°C at 10°C/min and 230°C at 300°C/min.

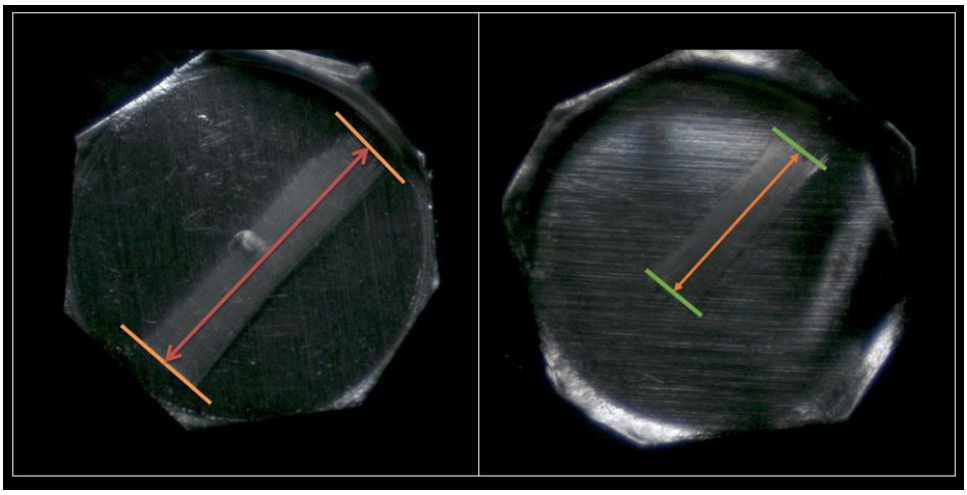

Fig 30: Image from the optical microscope showing the length of fibre bundle inside a DSC pan (before and after heating).

3.5 Change in Diameter

Just like shrinkage, fibre diameter is also used as one of the criteria to characterise fibre performance. Fibre diameter changes with heat, and hence tests were conducted to find out how exactly it changes with heat. The tests were conducted by heating yarn samples in oven and also in the DSC as with the shrinkage tests. The exact procedure is given below.

Experimental Procedure (Heating in an oven):

1. A single fibre was extracted from an unheated yarn of 7cm in length. The diameter of the fibre (outer wall-outer wall) was measured using an optical microscope at 400x magnification.

2. The first test was conducted by heating loose yarns of 7cm in length, in an oven at 220°C for 15 minutes. The procedure followed was the same as for the shrinkage test.
3. After heating, a single fibre was extracted from the yarn and placed under the optical microscope at 400x magnification and the diameter of the fibre (outer wall-outer wall) was measured.
4. This same test was done by extracting more fibres from the same heated yarn and the average was taken.

Experimental Procedure (Heating in DSC):

1. A single fibre was extracted from an unheated yarn of 7cm in length. The diameter of the fibre (outer wall-outer wall) was measured using an optical microscope at 400x magnification.
2. A small length of a fibre bundle was placed inside the DSC pan. The pan was sealed and heated in the DSC from 30°C to 210°C at 10°C/min.
3. The pan was taken out and a single fibre was extracted from the fibre bundle and placed under an optical microscope.
4. The diameter of the heated sample (outer wall-outer wall) was then measured using the optical microscope at 400x magnification (Figure 31).
5. The same process was repeated 9 times (taking random fibres from 3 heated DSC pans) and the average values were taken.
6. This test was repeated at different test conditions, i.e. 210°C at 300°C/min, 230°C at 10°C/min and 230°C at 300°C/min.

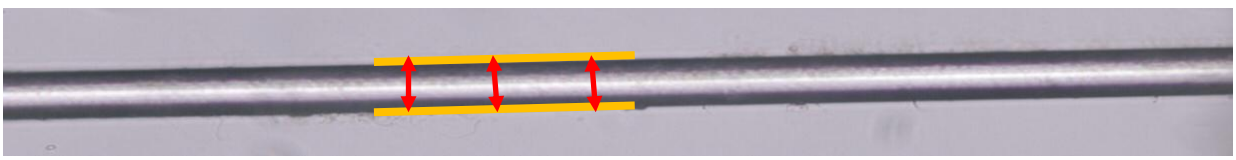

Fig 31: Single PA66 fibre under the optical microscope at 400x magnification.

Chapter 4: Results and Discussion

This chapter includes all the results from the experimental work described in the previous chapter. The chapter also includes detailed discussions and explanations of the results obtained.

4.1 DSC

The DSC heating curve shows the effect of heat on the fibre in the as-received state. The peak value of the curve in Figure 32 shows the temperature at which the polymer melts completely and the area under the curve gives the enthalpy of melting, or Delta H.

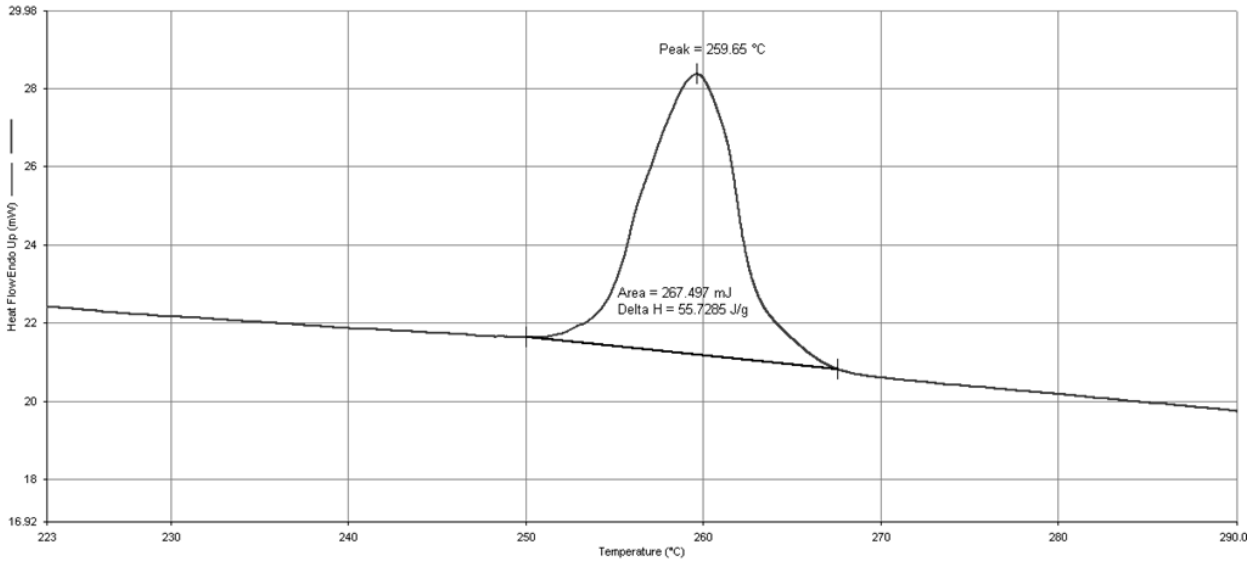

Fig 32: The scaled up version of the first heating curve.

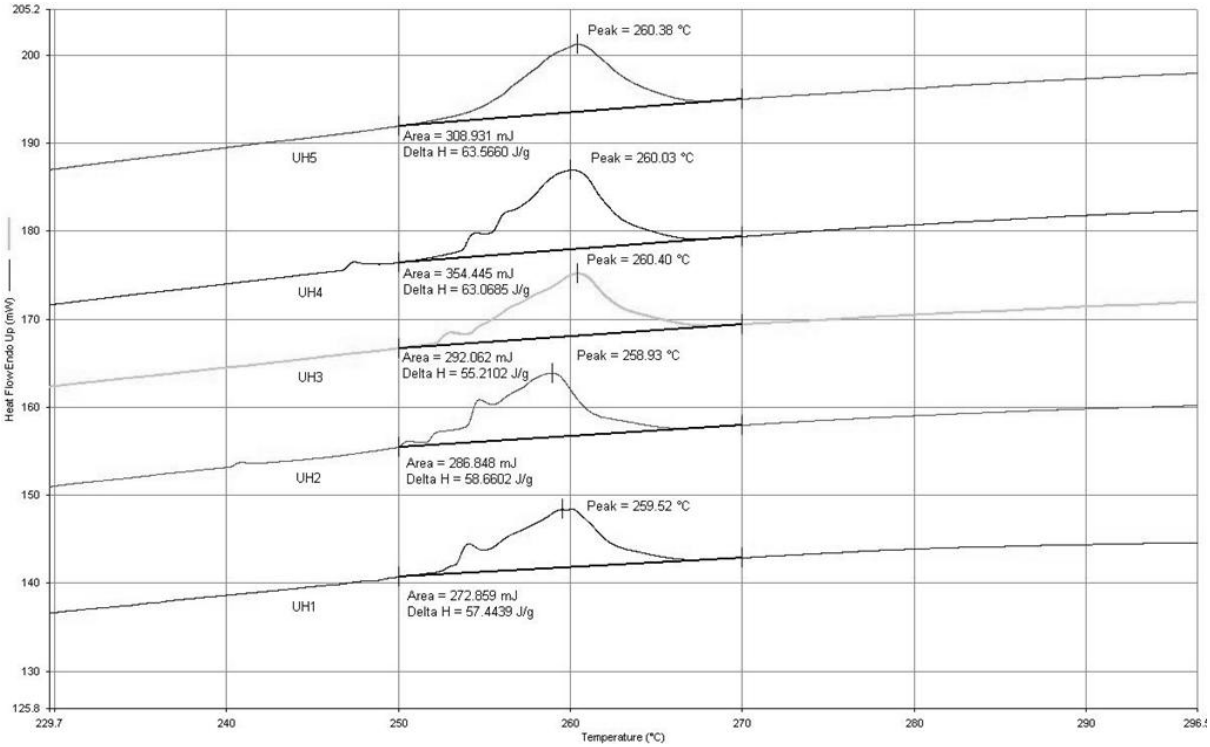

Fig 33: 5 virgin yarn samples tested in DSC.

5 virgin yarn samples were tested in the DSC and the average Delta H was calculated. Figure 33 shows the 5 curves. The average Delta H was calculated to be **59.6 ± 2.6 J/g**.

As was explained in the previous chapter, these tests were followed by tests on heated (with a hot air gun) samples. Figure 34 shows the curves for the 4 heated samples which were tested in the DSC. The average Delta H for the heated fibre samples was found to be **68.8 ± 2.1 J/g.**

The Delta H seems to increase when the fibre is heated, which indicates an increase in crystallinity. This happens because the heat causes the amorphous region of the fibre to gain sufficient energy to move and rearrange into ordered regions and hence undergoes recrystallization in the DSC (Bell, 1972).

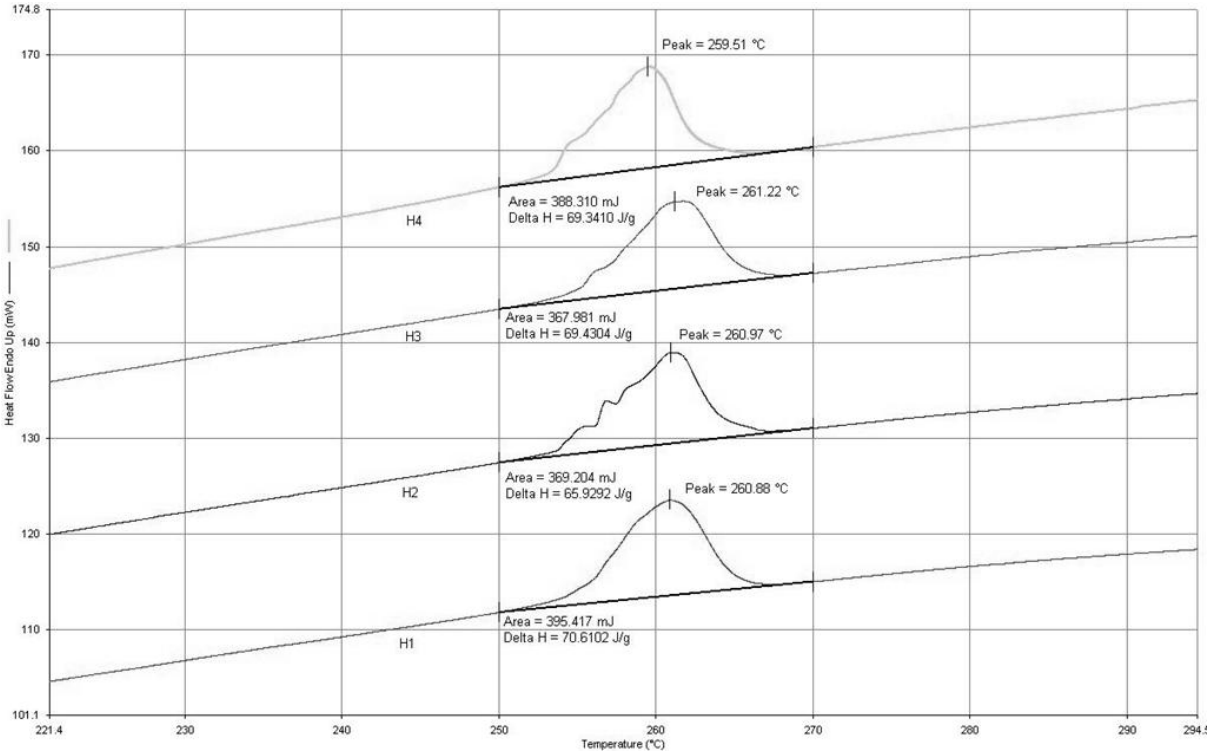

Fig 34: Heated fibre samples tested in the DSC

The effect of heating rate on Delta H was also investigated. Figure 35 shows the effect of 3 different heating rates (10, 100 and 300°C/min) on the Delta H of PA66 fibres.

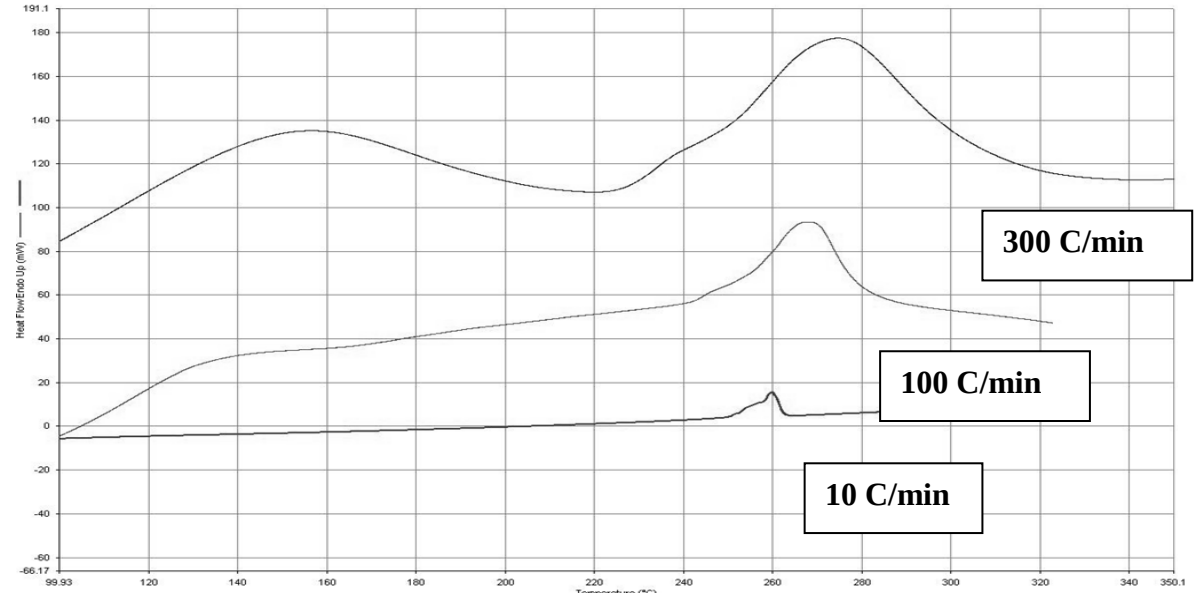

Fig 35: DSC Heating Curves for PA66 Fibres at different Heating Rates (10, 100 and 300°C/min)

As the heating rate increases, the curve and its peak is also seen to shift to the right (Figure 35), which means that the temperature at which the polymer melts increases. This is because the fibre is given less time at any particular temperature as the heating rate increases (Young and Lovell, 2011). Figure 36 shows how delta H varies with heating rate.

Heating Rate (C/min)	Average Delta H (J/g)
10	59.5 ± 1.6
100	64.5 ± 2.1
300	70.4 ± 2.7

Table 1: Average Delta H of PA66 Fibres at different Heating Rates

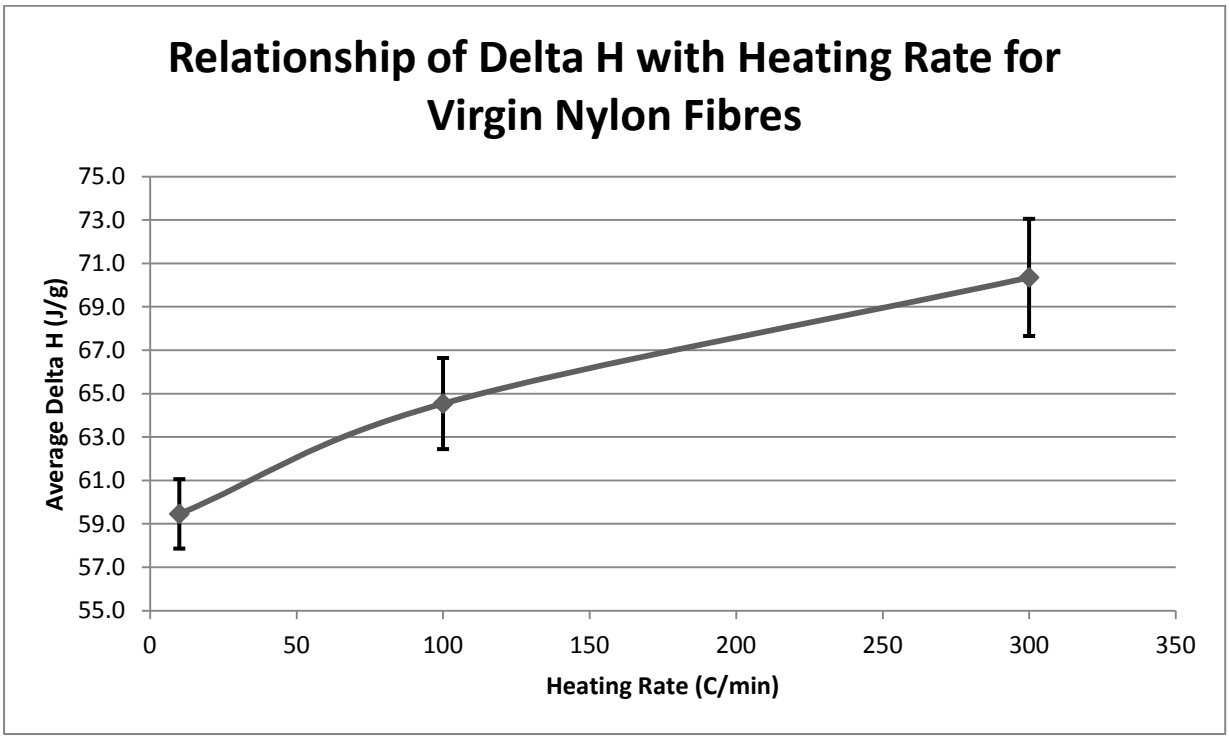

Fig 36: Relationship of Delta H with Heating Rate for PA66 Fibres

The increase in Delta H with heat is due to a process called "annealing". Annealing causes an increase in lamellar thickness of the polymer crystals. Annealing can only take place at high temperatures when there

is sufficient energy for molecular motion to take place. High temperature annealing also causes an increase in local ordering (Statton, 1972). The effect of annealing is to increase the overall crystallinity level and to reduce point-to-point variations in crystallinity. (Starkweather JR. et al., 1956)

This behaviour led to another investigation. If the heating rate has an effect, the cooling rate will most certainly have an effect on Delta H as well. Figure 37 shows the heating curves following the different cooling rates (5, 10, 20, 50, 100, 200, 300, 400, 500 and 600°C/min). The heating rate was constant at 10°C/min.

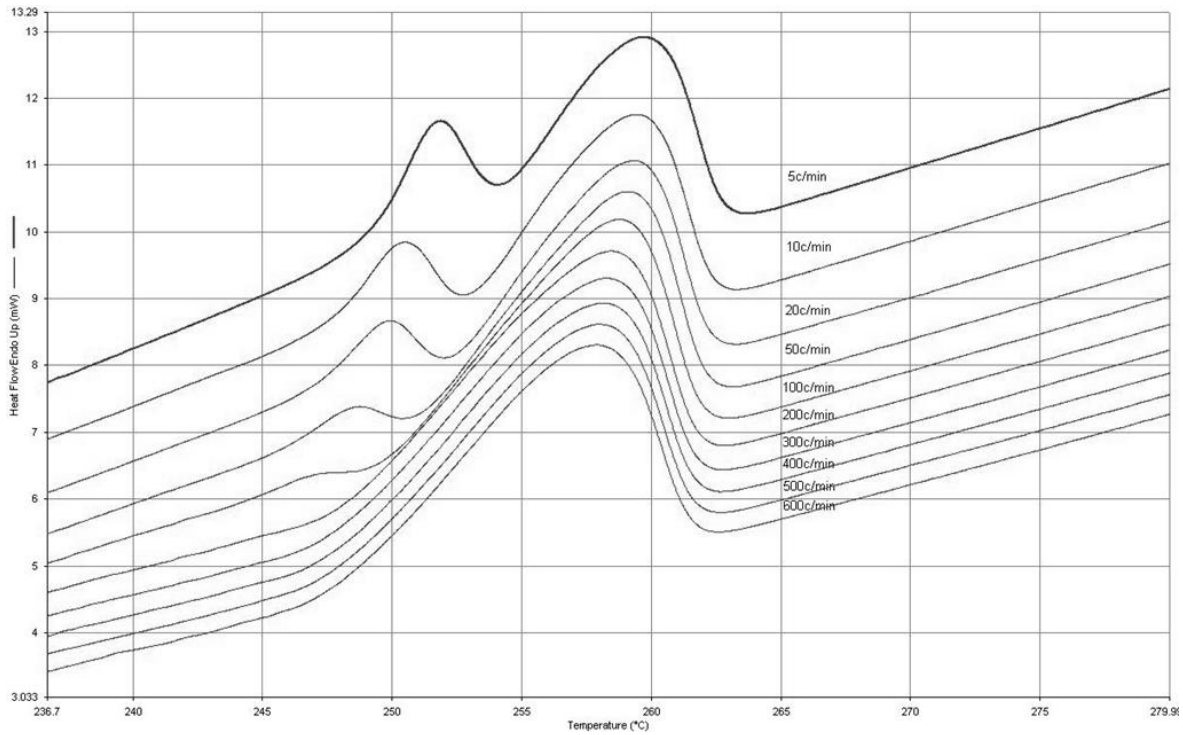

Fig 37: Effect of different cooling rates on Delta H of Nylon 6,6.

DSC melting curves of many semi-crystalline polymers including Nylon 6,6 sometimes show 2 peaks as shown in Figure 37. The intensity ratio of the 2 peaks depends on the thermal history and on the heating rate (Illers, 1975).

The double peak is due to the existence of 2 morphological species with different melting points according to Buchanan and Dumbleton, 1969. The upper melting point was attributed to folded chain crystals and the lower melting point to imperfect or small crystals with partially extended chains.

Others have explained the double peak differently. Illers, 1975 explained that the double peak is caused by re-crystallisation which occurs during heating small and/or imperfect crystals in the course of DSC measurements.

The explanation provided by Illers, 1975 is consistent with this research. Figure 37 shows that with very high cooling rates, the double peak is not observed. This means that at high cooling rates, the samples do not have enough time in the DSC to undergo re-crystallization.

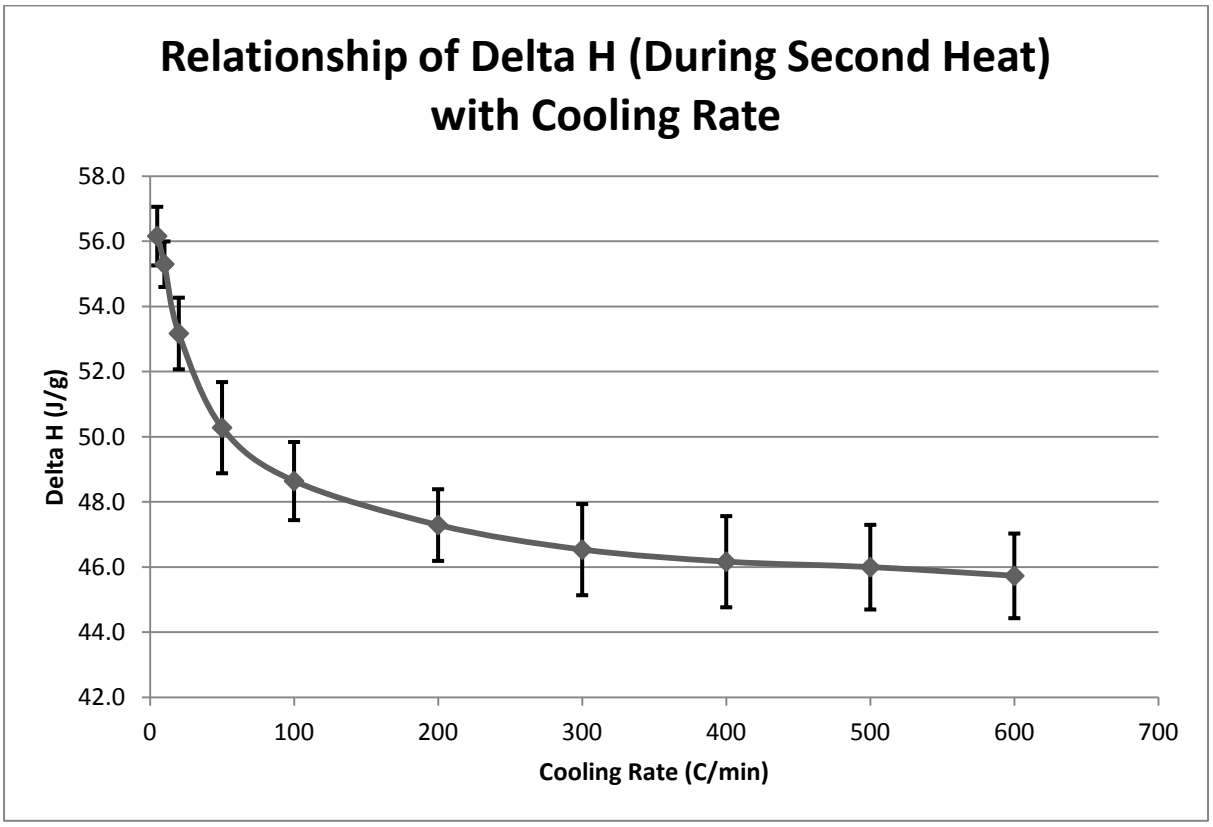

Fig 38: Relationship of Delta H (During Second Heat) with Cooling Rate for PA66 Fibres

Figure 38 shows that the Delta H on second heating decreases with an increase in cooling rate. This finding was very important, because it meant that for future heating tests on fibres, it had to be made sure that the samples cool at the same rate. If not, the results would have no meaning, as Delta H of heated fibres which have been cooled at different rates cannot be compared.

For tests on fabric level, DSC tests were done first on fabric from the vent region of both unfired and fired airbags as explained in the previous chapter. The curves followed a similar shape to the tests on fibre level. Several tests were conducted at different heating rates (10, 100 and 300°C/min).

The averages of these tests were taken and are given in Tables 2 and 3:

Sample	Delta H (J/g)
Avg. Unfired Vent 10°C/min	84.0 ± 2.3
Avg. Unfired Vent 100°C/min	90.1 ± 1.2
Avg. Unfired Vent 300°C/min	96.3 ± 1.6

Table 2: Average Delta H of unfired vent samples for 3 different heating rates

Sample	Delta H (J/g)
Avg. Fired Vent 10°C/min	86.4 ± 2.2
Avg. Fired Vent 100°C/min	91.1 ± 0.9
Avg. Fired Vent 300°C/min	97.2 ± 0.9

Table 3: Average Delta H of fired vent samples for 3 different heating rates

Figure 39 shows a graphical representation of the results.

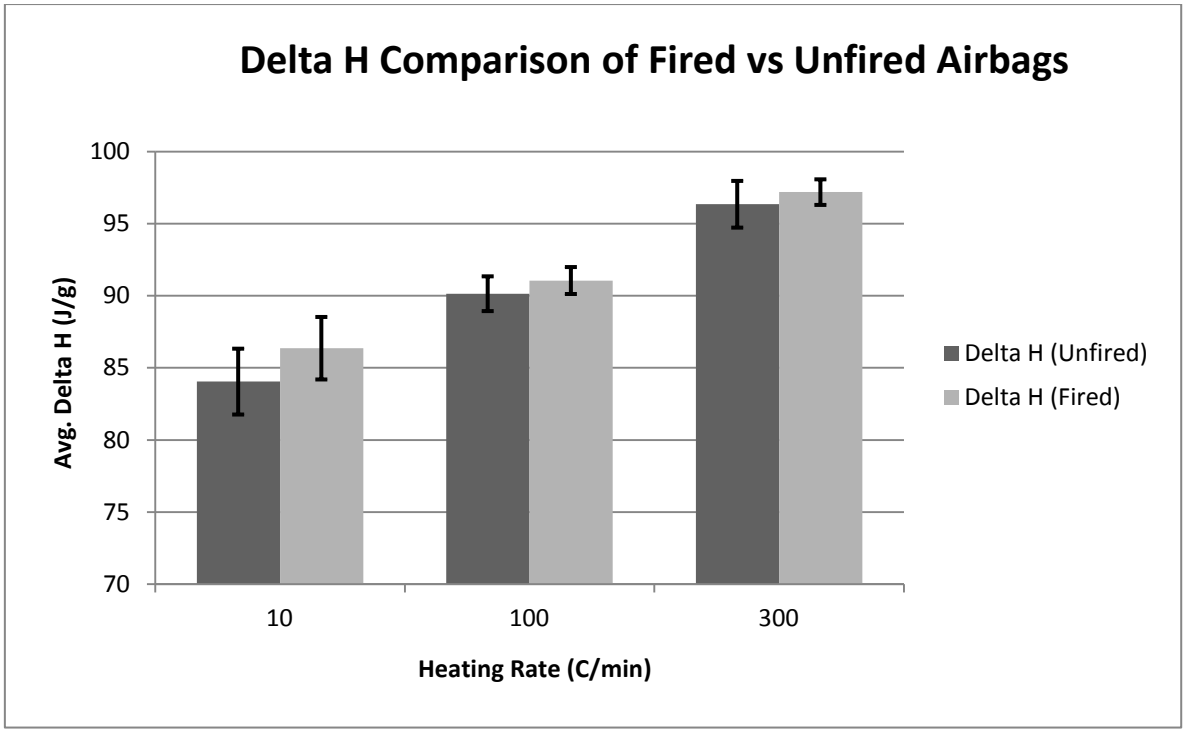

Fig 39: Comparison of Delta H for Fired and Unfired Airbag Fabrics from the Vent Region

Two things are noticeable from the chart above:

1. There is a general increase in Delta H for fired airbag vents compared to that of unfired airbag vents.
2. The Delta H for both fired and unfired airbags increases with increasing heating rates.

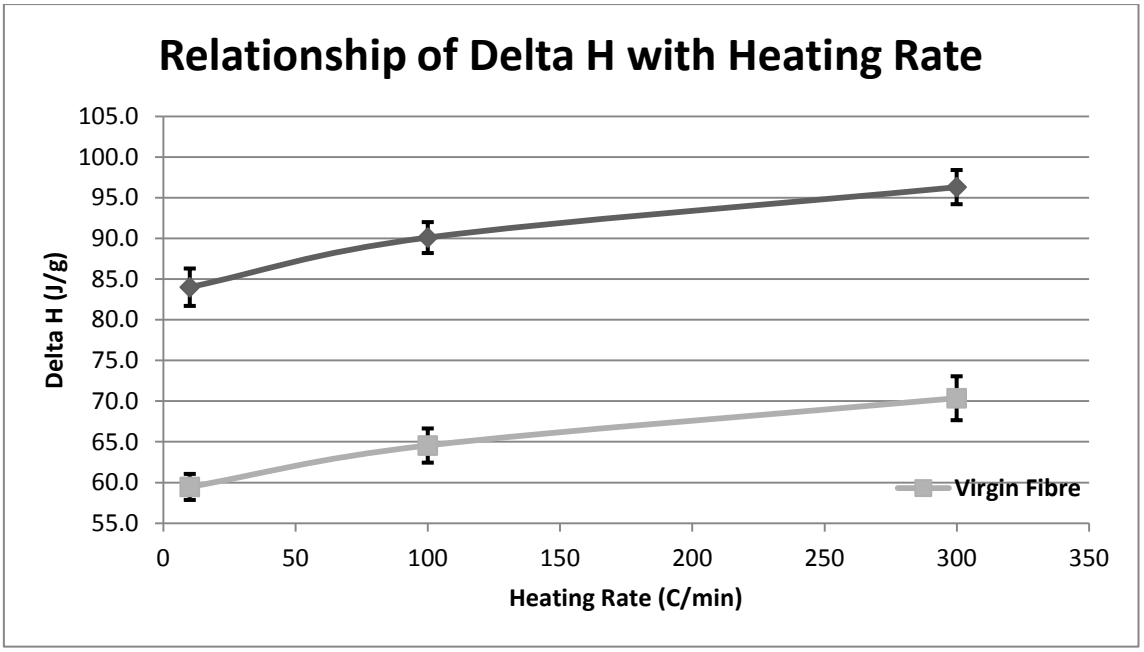

Fig 40: Comparison of Delta H of Unfired PA66 Fabric compared to Virgin PA66 Fibre

The trend and hence the shape of the curve for PA66 fabrics is similar to that of PA66 fibres. However, there is an important difference. The Delta H values for the fabric samples are much higher than that found for fibre samples. This is illustrated in Figure 40.

Although they follow the same trend, the fact that the Delta H values are much higher for the fabric sample than the fibre sample is thought to be caused by the construction of the fabric which is of course very different to that of individual fibres.

As mentioned in the previous chapter, DSC tests were conducted at 300°C/min by taking fabric from different regions (inflator side and vent) for both fired and unfired airbags. Table 4 shows the results.

	Unfired Bag	**Fired Bag (Inflator Side)**	**Fired Bag (Vent)**
Average Delta H (J/g)	96.4 ± 1.9	97.0 ± 1.7	98.3 ± 2.2

Table 4: Average Delta H of Fired Airbag in different regions

Figure 41 illustrates how the Delta H varies depending on the region of a fired airbag.

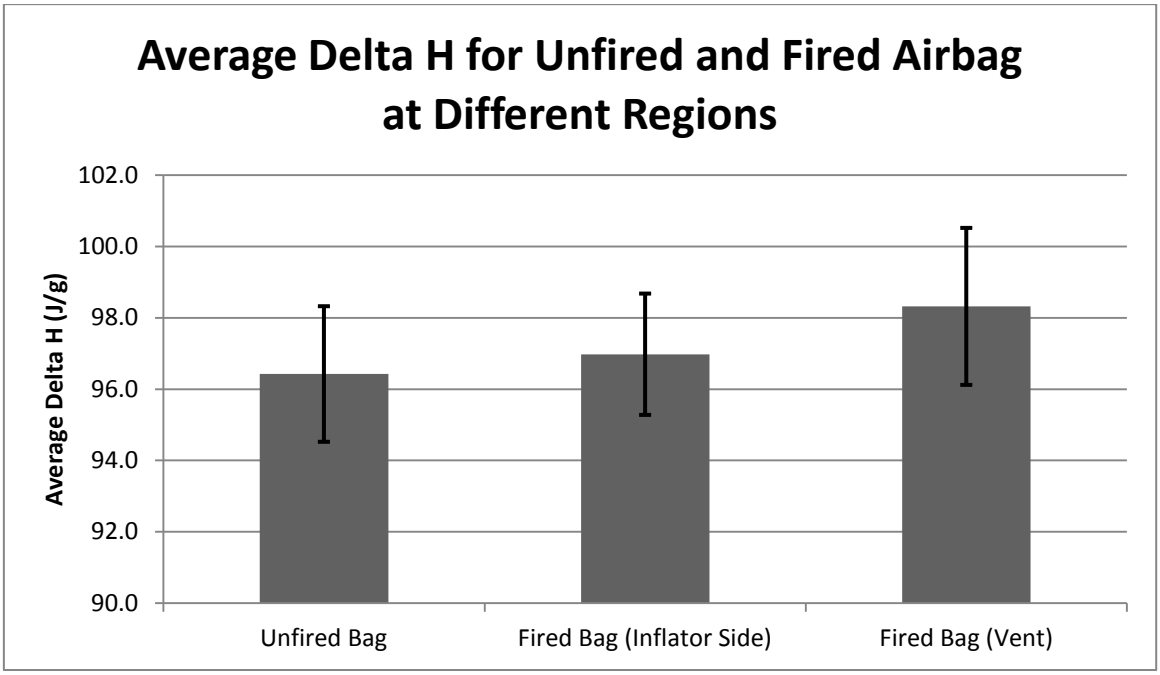

Fig 41: Delta H for Unfired and Fired Airbag at Different Regions

From Figure 41 it can be noticed that the Delta H increases for the fired airbag as expected. However, it does not increase uniformly across the entire bag. The Delta H is higher in the vent region compared to the inflator side of the bag.

Heat from the inflator radiates outward, and hence the inflator side of the bag is exposed to less heat as compared to the side which is opposite the inflator and hence directly facing the inflator. The vent region is exposed to a significant amount of heat as the hot gas escapes through the vent at a very high pressure.

The previous chapter mentioned that there is another type of DSC which is commonly used and that is "heat-flux DSC". Heat-flux DSC was carried out on unfired and fired airbags following the same procedure as power-compensation DSC. Heat-flux DSC allows for more extreme temperature

limits, and this was used to get a broader perspective. However, one limitation of the heat-flux DSC is that it cannot run at very high heating rates and thus tests were only done at 10°C/min. Figure 42 shows a typical curve, this particular one being that of a fired airbag heated at 10°C/min from -50°C to 350°C.

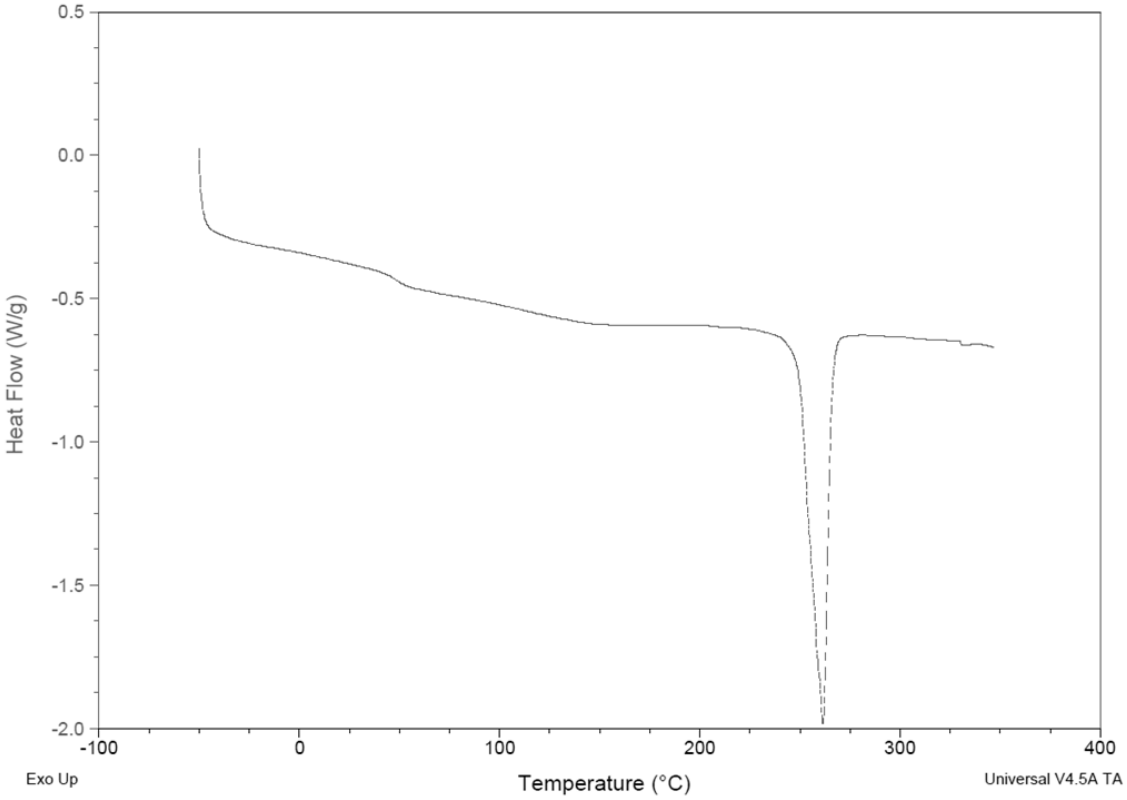

Fig 42: Heat-flux DSC curve for a Fired Airbag

From the figure above it can be seen that the peak observed in heat-flux DSC is upside-down if compared to a curve from power compensation DSC. In a power-compensation DSC, the endothermic peaks – those events which require energy point up – because the instrument must supply more power to the sample to keep the sample and reference furnaces at the same temperature. In a heat flux DSC, these same events cause the sample to absorb heat and be cooler than the furnace, so they point down. The reverse logic applies to exothermic events where energy is released (Young and Lovell, 2011)

It can be seen from the curve that melting peak is located at the same temperature as observed with power-compensation DSC. As before, the peak can be integrated to find out the enthalpy of melting. Table 5 shows the average results for Heat-Flux DSC.

Heat-Flux DSC	
Avg. Delta H (Unfired Airbag)	**Avg. Delta H (Fired Airbag)**
80.9 ± 2.9	83.8 ± 2.7

Table 5: Average Delta H for Unfired and Fired Airbag using Heat-Flux DSC

As these results show, there is very little difference between the results obtained. This indicates that the Delta H values are independent of the type of DSC used. The table above compares the Delta H values of unfired and fired airbags heated in power-compensation and heat-flux DSC at 10°C/min.

4.2 DMA

The previous chapter explained how DMA was used to characterise the fibre modulus. Figure 43 shows how the storage modulus of the fibre changes as it is heated from sub-zero temperature to beyond the melting point of the fibre.

It can be seen from Figure 43 that the storage modulus drops sharply in two regions, the glass transition and the crystalline melting. Outside of these 2 regions, the storage modulus continues to fall although at a slower rate.

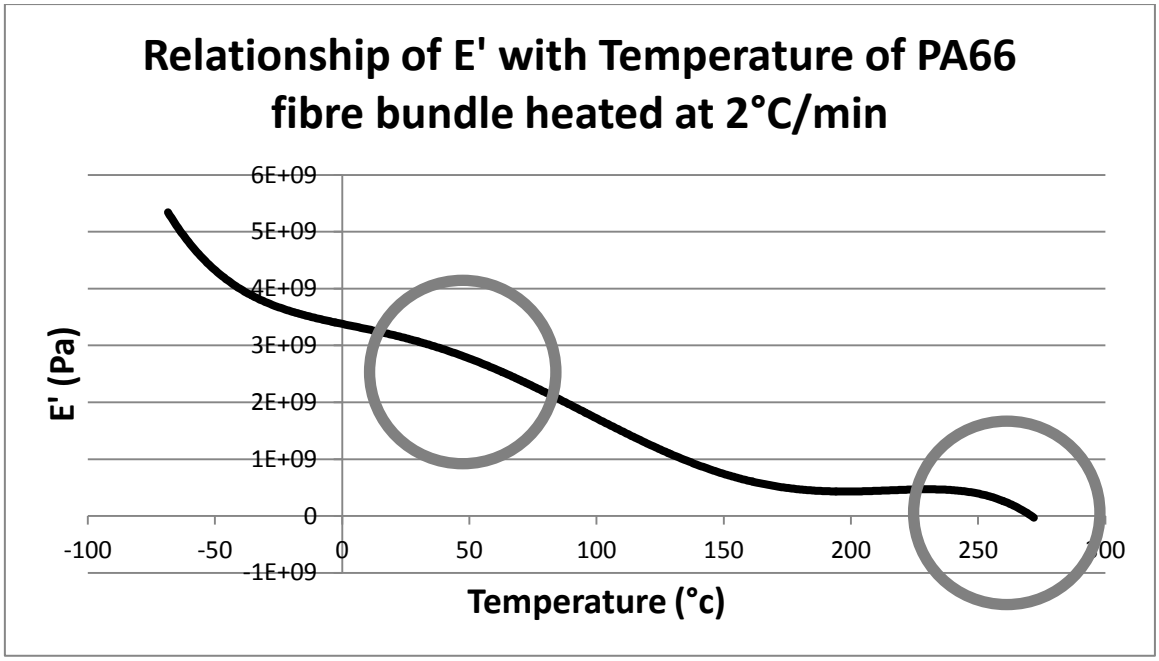

Fig 43: Relationship of E' with Temperature of PA66 fibre bundle heated at 2°C/min

Fibres with higher draw ratios would be expected to show a smaller drop in modulus in the relaxation regions. Higher draw ratios lower the segmental mobility of molecules in amorphous regions which results from chain orientation and the presence of taut tie-molecules (Leung et al., 1984).

DMA results of actual airbag yarns obtained here can be incorporated in future modelling work as it shows the path which the modulus takes as it drops while being heated. When modelling, the modulus associated with any given temperature can be easily found out from these results.

4.3 X-Ray

As previously mentioned, X-ray scattering was carried out on fabric extracted from the vent and inflator side of both fired and unfired airbags. Figure 44 shows the scattering pattern from the sample.

The scattering intensity can be seen to drop, which suggests a decrease in crystallinity. By calculating the areas under the crystalline peaks and the amorphous halo, it is found that the crystallinity has dropped by 35%. This is different to the DSC findings which showed an increase in crystallinity. In X-ray measurements, there is no heat involved and hence no scope for annealing.

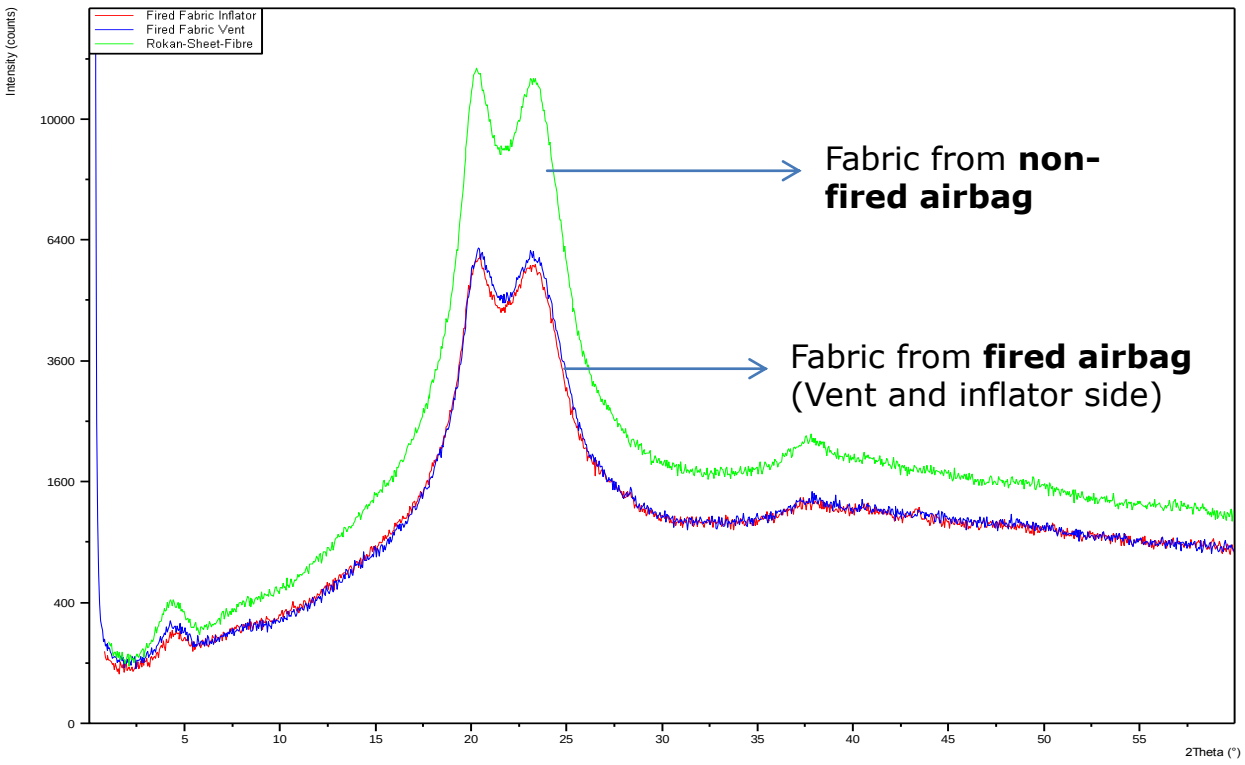

Fig 44: X-ray scattering of Fired and Unfired Airbag Fibres

The two strong peaks which can be seen in Figure 44 is likely due to lateral order and a high degree of hydrogen bonding in the crystallites (Narten et al., 1991). There is also a fall in the area under the peak for the fired airbag fabric sample as compared to the unfired airbag fabric sample. It can also be noted that the peaks are slightly offset, which suggests that the internal structure of the fibre is likely to have changed.

4.4 Tensile Tests

As mentioned in the previous chapter, tensile tests were also carried out on heated and unheated fibres. Figure 45 shows the results obtained from tensile tests on fibres which were placed inside an airbag and then fired (uncontrolled heating).

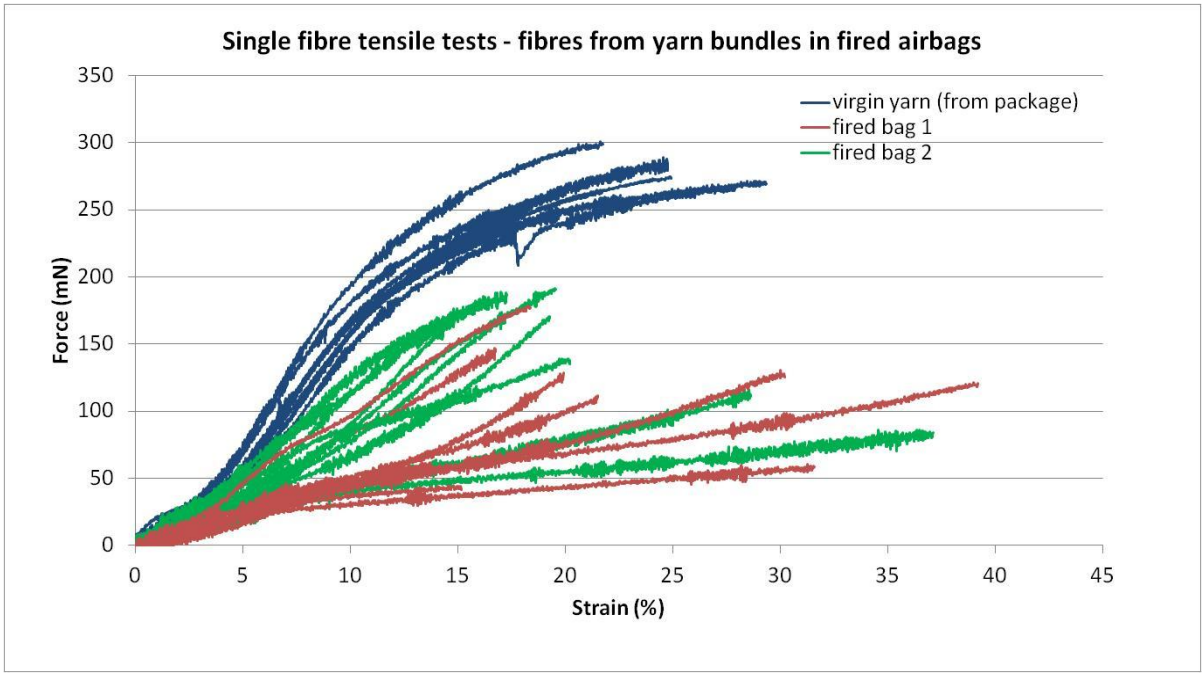

Fig 45: Single fibre tensile tests on virgin PA66 and heated (inside airbag) PA66.

The results in Figure 45 show that there is a definite decrease in the modulus for the yarns exposed to an actual airbag deployment compared to that of the virgin yarn sample. There is also a definite decrease in the force required to break the fibre samples. The effect on strain to failure is not very clear as the some of the samples broke at low strains while others broke at high strains.

These tests were followed by the tests on fibres which were heated using the DSC. Figure 46 shows the results from these tensile tests. These results show that the there is a definite decrease in modulus for fibres which were exposed to heat than that of virgin fibres. It can also be seen

that the modulus decreases with an increase in temperature and also an increase in heating rate. Elad and Schultz, 1984 reported that the rate of decrease of modulus of Nylon 6,6 fibre increases with increasing temperature.

The force at which the fibre breaks also decreases for the fibres which were subjected to heat. This is in agreement with Jain and Vijayan, 2002 who applied isothermal heat treatment on Nylon 6,6 and reported a drop in breaking force with temperature.

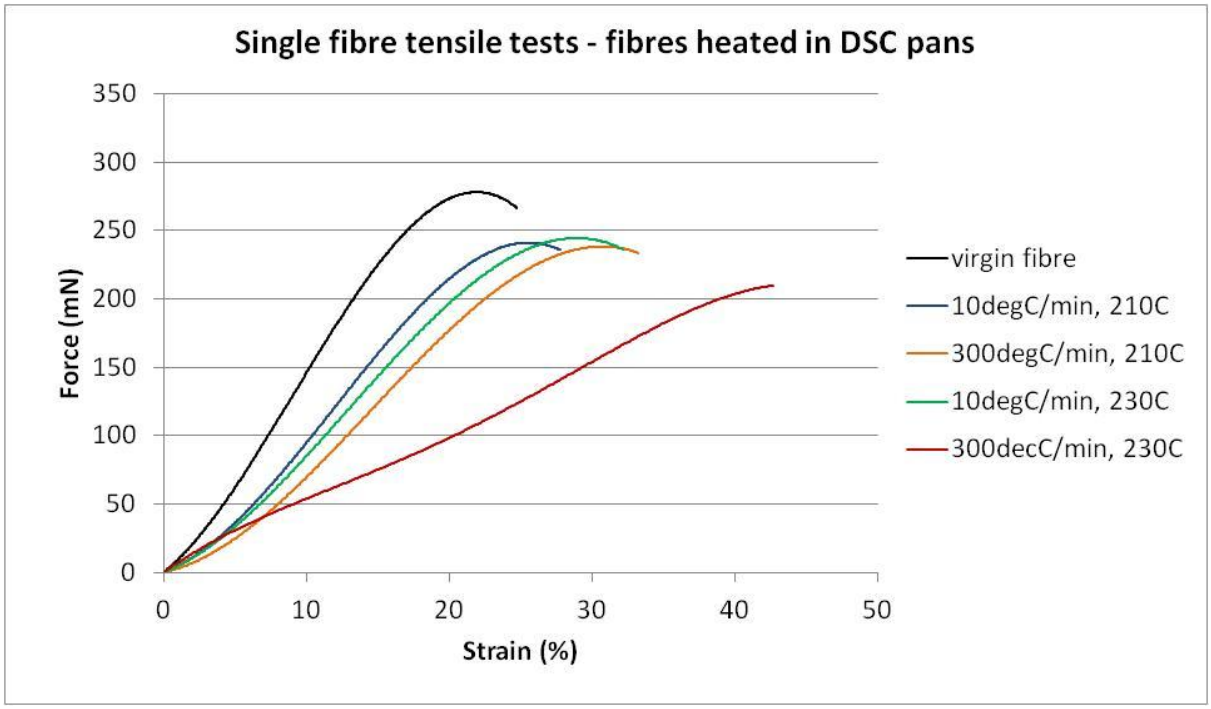

Fig 46: Single fibre tensile tests (at room temperature) on virgin PA66 and heat treated (in DSC) PA66.

The change in tensile properties is likely due to the change in chain extension and orientation. If the molecular chains are extended and highly oriented, it gives rise to an increase in stiffness and strength, as the mechanical properties of the fibre become predominantly determined by the strong covalent bonds along the chain backbone rather than by the

weak Van der Waals bonds between neighbouring chain molecules (Frank and Wendorff, 1988).

An increase in tenacity and a decrease in elongation with crystalline and amorphous orientation of Nylon 6,6 fibres have also been reported by Simpson et al., 1981. The authors, however, suggested that for chain-folded Nylon morphologies, the fibre structure was more sensitive to the state of the amorphous orientation than to the crystalline orientation because the amorphous tie-chains were the load bearing units. Increased tenacity is obtained by stretching the tie-chains out in the fibre direction. Reduction of strength and modulus of Nylon fibres with a decrease in oriented amorphous fraction has also been reported by Murthy, 1997.

As mentioned before, these tests were followed by cycling tests on the tensile tester to find the strain recovery for virgin and heated fibres. Figure 47 shows the results from the cyclic tests.

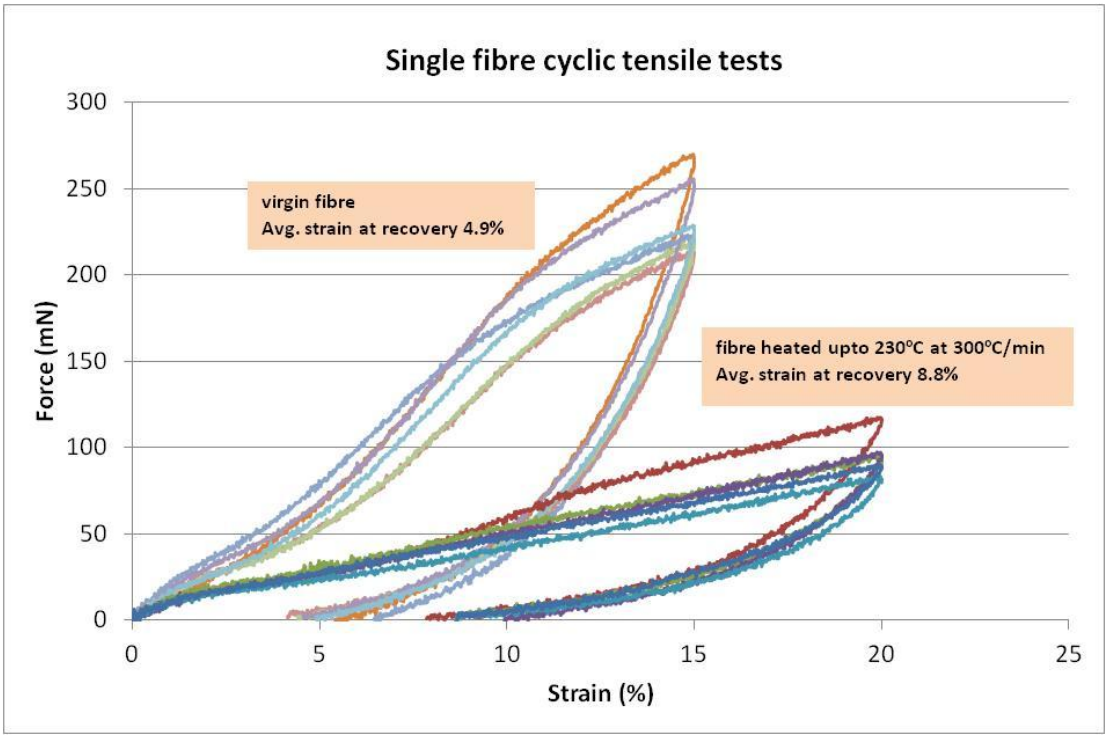

Fig 47: Single fibre cycling tensile tests on virgin and heated PA66.

It can be seen from Figure 47 that virgin fibres have better strain recovery performance than the heated fibres. The average strain at recovery for virgin fibres was 4.9% while the average strain at recovery for the heated (230°C at 300°C/min) fibre was 8.8%. This means that the unheated fibre has recovered 67% of the applied strain while the heated fibre has only recovered 56% of the applied strain.

The heated fibre was taken to a higher strain because the fibre was able to withstand the higher strain. The heat caused to fibre to allow more elongation. The fact that the heated fibres recovers less than the unheated fibre suggests there has been a reduction in orientation and/or breakage of bonds between molecules which might have led to a less elastic fibre.

4.5 Shrinkage

The previous chapter mentioned that shrinkage tests were carried out to see if there was a change in orientation. The results for shrinkage of both yarns and fabrics are given in Table 6.

	Fabric (Weft)	**Fabric (Warp)**	**Yarn**
Shrinkage %	5.71 ± 0.23	7.86 ± 0.34	8.29 ± 0.38

Table 6: Shrinkage (%) of PA66 Yarns and Fabrics (warp and weft direction)

Figure 48 illustrates the amount of shrinkage.

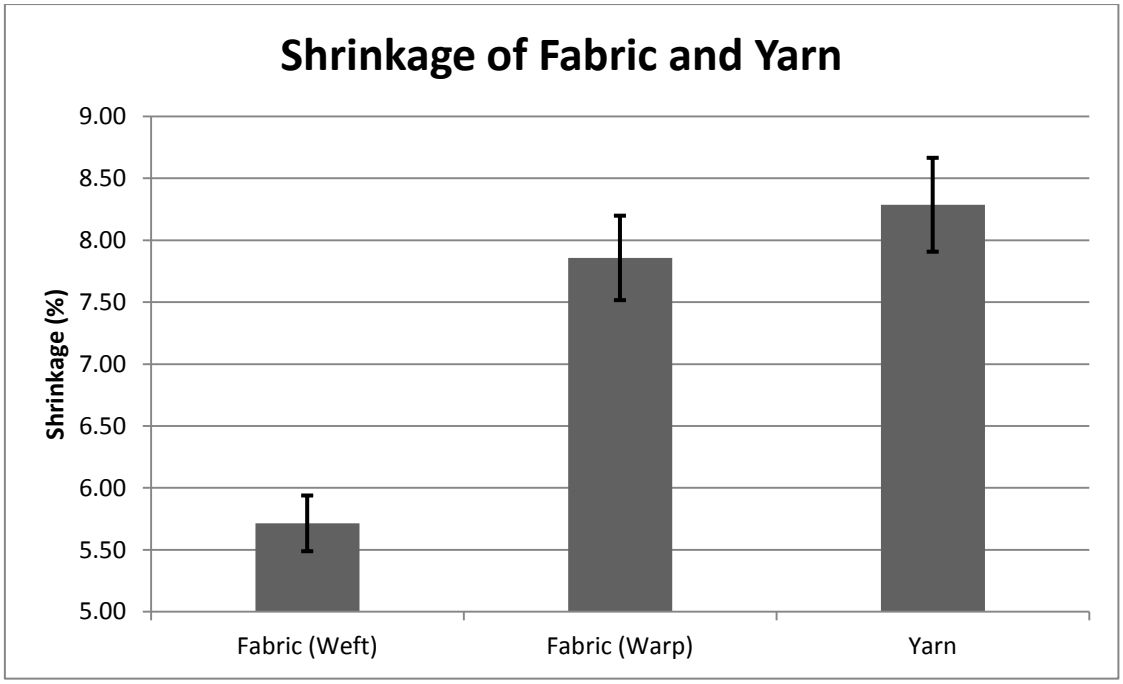

Fig 48: Chart showing Shrinkage (%) of PA66 Fibres and Fabrics (warp and weft direction)

From the results above if can be seen that the yarn shrinks more than the fabric. When it comes to the fabric, the shrinkage is not uniform. There is more shrinkage in the warp direction of the fabric as compared to the weft direction which is due to the differences in tension between the yarns in the warp and weft direction.

Apart from shrinkage, the fabric also changed colour due to the heat. A yellow-brown discolouration was observed. This discolouration of Nylon is a likely indication of the production of a conjugated structure. (Holland and Hay, 2000)

As mentioned in the previous chapter, shrinkage tests were also carried out on yarns by heating them in the DSC at different maximum temperatures and different heating rates. These maximum temperatures and heating rates were the same as those used for the tensile test samples. The results are given in Table 7.

	210°C at 10°C/min	210°C at 300°C/min	230°C at 10°C/min	230°C at 300°C/min
% Shrinkage	18.10 ± 0.69	21.19 ± 0.71	35.88 ± 0.93	41.17 ± 0.96

Table 7: Shrinkage (%) of PA66 Yarn at different Maximum Temperatures and Heating Rates

Figure 49 illustrates the different amounts of shrinkage for PA66 fibres.

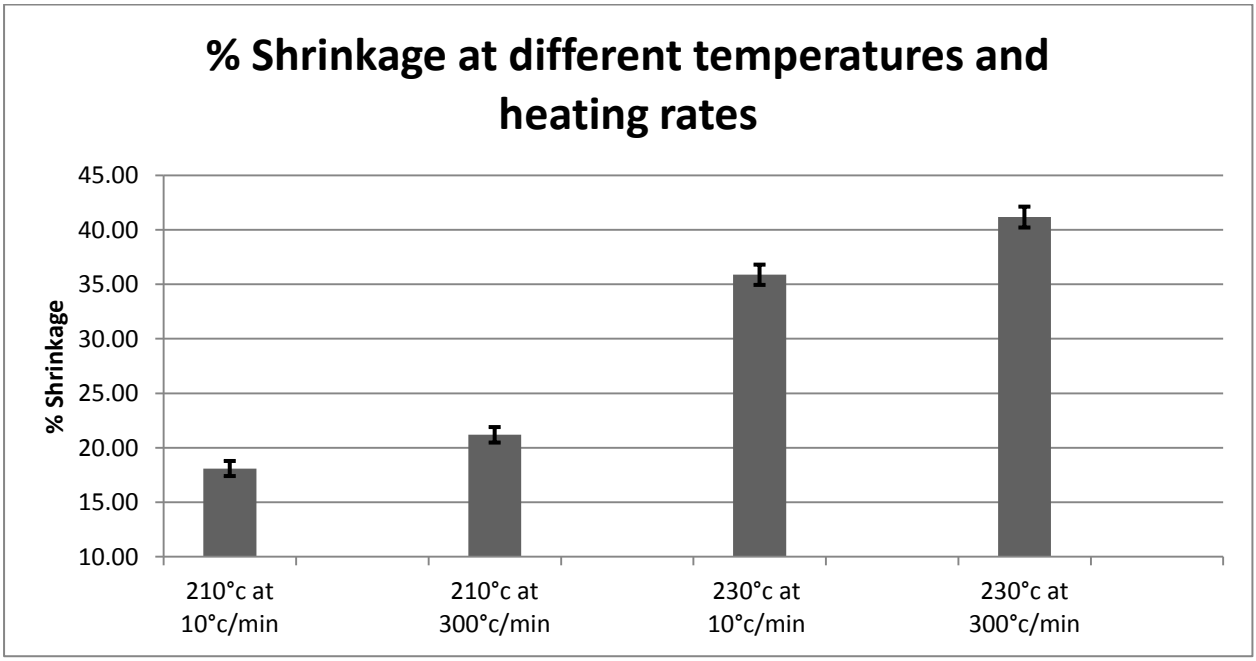

Fig 49: Chart showing Shrinkage (%) of PA66 Fibres at different Maximum Temperatures and Heating Rates

A trend can be seen from Figure 49. It can be seen that the shrinkage (%) increases with both an increase in heating rate and an increase in maximum temperature.

These shrinkage results suggest that the heat provided is sufficient to change the structure of the material. The change in structure results in a loss in orientation of the molecules, hence causing shrinkage. This is in agreement with Prevorsek and Tobolsky, 1965 who found that the free shrinkage of Nylon 6,6 fibres increased with temperate (100°C to melting

point). The authors concluded that during the free shrinkage of an oriented fibre, there is considerable disorientation of the primary axes of the polymer crystallites, and the polymer reverts to the amorphous state on melting.

However, others have explained free thermal shrinkage differently. Dismore and Stratton, 1966 believed that the free thermal shrinkage of oriented polymers involves a structural transformation between two crystalline forms – the extended-chain and folded-chain conformations, rather than a disorientation of the primary axes of polymer crystallites. The authors explained that heat causes the intermolecular bonds to loosen, and the chains move into folded conformation in which the bond distances are smaller and the bond energies are lower.

The difference in views is likely due to the difference in temperature range in which the authors have conducted their studies (Ribnick, 1969). Unlike Dismore and Stratton, 1966, Prevorsek and Tobolsky, 1965 examined samples which were heated close to their melting temperatures at which point appreciable disorientation of the principal axis might be observed.

Buchanan and Dumbleton, 1969 analysed shrinkage behaviour of drawn Nylon 6,6 yarns by annealing the yarns in air and in oil. The purpose of this was to get different heating rates as the yarn absorbed heat from hot oil much more rapidly than that from hot air. In both cases, the authors found that the shrinkage increases with increasing annealing temperature, however, the degree and also the rate of change is much greater for the oil-annealed samples. This correlates well with the results obtained in this research, i.e. shrinkage increases with both temperature and heating rate.

4.6 Change in Diameter

The previous chapter mentioned that tests were carried out to find out the associated change in diameter of the fibres due to shrinkage. The results are given in Table 8.

	Unheated Fibre	Heated Fibre	% Increase
Diameter (μm)	18.6 ± 0.6	19.8 ± 0.9	6.42

Table 8: Diameter of PA66 Fibre before and after Heating

Figure 50 illustrates the change in diameter.

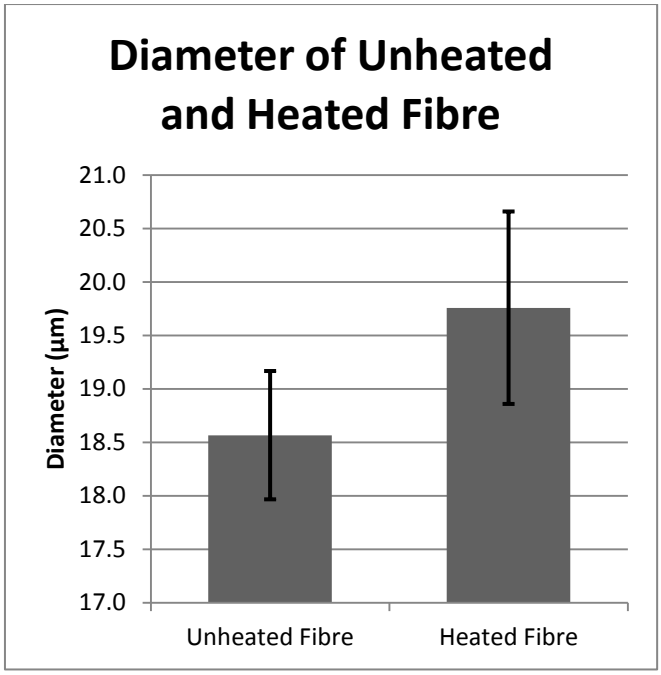

Fig 50: Chart showing the Diameter of PA66 Fibre before and after Heating.

The diameter of the fibre increases as the fibre was heated without any tension. The internal forces in the fibre relax when subjected to heat which makes it swell in the radial direction giving a rise in diameter. Under

tension heating, the diameter would be expected to go down (Zhang et al., 2012).

Change in diameter tests were also carried out on yarns by heating them in the DSC at different maximum temperatures and different heating rates. These maximum temperatures and heating rates were the same as those used for the tensile test samples. The results are given in Table 9.

	Virgin	**210°C @ 10°C/min**	**210°C @ 300°C/min**	**230°C @ 10°C/min**	**230°C @ 300°C/min**
Diameter (µm)	18.6 ± 0.2	19.7 ± 0.3	19.8 ± 0.3	20.1 ± 0.4	20.2 ± 0.4

Table 9: Diameter of PA66 Fibre before and after Heating at different Maximum Temperatures and Heating Rates

Just like shrinkage, the change in diameter also depends on the maximum temperature and heating rate used. Figure 51 illustrates this.

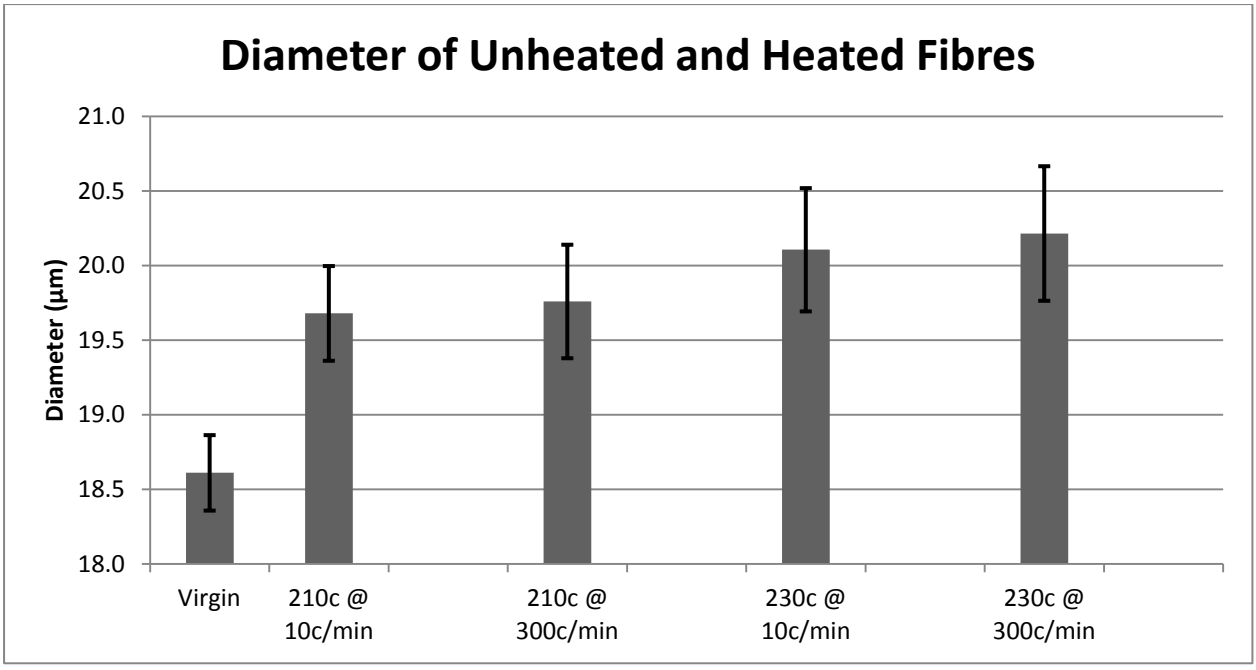

Fig 51: Chart showing the Diameter of PA66 Fibre before and after Heating at different Maximum Temperatures and Heating Rates

This is in good agreement with the shrinkage results. Higher shrinkage is expected to give rise to higher diameter when the fibre is heated under no tension. The result is also in agreement with the results obtained by Zhang et al., 2012, although the authors have conducted their study using PSU fibres. The authors have shown that the diameter increases with treatment temperature. However, no relationship with heating rate was mentioned. This study has shown that the diameter increases with both temperature and heating rate.

During relaxation heating, the movement of the molecules cause the internal force of the fibre to relax, therefore the fibre tended to shrink and swell in the radial direction which explains the increase in diameter (Zhang et al., 2012). Experiments done by Murthy, 1997 show that during annealing, the diameter of drawn Nylon 6 increases. The author attributed this increase to the crystallisation of the inter-fibrillar amorphous chain segments, and melting and re-crystallisation of the smaller crystallites, both of which could also contribute to fibre shrinkage.

Both shrinkage and diameter is seen to be influenced by heat and the heating rate. The diameter of the fibre increases with an increase in temperature and heating rate while the length of the fibre decreases (increase in shrinkage). Figure 52 shows the relationship between the shrinkage and the diameter of PA66 fibres.

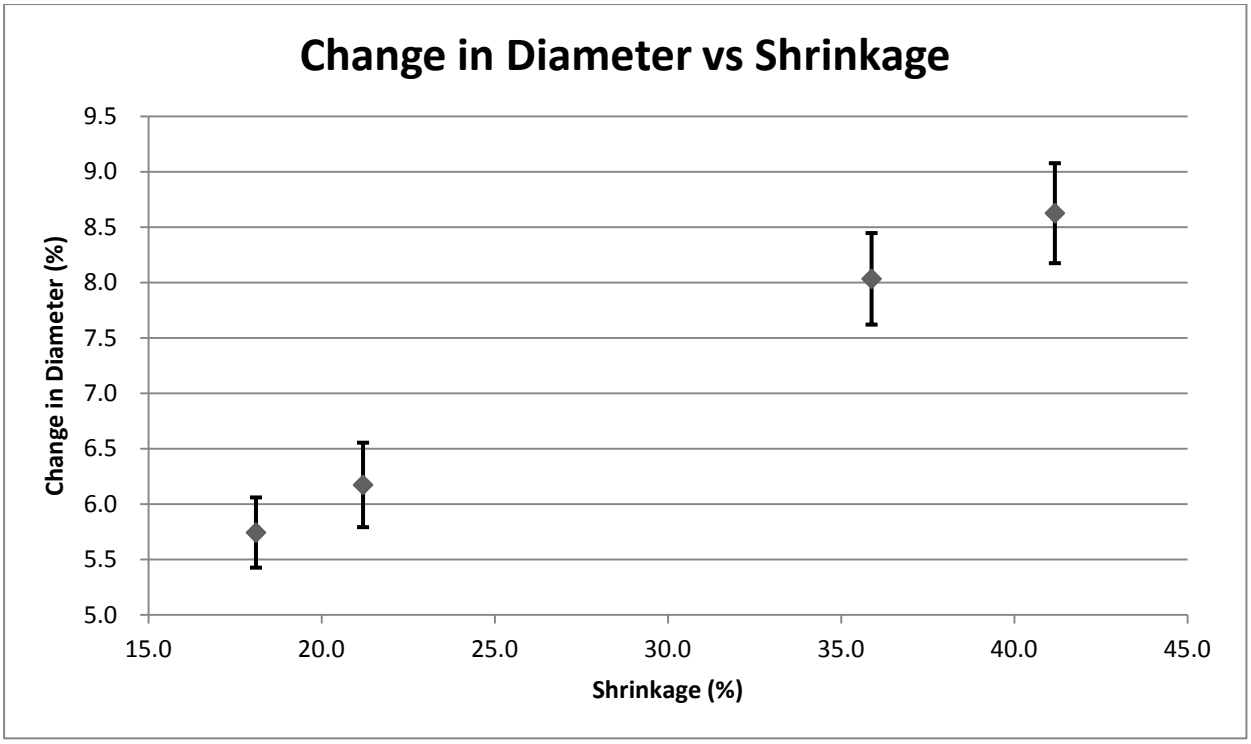

Fig 52: Relationship between Change in Diameter and Shrinkage of PA66 Fibres heated at different Temperatures and Heating Rates

4.7 Correlation between Shrinkage and Tensile Properties

From the tensile results, it was seen that PA66 fibres experienced significant changes to tensile properties after being exposed to actual airbag deployment conditions. The tests conducted in the DSC were seen to give similar results.

Firstly, it was seen that there was a decrease in the average force at failure. At the same time the average strain at failure increased after the fibres were exposed to heat. Figure 53 shows the relationship between the breaking force and the breaking strain for PA66 fibres heated at different temperatures and heating rates.

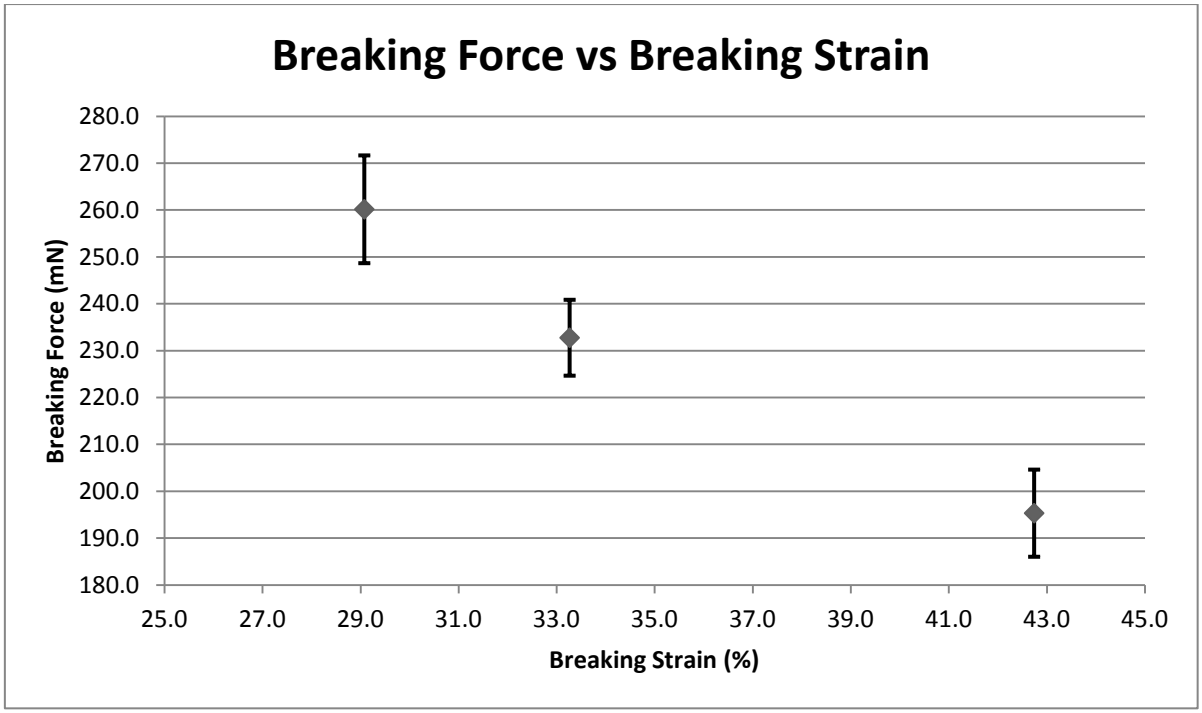

Fig 53: Relationship of Breaking Force with Breaking Strain for PA66 Fibres Heated at different Temperatures and Heating Rates

Secondly, it was seen that there is a decrease in initial stiffness of the fibres after being exposed to heat. This decrease in stiffness is thought to arise due to the loss in orientation of the molecules in the PA66 fibres, which was confirmed by the shrinkage results. Orientation of molecular chains gives rise to an increase of stiffness (Frank and Wendorff, 1988). Since shrinkage is caused by a decrease in orientation, the stiffness in this case is expected to go down.

Simpson et al., 1981 also found that tenactiy increases with increasing crystalline and amorphous orientaion for Nylon 6,6 fibres while the elongation decreases. Higher tenacity and lower elongation result from higher stiffness. A reduction is molecular orientation (higher shrinkage) will thus cause a reduction in stiffness. Figure 54 shows the relationship between the stiffness and the shrinkage of PA66 heated at different temperatures and heating rates.

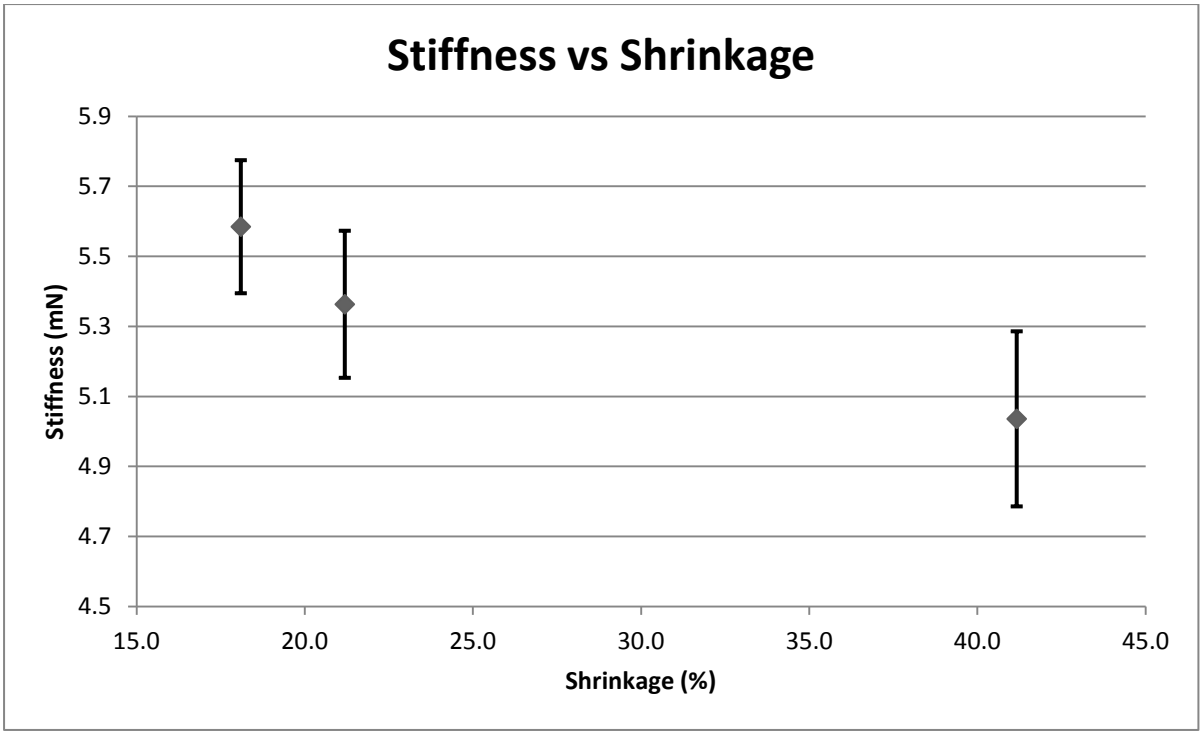

Fig 54: Relationship of Initial Stiffness with Shrinkage for PA66 Fibres Heated at different Temperatures and Heating Rates

Similarly, the loss in orientation confirmed by the shrinkage tests is thought to be the main cause for the fall in breaking force and the resulting increase in breaking strain. Ribnick, A. 1969 studied the stress dependency of thermal shrinkage for Nylon 6,6 yarns.. The author applied a load to a yarn, heated it to a certain temperature and then removed the load to measure shrinkage. It was found that increasing the load reduced thermal shrinkage. It was also found that the final shrinkage was reached in a shorter time as the load was increased.

Figures 55 and 56 show the relationships between the breaking force and shrinkage, and the breaking strain and shrinkage respectively. It has not been possible to outline an exact relationship due to a lack of data points, however, Ribnick, A. 1969 found that thermal shrinkage fell rapidly with increasing load which suggests that the relationships are likely to be exponential.

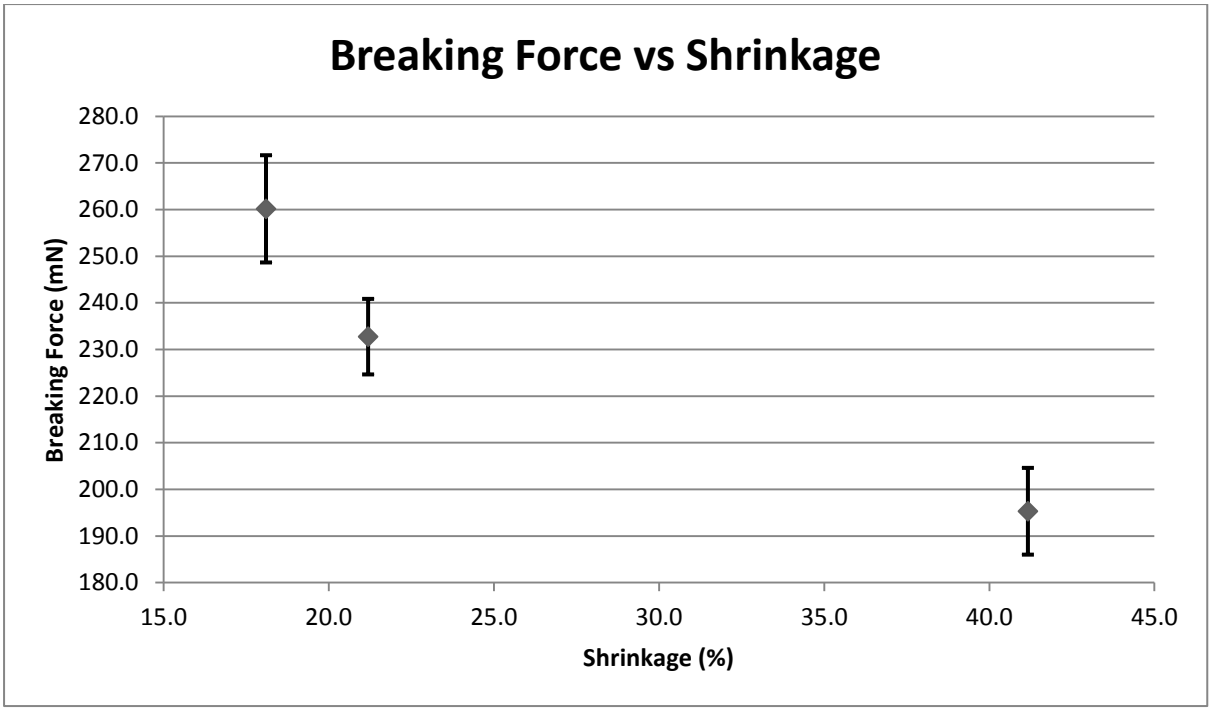

Fig 55: Relationship of Breaking Force with Shrinkage for PA66 Fibres Heated at different Temperatures and Heating Rates

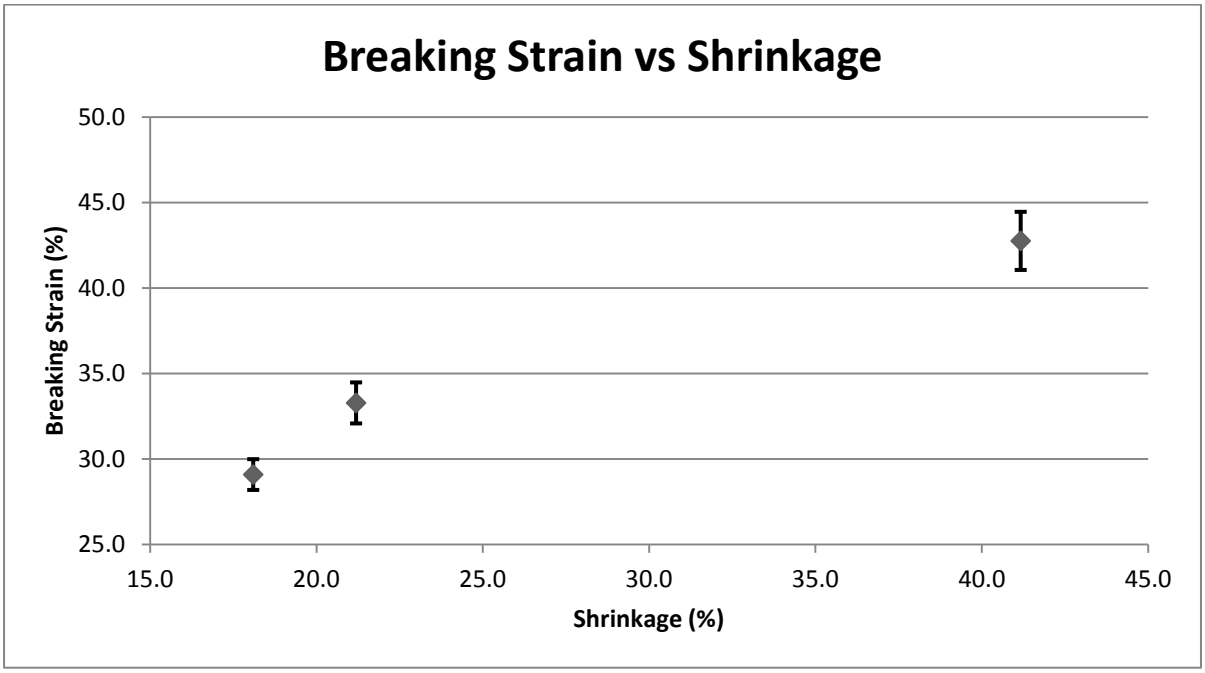

Fig 56: Relationship of Breaking Strain with Shrinkage for PA66 Fibres Heated at different Temperatures and Heating Rates

Chapter 5: Conclusions and Further Research

This chapter summarises and concludes the major findings in this research. It also suggests further areas of research which can be very useful in order to better understand the effects of airbag deployment on the airbag material.

5.1 Conclusions

Thermal tests were conducted on airbag fibres and fabrics. DSC was used to measure the difference in enthalpy between fired and unfired airbags, and between heated and unheated airbag fibres. DMA was used to establish a path which the storage modulus takes as an airbag yarn is heated from sub-zero temperature to melting temperature. The data obtained from DMA will be used in future modelling work.

DSC results show that the fired airbag fabrics and the heated airbag fibres show a higher value of delta H as compared to the unfired airbag fabric and virgin airbag fibre. For both unheated and heated fibres and also for unfired and fired fabrics, the delta H values seemed to be heating rate dependant. The higher the heating rate used, the greater the value of delta H obtained. Although the same trend was seen for both fibres and fabrics, the actual delta H values were higher for fabrics that those of fibres. DSC tests on fired airbags were done by extracting samples from different regions of the bag. Compared to the unfired airbag, the delta H value was higher for both the regions – inflator side and the vent. However, the increase in delta H was greater for the vent region than that of the inflator side.

DSC was also used to analyse the effect of cooling rate of delta H. The delta H on second heating seemed to decrease with increasing cooling rate. The delta H drops sharply between cooling rates of 10°C/min and 100°C/min. From 100°C/min to 600°C/min, the delta H continues to drop, but at a much slower rate.

DMA was conducted on airbag yarns straight from a bobbin. The storage modulus dropped as the sample was heated from sub-zero temperature to melting point of the material. The drop was sharp in two regions – the glass-transition and the melting point. As mentioned before, the main purpose of conducting DMA was to establish a path which the storage modulus takes when heated to be used in future modelling work.

Tensile tests were initially done on single fibres extracted from virgin yarns and from yarns fired inside an airbag. There is a clear drop in modulus and tensile strength. A range of values is found for modulus and breaking force, with some fibres having a very low modulus breaking at very low forces while some fibres seem to have a relatively high modulus and breaking at higher forces. This breaking force is still lower than that of virgin fibres. The range of values is likely due to the fact that fibres were extracted randomly from the fired yarn, i.e. some of the fibres originated from the surface of the yarn while some from the core of the yarn.

Tensile tests were also carried out on fibres which were heated in a DSC in a controlled environment. A similar trend was seen compared to the uncontrolled heating environment, i.e. the modulus and breaking force seemed to drop with heat. To be more precise, the modulus and breaking forced dropped with increasing temperature and increasing heating rate.

DSC results showed that delta H increased with heat, which means that there is a slight increase in crystallinity. At the same time, tensile results

showed that the modulus and breaking force decrease with heat. As the modulus dropped, the fibre showed higher elongation at break but at the same time becomes less elastic. This is confirmed by the drop in elastic recovery of the fibre.

The drop in strength despite a rise in crystallinity can be explained by a change in molecular orientation of the fibre. Change in orientation is confirmed by shrinkage when the fibre is heated under no tension. Shrinkage seemed to increase with temperature and heating rate which led to an increase in fibre diameter which also followed the same trend and increased with temperature and heating rate. Correlations of stiffness, breaking force and breaking strain with shrinkage showed that stiffness and breaking force decreases with increasing shrinkage while breaking strain increases with increasing shrinkage.

5.2 Scope for Further Research

This project has been able to shed some light on what actually happens at the fibre and fabric level when automotive airbag materials are subjected to deployment conditions. However, further research is necessary in order to fully understand the heat effects on automotive airbags.

- Change or loss in orientation: this research has concluded that there is a loss in orientation of the fibre molecules which results in the drop in some tensile properties such as modulus and tensile strength. However, it will be useful to look at exactly what orientation these molecules take after heating. This can be achieved using Raman Spectroscopy or Flat-plate X-ray diffraction for example.

- Test coated airbags: this research has only looked at uncoated airbags, but coated airbags are also used widely in the industry.

Coated airbags might have a very different reaction to heat. The properties of coated airbags after heating will be very interesting to consider as the heat tends to cause physical degradation of the coating material and the fabric, but it may also form some sort of a composite structure.

- Dynamic thermo-mechanical testing: the tests conducted in this project were mostly static. To understand how heat and mechanical loading works in combination to alter the properties of airbag materials, dynamic thermo-mechanical testing needs to be carried out. This can be done on both yarns and fabrics by developing high strain rigs with bi-axial loading capability and with a controllable heat source.

References

Airbag Inflators [Online]. The Clemson University Vehicular Electronics Laboratory. Available: http://www.cvel.clemson.edu/auto/actuators/airbag.html [Accessed 29th August 2012].

Airbags 101 [Online]. Available: http://nettleslawblog.com/blog-old/?currentPage=45 [Accessed 19th August 2012].

Crash Test - Driver Airbag [Online]. Autoliv. Available: http://adam.autoliv.com/Standard/CatalogAuto.jsp [Accessed 29th September 2012].

European Commission [Online]. Available: http://ec.europa.eu/health/opinions/en/dental-amalgam/glossary/pqrs/polymer.htm [Accessed 17th August 2012].

Lexus [Online]. Available: http://www.lexus.com/models/IS/features/safety/airbags.html [Accessed 2nd May 2012].

International Union of Pure and Applied Chemistry [Online]. Available: http://pac.iupac.org/publications/pac/pdf/1974/pdf/4003x0477.pdf [Accessed 6th July 2013].

ARAKAWA, T., NAGATOSHI, F. & ARAI, N. 1969. Melting Behavior and Morphology of Drawn Nylon 6. *Journal of Polymer Science,* 7**,** 1461-1472.

BELL, J. P. 1972. The Effect of Rate and Temperature of Drawing on the Properties of Nylon 6,6 Fibers. *Textile Research Journal,* 42**,** 292-297.

BELL, J. P. & HUGHES, A. J. 1978. Selective Degradation of Nylon 6,6. II. Application of the Degradation Technique to Commercially Drawn Fibers. *Journal of Polymer Science: Polymer Physics Edition,* 16**,** 215-222.

BOWER, D. I. 2002. *An Introduction to Polymer Physics*, Cambridge University Press.

BUCHANAN, D. R. & DUMBLETON, J. H. 1969. Effect of Annealing Conditions in the Structure of Drawn Nylon 66 Yarns. *Journal of Polymer Science,* 7**,** 113-122.

CRYSTAL, R. G. & HANSEN, D. 1968. Morphology of Cold-Drawn Nylon 66. *Journal of Polymer Science, Part A-2*, 6, 981-993

BUNN, C. W. & GARNER, E. V. 1947. The Crystal Structures of Two Polyamides (Nylons). *Proceedings of the Royal Society of London - Mathematical, Physical and Engineering Sciences,* 189**,** 39-68.

DISMORE, P. E. & STRATTON, W. O. 1966. Chain Folding in Oriented Nylon 66 Fibers. *Journal of Polymer Science,* 13**,** 133-148.

ELAD, J. & SCHULTZ, J. M. 1984. Microstructural Rearrangement during Heat Treatment of Drawn Nylon 66 Fiber *Journal of Polymer Science,* 22**,** 781-792.

EMRI, I., BERNSTORFF, B. V. & VOLOSHIN, A. 2006. Effect of Heating on Fiber Shrinkage. P*roceedings of the 2006 SEM Annual Conference and Exposition on Experimental and Applied Mechanics*, Paper 23

FRANK, O. & WENDORFF, J. H. 1988. Polyamide 6,6 fibers: Tensile deformation behavior and chain scission. *Colloid & Polymer Science,* 266**,** 216-226.

FULLER, C. S. 1940. The investigation of synthetic linear polymers by x-rays. *Chemical Reviews,* 26**,** 143-167.

FULLER, C. S., BAKER, W. O. & PAPE, N. R. 1940. Crystalline behavior of linear polyamides. Effect of heat treatment. *Journal of the American Chemical Society,* 62**,** 3275-3281.

HOLLAND, B. J. & HAY, J. N. 2000. Thermal degradation of nylon polymers. *Polymer International,* 49**,** 943-948.

HOU, Y., SUN, T., WANG, H. & WU, D. 2008. Effect of Heating Rate on the Chemical Reaction during Stabilization of Polyacrylonitrile Fibers. *Textile Research Journal,* 78**,** 806-811.

ILLERS, K. H. 1975. Dynamic mechanical behaviour of drawn nylon 66 and poly(ethylene terephthalate). *Colloid and Polymer Science,* 253**,** 329-331.

JAIN, A. & VIJAYAN, K. 2002. Effect of thermal ageing on Nylon 6,6 fibres. *Journal of Materials Science,* 37**,** 2623-2633.

JENEKHE, S. A. & ROBERTS, M. F. 1993. Effects on Intermolecular Forces on the Glass Transition of Polymers. *Macromolecules,* 26**,** 4981-4983.

KESHAVARAJ, R., TOCK, R. W. & NUSHOLTZ, G. S. 1996. A Realistic Comparison of Biaxial Performance of Nylon 6,6 and Nylon 6 Fabrics Used in Passive Restraints - Airbags *Journal of Applied Polymer Science,* 61**,** 1541-1552.

KONG, Y. & HAY, J. N. 2002. The measurement of the crystallinity of polymers by DSC. *Polymer,* 43**,** 3873-3878.

LEUNG, W. P., HO, K. H. & CHOY, C. L. 1984. Mechanical Relaxations and Moduli of Oriented Nylon 66 and Nylon 6 *Journal of Polymer Science: Polymer Physics Edition,* 22**,** 1173-1191.

MORTON, W. E. & HEARLE, J. W. S. 1993. *Physical properties of textile fibres*, Textile Institute.

MUKHOPADHAY, S. K. & PARTRIDGE, J. F. 1999. Automotive Textiles. *Textile Progress,* 29**,** 1-125.

MURTHY, N. S. 1997. Fibrillar Structure and Its Relevance to Diffusion, Shrinkage, and Relaxation Processes in Nylon Fibers. *Textile Research Journal,* 67**,** 511-520.

NARTEN, A. H., HABENSCHUSS, A. & XENOPOULOS, A. 1991. Diffraction pattern and structure of amorphous and crystalline regions in semicrystalline nylon 6.6. *Polymer,* 32**,** 1923-1927.

PAI, C., JENG, J., GROSSMAN, S. J. & HUANG, J. 1989. Effects of Moisture on Thermal and Mechanical Properties of Nylon-6,6. *Advances in Polymer Technology,* 9**,** 157-163.

PREVORSEK, D. & TOBOLSKY, A. V. 1965. Determination of Non-Flow Shrinkage in Oriented Fibers. *Textile Research Journal,* 33**,** 795-802.

RAMESH, C., KELLER, A. & ELTINK, S. J. E. A. 1994. Studies on the crystallization and melting of nylon-6,6: 1. The dependence of the Brill transition on the crystallization temperature. *Polymer,* 35**,** 2483-2487.

RIBNICK, A. 1969. Thermal Shrinkage of Oriented Nylon 66 Yarns as a Function of Time, Temperature, and Stress. *Textile Research Journal,* 39**,** 428-434.

SEPE, M. 2011. *The effects of temperature* [Online]. Plastics Technology. Available: http://www.ptonline.com/columns/the-effects-of-temperature [Accessed 15th August 2012].

SIMPSON, P. G., SOUTHERN, J. H. & BALLMAN, R. L. 1981. Nylon 6,6 Fiber Tensile Properties as a Function of Morphology. *Textile Research Journal,* 51**,** 97-100.

STACK, G. M., MANDELKERN, L. & VOIGT-MARTIN, I. G. 1982. Changes in Crystallite Size Distribution During the Isothermal Crystallization of Linear Polyethylene *Polymer Bulletin,* 8**,** 421-428.

STARKWEATHER JR., H. W., MOORE, G. E., HANSEN, J. E., RODER, T. M. & BROOKS, R. E. 1956. Effect of Crystallinity on the Properties of Nylons. *Journal of Polymer Science,* 21**,** 189-204.

STATTON, W. O. 1972. High-Temperature Annealing of Drawn Nylon 66 Fibers. *Journal of Polymer Science,* 10**,** 1587-1592.

SUN, J. & BARNES, J. A. 2010. Materials Selection for Airbag Fabrics. Du-Pont. Available: http://www2.dupont.com/Automotive/en_US/assets/downloads/materialssselectionairbagfabrics.pdf [Accessed 12th September 2012].

WHITE, J. L. & CAKMAK, M. 1986. Orientation Development and Crystallization in Melt Spinning of Fibers *Advances in Polymer Technology,* 6**,** 295-338.

YONGQIANG, X., QINGSHENG, Z. & CHUNHUI, L. 2001. The Thermodynamic Relations between the Melting Point and the Size of Crystals. *Journal of Colloid and Interface Science,* 243**,** 388-390.

YOUNG, R. J. & LOVELL, P. A. 2011. *Introduction to Polymers*, CRC Press, Taylor & Francis Group LLC.

ZHANG, L., LIU, L., PAN, F., WANG, D. & PAN, Z. 2012. Effects of Heat Treatment on the Morphology and Performance of PSU Electrospun Nanofibrous Membrane. *Journal of Engineered Fibers and Fabrics***,** 7-16.